



SCHOOL of
GRADUATE STUDIES
EAST TENNESSEE STATE UNIVERSITY

East Tennessee State University
Digital Commons @ East
Tennessee State University

Electronic Theses and Dissertations

Student Works

12-2014

Biochemical Characterization of SBIP-470 and its role in SA-mediated Signaling in Plants

Danda P. Chapagai

East Tennessee State University

Follow this and additional works at: <https://dc.etsu.edu/etd>



Part of the [Biology Commons](#)

Recommended Citation

Chapagai, Danda P., "Biochemical Characterization of SBIP-470 and its role in SA-mediated Signaling in Plants" (2014). *Electronic Theses and Dissertations*. Paper 2428. <https://dc.etsu.edu/etd/2428>

This Thesis - Open Access is brought to you for free and open access by the Student Works at Digital Commons @ East Tennessee State University. It has been accepted for inclusion in Electronic Theses and Dissertations by an authorized administrator of Digital Commons @ East Tennessee State University. For more information, please contact digilib@etsu.edu.

Biochemical Characterization of SBIP-470 and its role in SA-mediated Signaling in Plants

A thesis

presented to

the faculty of the Department of Biological Sciences

East Tennessee State University

In partial fulfillment

of the requirements for the degree

Master of Science in Biology

by

Danda Pani Chapagai

December 2014

Dhirendra Kumar, PhD Chair

Aruna Kilaru, PhD

Ranjan Chakraborty, PhD

Keywords: Plant Defense, Salicylic Acid, Systemic Acquired Resistance, Salicylic Acid Binding

Protein 2, Lipid Transfer Protein, Lipid binding, Lipid Transfer

ABSTRACT

Biochemical Characterization of SBIP-470 and its role in SA-mediated Signaling in Plants

by

Danda Pani Chapagai

Salicylic acid binding protein 2 (SABP2) is known to play a key role in Salicylic acid mediated defense pathway. SBIP-470 is SABP2 interacting protein that might be putatively involved in transfer of lipids. SBIP-470 was cloned without the signal peptide and expressed in *E. coli*. In vitro lipid binding assay using recombinant SBIP-470 failed to detect lipid binding. In vitro lipid transfer assay showed recombinant SBIP-470 does not transfer phospholipid. Study has shown that SBIP-470 is highly inducible upon infection with viral as well as bacterial pathogens.

Induction of *SBIP-470* expression upon the TMV infection most likely depends upon the SABP2 while its expression upon non-host bacterial pathogens is most probably inhibited by the SABP2.

A study of *Arabidopsis* knockout mutants (*ltp12* mutant and *ltp2* mutant) lacking the *SBIP-470* homolog genes showed defects in growth phenotype, and they were found susceptible to bacterial pathogens.

ACKNOWLEDGEMENTS

I would like to thank my committee members, Dr. Dharendra Kumar, Dr. Aruna Kilaru, and Dr. Ranjan Chakraborty for their valuable suggestions and guidance throughout the project. I am extremely grateful to Dr. Dharendra Kumar for his encouragement, guidance, and support all the way through the research. I would like to thank all the faculty and staff from Department of Biological Sciences. I would like to thank ETSU Graduate School for graduate assistantship and also would like to thank ETSU RDC grant (14-021M to DK) and NSF grant (MCB 1022077 to DK) for financial support. A special thanks to my lab colleagues for their help, and I am thankful to all my family members and friends for their love and support.

TABLE OF CONTENTS

	Page
ABSTRACT.....	2
ACKNOWLEDGEMENTS.....	3
LIST OF TABLES.....	9
LIST OF FIGURES	10
 Chapter	
1. INTRODUCTION	13
Plants Natural Defense.....	13
Signaling Pathways.....	14
Salicylic Acid (SA).....	14
SA Dependent/Independent Pathway	15
Systemic Acquired Resistance (SAR)	16
Jasmonic Acid (JA).....	18
Ethylene (ET).....	18
Abscisic Acid (ABA).....	19
Salicylic Acid Binding Protein 2 (SABP2).....	19
SABP2 interacting protein (SBIP).....	19
Lipid Transfer Proteins (LTPs).....	20
Family 1: Nonspecific Lipid Transfer Protein (nsLTP1) and Binding Mechanism.....	20
Family 2: Nonspecific Lipid Transfer Protein (nsLTP2) and Binding Mechanism.....	21
Roles of Lipid Transfer Protein in Plant Defenses	21
Defective in Induced Resistance 1 (DIR1) in Systemic Acquired Resistance (SAR).....	22

Tobacco Lipid Transfer Protein 1 (NtLTP1) in Pathogen Resistance	23
Lipid Transfer Protein in Vegetative Growth and Reproduction.....	24
<i>Arabidopsis</i> LTP2 and LTP12	25
<i>Arabidopsis</i> LTP2	25
<i>Arabidopsis</i> LTP12	25
<i>Arabidopsis ltp2</i> Mutant	26
<i>Arabidopsis ltp12</i> Mutant	26
Gene Expression of <i>SBIP-470</i> upon Pathogen Infection	26
<i>SBIP-470</i> Expression upon <i>Tobacco Mosaic Virus (TMV)</i> Infection.....	26
<i>SBIP-470</i> Expression upon <i>Pseudomonas syringae pv. tabaci (P.s. tabaci)</i>	
Infection	27
<i>SBIP-470</i> Expression under <i>Pseudomonas syringae pv. tomato DC3000</i>	
(<i>Pst DC3000</i>)	28
<i>SBIP-470</i> Expression under <i>Pseudomonas syringae pv. phaseolicola (P.s.</i>	
<i>pv. phaseolicola)</i>	29
Hypotheses	31
Hypothesis I: Tobacco <i>SBIP-470</i> is a Lipid Transfer Protein	31
Hypothesis II: <i>Arabidopsis ltp2</i> Mutant and <i>ltp12</i> Mutant Have Defective	
Growth Phenotype and are Susceptible to Pathogens.....	32
2. MATERIALS AND METHODS.....	33
Plant Material.....	33
Chemicals and Reagents	33
Other Materials	34
Biochemical Characterization of <i>SBIP-470</i> (Hypothesis I).....	34
Bioinformatics Analysis.....	34
Conserved domain prediction	34
Prediction of <i>SBIP-470</i> properties	34
Subcellular localization.....	34

Signal peptide and cleavage site prediction	34
3D structure prediction	34
Phylogenetic analysis.....	35
Cloning of <i>SBIP-470</i> without the Signal Peptide (<i>SBIP-470-25</i>).....	35
cDNA Synthesis.....	35
Agarose Gel Electrophoresis.....	36
PCR Purification	36
Quantitation of <i>SBIP-470</i>	37
Agarose Gel Electrophoresis.....	37
BP Recombination Reaction	37
Transformation to Competent <i>E. coli</i> Cells	37
Plasmid Isolation.....	38
Sequencing.....	38
LR Recombination Reaction.....	39
Transformation of Competent <i>E. coli</i> (DH5 α).....	39
Plasmid Isolation.....	39
Transformation of Competent <i>E. coli</i> Magic Cell (BL21DE3)	40
Expression of Recombinant SBIP-470 in <i>E. coli</i>	40
Solubility Test of Recombinant SBIP-470 in <i>E. coli</i>	41
Purification of Recombinant SBIP-470	41
Ni-NTA column chromatography.....	41
Q-sepharose column chromatography	42
Ni-NTA column chromatography.....	42
SDS PAGE.....	42
Western Blot Analysis	43
Dialysis of recSBIP-470	44
Quantification of recSBIP-470	44
Biochemical Characterization.....	45

In Vitro Lipid Binding Assay	45
In Vitro Lipid Transfer Assay.....	47
Characterization of Arabidopsis Mutants (Hypothesis II)	48
Arabidopsis Mutant Screening.....	48
Mutant screening using cDNA.....	49
Reverse transcriptase (RT)-PCR.....	49
cDNA synthesis	50
Phenotype Analysis.....	51
Toluidine Blue (TB) Test.....	51
Pathogen Growth Assay.....	51
3. RESULTS	53
Biochemical Characterization of SBIP-470 (Hypothesis I).....	53
Computational Analysis of SBIP-470.....	53
Predicted Properties of SBIP-470	53
Conserved Domain.....	54
Subcellular Localization	55
Signal Peptide Cleavage Site	56
SBIP-470 <i>Arabidopsis</i> Homolog	58
Predicted 3D Structure	59
Phylogeny Tree	60
Cloning of <i>SBIP-470</i>	61
cDNA Synthesis.....	61
PCR Purification.....	62
pDONR221- <i>SBIP-470-25</i> Entry Clone Validation.....	63
pDEST17- <i>SBIP-470-25</i> Validation	65
Expression of Recombinant SBIP-470	66
Expression.....	66
Solubility Test.....	67

Expression of SBIP-470 under Soluble Condition	68
Ni-NTA Column Chromatography	68
Q-Sepharose Column Chromatography	69
Ni-NTA Column Chromatography	71
Biochemical Characterization	72
Lipid Binding Assay	72
In Vitro Lipid Transfer Assay.....	74
Phenotype Analysis of <i>Arabidopsis</i> Mutants (Hypothesis II)	75
T-DNA Based Mutant Screening.....	75
RT-PCR Based Mutant Screening	77
Growth Phenotype of <i>ltp12</i> and <i>ltp2</i> Mutant	77
Toluidine Blue (TB) Test.....	84
Pathogen Growth Assay.....	85
4. DISCUSSION.....	89
Characterization of SBIP-470.....	91
<i>SBIP-470</i> Gene Expression upon Pathogen Infection	91
Mutant Analysis	92
Pathogen Growth Assay.....	93
Toluidine Blue Test.....	94
Lipid binding and transfer test	94
Gene expression and pathogen growth	94
Future Direction	96
REFERENCES	96
APPENDICES	101
Appendix A: Abbreviations	101
Appendix B: Buffers and Reagents.....	103
VITA.....	107

LIST OF TABLES

Table	Page
1. Nomenclature of Various Phospholipids Spotted on PIP Strips.....	46
2. PLTP Activity Assay Kit Work Flow.....	48
3. Predicted Properties of SBIP-470.....	54
4. Subcellular Localization of SBIP-470.....	56

LIST OF FIGURES

Figure	Page
1. Chemical Structure of Salicylic Acid	15
2. NPR Dependent SA Signaling and NPR Independent SA Signaling	16
3. SAR Development in Plant.....	17
4. Chemical Structure of Jasmonic Acid.....	18
5. <i>SBIP-470</i> Gene Expression upon <i>TMV</i> Infection in C3 and 1-2 Plants.....	27
6. <i>SBIP-470</i> Gene Expression upon <i>P.s. tabaci</i> in C3 and 1-2 Plant.....	28
7. <i>SBIP-470</i> Gene Expression upon <i>Pst DC3000</i>	29
8. <i>SBIP-470</i> Gene Expression upon <i>P.s. pv. phaseolicola</i>	30
9. <i>SBIP-470</i> DNA Sequence (345 Bases) Obtained from Y2H Screening.....	53
10. <i>SBIP-470</i> Amino Acid Sequence (114 aa) Translated from Nucleotide Sequence by <i>ExPASy Bioinformatics Research Portal</i>	53
11. Result Showing Protein BLAST of <i>SBIP-470</i>	54
12. Conserved Domain of nonspecific Lipid Transfer Protein-1 (nsLTP1)	55
13. Subcellular Localization of <i>SBIP-470</i>	56
14. <i>SBIP-470</i> Signal Peptide Cleavage Site Prediction	57
15. Analysis of Amino Acid Residues at Signal Peptide Cleavage Site of Tobacco <i>SBIP-470</i> and Tobacco LTP	58
16. Multiple Sequence Alignment between Tobacco <i>SBIP-470</i> , <i>Arabidopsis</i> LTP12, and <i>Arabidopsis</i> LTP2	59
17. Predicted Protein Model of <i>Arabidopsis</i> LTP12, <i>Arabidopsis</i> LTP2, and Tobacco <i>SBIP-470</i>	60
18. Rooted Phylogeny Tree (Maximum Likelihood, Character State Method) between Tobacco, Potato, <i>Arabidopsis</i> , <i>Citrus sinensis</i> , and <i>Plasmodium cynomolgi</i> LTP Protein Family.....	61

19. 1.2% Agarose Gel Picture of <i>SBIP-470-25</i> Amplified from Verified Clone, pDONR221- <i>SBIP-470</i> Construct.....	62
20. 1.2% Agarose Gel Picture of Purified <i>SBIP-470-25</i>	62
21. Agarose Gel Showing Purified <i>pDONR221-SBIP-470-25</i> Entry Clone by QIAprep Spin MiniPrep Kit.....	64
22. Sequence Alignment of <i>SBIP-470-25</i> with attB Sites (#470-attBs) and <i>pDONR221-</i> <i>SBIP-470-25</i> Entry Clone (#ENC).....	65
23. Agarose Gel Showing Purified pDEST17- <i>SBIP-470-25</i> DNA Construct by QIAprep Spin MiniPrep Kit.....	66
24. Solubility Test of recSBIP-470-25 Obtained from 37°C and 17°C Culture.....	68
25. Purification of recSBIP-470-25 using Ni-NTA Column Chromatography	69
26. Chromatography Profile of Protein in Q Sepharose Column Chromatography	70
27. Purification of recSBIP-470-25 using Q Sepharose Column Chromatography	71
28. Purification of recSBIP-470-25 using Ni-NTA Column Chromatography	72
29. Lipid Binding Assay of recSBIP-470-25 using PIP Strips (Catalog P-6001)	73
30. Lipid Binding Assay of recSBIP-470-25 using PIP Strips (Catalog P-6002)	74
31. Time Dependent Phospholipid Transfer Activity of recSBIP-470-25.....	75
32. Confirmation of T-DNA Insertion at <i>LTP12</i> and <i>LTP2</i> Gene	76
33. RT-PCR Analysis of <i>Arabidopsis LTP12</i> and <i>LTP2</i> (Partial) Genes	77
34. Growth Phenotype Analysis of <i>ltp12</i> Mutant, <i>ltp2</i> Mutant, and Col-0.....	79
35. Height of <i>Arabidopsis</i> Plant at 15, 22, 30, and 39 DAG	81
36. Numbers of Leaf of <i>ltp12</i> Mutant, <i>ltp2</i> Mutant, and Col-0 at 30 DAG.....	81
37. Length of Longest Leaf in <i>ltp12</i> Mutant, <i>ltp2</i> Mutant, and Col-0	82
38. Bolting Time of <i>ltp12</i> Mutant, <i>ltp2</i> Mutant, and Col-0	82
39. Time of Inflorescence Emergence in <i>ltp12</i> Mutant, <i>ltp2</i> Mutant, and Col-0.....	83
40. Time of Silique Formation in <i>ltp12</i> Mutant, <i>ltp2</i> Mutant, and Col-0	83
41. Height of Inflorescence at 39 DAG in <i>ltp12</i> Mutant, <i>ltp2</i> Mutant, and Col-0.....	84

42. Application of Toluidine Blue on Plant Surface to Detect Permeable Epidermal Surface	85
43. Bacterial Population of <i>Pst DC3000</i> in Col-0 and <i>ltp12</i> Mutant at 1 dpi (Days after Post Inoculation)	86
44. Bacterial Population of <i>Pst DC3000</i> in Col-0 and <i>ltp12</i> Mutant at 4 dpi	86
45. Bacterial Population of <i>Pst DC3000</i> in Col-0 and <i>ltp2</i> Mutant at 1 dpi	87
46. Bacterial Population of <i>Pst DC3000</i> in Col-0 and <i>ltp2</i> Mutant at 4 dpi	87
47. Bacterial Population of <i>Pst DC3000 AvrRPT2</i> in Col-0 and <i>ltp12</i> Mutant at 3 dpi	87
48. Bacterial Population of <i>Pst DC3000 AvrRPT2</i> in Col-0 and <i>ltp12</i> Mutant at 4 dpi	88
49. Bacterial Population of <i>Pst DC3000 AvrRPT2</i> in Col-0 and <i>ltp2</i> Mutant at 3 dpi	88
50. Bacterial Population of <i>Pst DC3000 AvrRPT2</i> in Col-0 and <i>ltp2</i> Mutant at 4 dpi	88

CHAPTER1

INTRODUCTION

Plants are a rich source of nutrients for vertebrates, bacteria, fungi, and insects. Humans mainly depend upon plants for food, timber, medicines, cosmetics, and industrial chemicals (Beattie 2008). Plants face many challenges from a wide range of pathogens such as microorganisms (viruses, bacteria, and fungi), nematodes, insects, and more at all stages in all organs (De Vos et al. 2006). A significant amount of crop yield is lost because of the diseases caused by pathogens every year worldwide (Oerke 2005).

Various strategies can be applied to decrease the crop lost by pathogen infections. For instance, people have used fungicides and pesticides to control pathogens and pests respectively, and developed transgenic plant producing insecticide (i.e. BT cotton). However, several of these chemicals are toxic to human consumption; some of them may concentrate in food chain, and they may alter the ecosystem. Moreover, pathogens develop resistance to chemicals when used continuously (Pal et al. 2006).

Plants Natural Defense

Plants have both innate and adaptive immunity. Innate immunity, a first line of immunity, does not last for long time. In the innate immunity, plant responds to pathogen using 2 branches of immune systems. The first branch recognizes and responds to molecules that are common to pathogens. In the first branch the Pattern Recognition Receptors (PRRs) present on surface of plants detects Pathogen Associated Molecular Patterns (PAMPs). Consequently, plants develop PAMP-Triggered Immunity (PTI). Then, PTI initiates the production of Reactive Oxygen Species (ROS), defense gene expression, hormone signaling, and more. Pathogens that are able to suppress the PTI, release the virulence effector proteins, causing development of Effector-Triggered Susceptibility (ETS). In second branch of immunity effector is then specifically recognized by one

of Nucleotide Binding (NB) and Leucine Rich Repeat (LRR) proteins that develops ETI. Thus, developed immunity causes cell death at the site of pathogen infection (Jones and Dangl 2006). ETI and PTI activate different signaling pathways. ETI stimulates the Salicylic Acid (SA) biosynthesis that eventually leads to development of Local Resistance (LR) as well as Systemic Acquired Resistance (SAR) against the biotrophic pathogens (Métraux et al. 1990), whereas PTI stimulates Ethylene (ET) biosynthesis (Felix et al. 1999). Ethylene and Jasmonic Acid (JA) coordinate to activate the defense pathway against the necrotrophic pathogens (Thomma et al. 1998). Different but interconnecting signaling pathways have been found to function while studying the mutants compromised in the resistance to pathogens. Plant signaling molecules such as SA, JA, abscisic acid, and ET involve in interconnecting pathways (Figure 2) (Shah 2003).

Signaling Pathways

Salicylic Acid (SA)

SA (Figure 1), 2-hydroxybenzoic acid is involved in activating the defense signaling pathway in plants. Biosynthesis of SA has been unraveled to some extent but the detail mechanism is still unknown. Two pathways are known that are responsible for synthesizing SA in plants, the phenylalanine ammonia lyase (PAL) mediated and isochorismate synthase (ICS) mediated pathways. Chorismate, a product of shikimate pathway, is converted into SA by either via PAL or ICS mediated pathway (Chen et al. 2009; Dempsey and Klessig 2012).

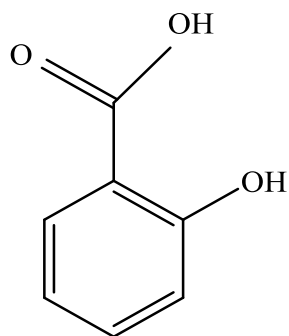


Figure 1. Chemical Structure of Salicylic Acid

Phenylalanine is converted by PAL to cinnamate, which is converted to SA via benzoate (Chen et al. 2009; Dempsey et al. 2011). On the other side, based on genetic study, ICS converts chorismate to isochorismate then it is converted to SA, which is not fully understood (Chen et al. 2009).

SA undergoes several modifications after its synthesis such as glycosylation, methylation, amino acid conjugation, etc. Most of modifications of SA make it inactive but leads to proper functioning at the right time and right place. Glycosylation also inactivates the SA but allows a high amount of SA to be stored in vacuoles. Methylation increases its permeability to cross the hydrophobic lipid bilayer membrane. Methylation is very important especially for the long distance signaling during pathogen infection. Amino acid conjugation of SA is not well understood yet (Dempsey et al. 2011).

SA Dependent/Independent Pathway

Two types of SA-mediated pathways are known that are, non-expressor of pathogenesis-related genes (NPR) dependent SA signaling and NPR independent SA signaling (Dong 2001). In the NPR dependent SA signaling, SA stimulates the translocation of NPR1 monomers into nucleus where it interacts with TGA class of transcription factors (Kinkema 2000). In the NPR independent SA signaling pathway, NPR1 is not necessary for the expression of

pathogenesis-related (PR) genes and subsequent resistance to pathogen. A second signal is required in addition to SA and the signal can be cell death. ET and JA signal through the NPR independent pathway (Figure 2) (Clarke et al. 2000; Dong 2001).

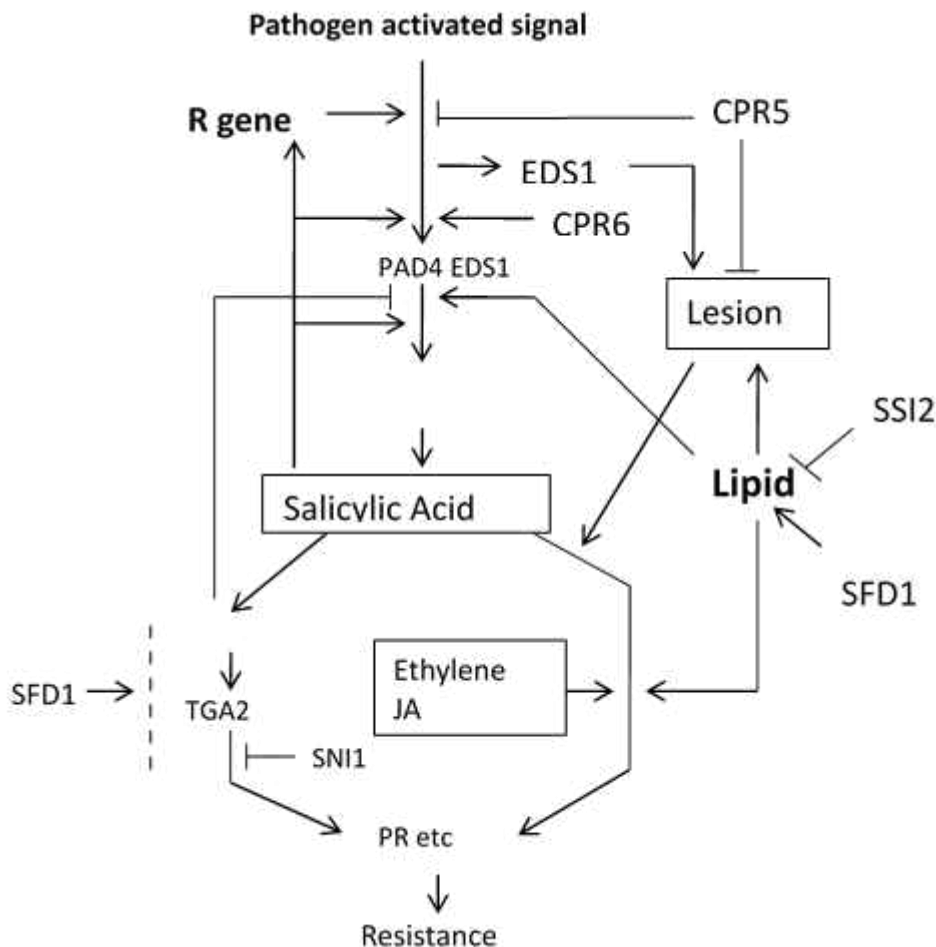


Figure 2. NPR Dependent SA Signaling and NPR Independent SA Signaling. In the NPR dependent SA signaling pathway, NPR1, activated by SA, is necessary for expression of pathogenesis related (*PR*) genes and subsequent resistance to pathogen. Whereas in the NPR independent SA signaling, the NPR1 is not essential for *PR* gene expression but a second signal in addition to SA is necessary (redrawn from Shah 2003).

Systemic Acquired Resistance (SAR)

Plants exhibiting resistance against pathogens produces high amount of SA that activates defense pathway (Malamy et al. 1990). When pathogen attacks plants, the SA level increases in the primary infected tissue (Ryals et al. 1996). SA methyl transferase 1 (SAMT1) converts some of SA

to Methyl Salicylate (MeSA) (Park et al. 2007). MeSA esterase (MSE) activity of salicylic acid-binding protein 2 (SABP2) can convert back the MeSA to SA by demethylating the MeSA, but the high amount of SA inhibits the MSE activity (Park et al. 2007). Some of the accumulated MeSA moves to systemic tissue where MSE converts the MeSA to SA (Park et al. 2007). As a result, the plant develops a SAR, (Figure 3) (Park et al. 2007). In primary infected tissues defective in induced resistance 1 (DIR1), a lipid transfer protein, and suppressor of fatty acid desaturase1 (SFD1) form *Arabidopsis thaliana* DIR1 and SFD1 dependent lipid complex (XY) that moves to the systemic tissue. The lipid derived factor (XY) directly or indirectly suppresses SABATH methyltransferase *BSMT1* (*BSMT1*) expression thus allowing the SA accumulation in systemic tissue (Liu et al. 2011).

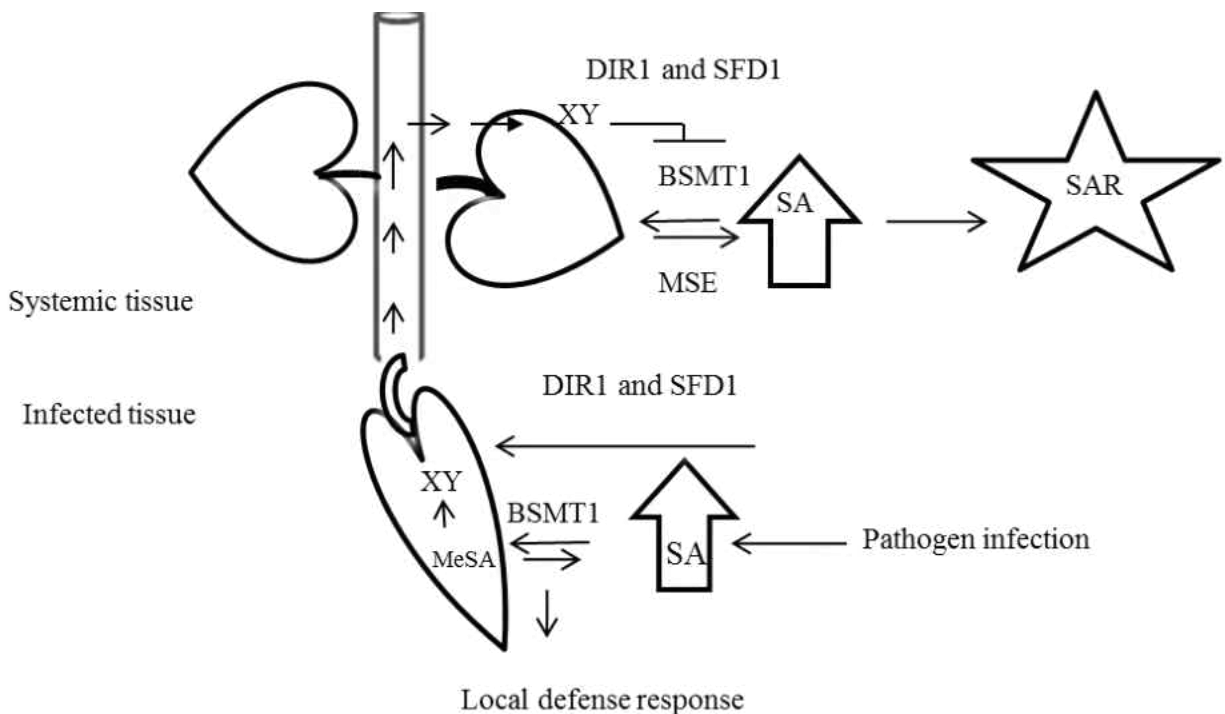


Figure 3. SAR Development in Plant. When pathogen attacks plants, the SA level rises in the primary infected tissue. SAMT1 converts some of SA to MeSA in primary infected tissue. The accumulated MeSA moves to systemic tissue where MSE converts the MeSA to SA to develop SAR. In primary infected tissue, Arabidopsis DIR1 and SFD1 form a lipid derived factor (XY) which moves to systemic tissue. In the systemic tissue, the lipid derived factor (XY) suppresses BSMT1 expression thus allowing the SA accumulation.

Similarly, in a chimeric tobacco plant (generated by grafting plants with different genetic backgrounds), SABP2, which has MSE activity, converts MeSA to SA when the plant is inoculated with a pathogen. Thus produced SA develops SAR (Park et al. 2007).

Jasmonic Acid (JA)

JA (Figure 4) is a member of Jasmonate class of plant hormones, which is produced from linolenic acid by an octadecanoid pathway. In *Arabidopsis thaliana* JA content increases rapidly in petiole exudes (PEX) collected from leaves inoculated with SAR eliciting virulent strain of *Pseudomonas syringe*. The increased levels of JA lead to rapid and systemic expression of JA-responsive genes. Similarly, Jasmonate-deficient 12-oxophytodienoate reductase 3 (*opr3*) and jasmonate-insensitive 1 (*jin1*) and jasmonate-insensitive 4 (*jai4*) mutants do not develop a SAR conferred resistance (Shah 2009). JA and its derivatives have roles in regulating plant responses to abiotic stresses as well as plant growth and development (Delker et al. 2006).

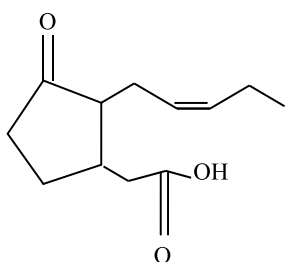


Figure 4. Chemical Structure of Jasmonic Acid

Ethylene (ET)

ET (C₂H₄ or H₂C=CH₂) is involved in diverse metabolic and developmental process such as seed germination, fruit ripening, and senescence (Wang et al. 2002). Environmental factors such as flooding, drought, chilling, wounding, and pathogen attack can induce ethylene synthesis in a plant (Yang 1984). ET with JA signals through the NPR independent pathway (Figure 2) (Clarke et al. 2000; Dong 2001).

Abscisic Acid (ABA)

ABA is an isoprenoid plant hormone that has various roles in plant such as in root growth, seed maturation and dormancy, protection from biotic and abiotic stress. It is derived from plastidial 2-C-methyl-D-erythritol-4-phosphate (MEP) pathway. ABA mediated signaling has a role in plant responses to environmental stress and pathogen infection (Nambara and Marion-Poll 2005).

Role of ABA in plant defense is not well understood. It may influence disease resistance through stomata closure or water relation. The role of ABA is considered as a negative regulator in plant disease resistance. It may be due to interference of ABA with SA, JA, and ET mediated biotic signaling pathway (Mauch-Mani and Mauch, 2005). Contrary to the negative role, recent studies have shown that it also promotes the disease resistance. Its roles in disease resistance depends upon several factors such as type of pathogen, pathogen's specific way of entering in host, timing of defense response, and tissue infected (Ton et al. 2009).

Salicylic Acid Binding Protein 2 (SABP2)

SABP2 is a 29 KDa soluble, low abundance protein that converts MeSA to SA. SABP2 has high affinity ($K_d = 90$ nM) for SA. In SABP2 silenced transgenic plants the local as well as the SAR against tobacco mosaic virus is disrupted (Kumar and Klessig 2003; Park et al. 2007).

SABP2 interacting protein (SBIP). Yeast two-hybrid screening using SABP2 as a bait and tobacco leaf proteins as a prey has shown that SABP2 physically interacts with several other tobacco proteins including i.e. SABP2 interacting protein-470 (SBIP-470) (Kumar et al. Unpublished). SBIP-470 is predicted to be a member of nonspecific lipid-transfer protein type 1 (nsLTP1) subfamily.

Lipid Transfer Proteins (LTPs)

LTPs are small, soluble, and basic proteins. Based on sequence similarity, LTPs are divided into 9 types, LTP I-IX. They have 8 cysteine residues and have a tunnel like hydrophobic cavity that binds different types of lipid substrates. Based on biochemical characteristics, LTPs are divided into 2 distinct families. Generally, LTPs from family 1 and 2 have molecular weight of ~9 KDa and ~7 KDa respectively. LTPs from both families are highly basic (pI ~9) and have 8 cysteine residues (C1-C8). They share 30% sequence similarity and have a common hydrophobic cavity formed by 4 α -helices. This hydrophobic cavity accommodates long chain fatty acids as substrates. One end of the hydrophobic cavity has a narrower opening and has nonpolar residues, and another end of the hydrophobic cavity has a wider mouth that is near to a flexible and polar region (Jean and Claude Kader 1996).

Family 1: Nonspecific Lipid Transfer Protein (nsLTP1) and Binding Mechanism

LTPs in this family have 3 amphiphilic α -helices parallel to central binding pocket. The rest part of the hydrophobic cavity is defined by the fourth α helix and a c-terminal loop in this family, Tyr₇₉ is conserved, which is involved in hydrogen bonding to polar head group of lipid ligands (Charvolin et al. 1999). Similarly, 2 oppositely charged residues at the beginning of the third α helix are also present in all nsLTP1 (Han et al. 2001). Based on equilibrium titration experiments, nsLTP1 are known to bind glycerolipids and fatty acids. According to crystal structure of LTP1 from wheat (*Triticum aestivum*) and rice (*Oryza sativa*) they (LTPs) bind L-a-myristoyl-phosphatidylcholine and palmitic acid. The study of protein structure has shown that 2 ligands share a common binding tunnel in tail to tail manner and they enter from opposite ends leaving their polar ends exposed to solvent (Charvolin et al. 1999; Cheng et al. 2004). In vitro lipid binding assay has shown that nsLTP1 binds acyl CoA. But, in vivo binding of nsLTP1 to hydroxyacyl-CoA, precursors of cutin and long aliphatic compound of waxes have not been

established. In an alternative model, it is proposed that nsLTP1 form a noncovalent bridge by binding 2 acyl moieties from neighboring cutin domains (Renan et al. 2003).

Family 2: Nonspecific Lipid Transfer Protein (nsLTP2) and Binding Mechanism

LTPs in this family also have the 4 α -helices bound by the disulfide bonds that enclose the hydrophobic lipid binding cavity. But, pairing pattern of cysteine (5 and 6) is switched. In nsLTP2, the disulfide bonding pattern is C1-C5 and C6 –C8, whereas in nsLTP1 bonding pattern is C1-C6 and C5-C8. Hydrophobic cavity is smaller in nsLTP2 than in nsLTP1 but it is more flexible, which can even accommodate wider varieties of lipids including sterols (Cheng et al. 2004). Proline 20 and 42 are evolutionary conserved and make a tight turns between helix 1 and helix 2, and between helix 3 and helix 4 respectively (Cheng et al. 2007).

Roles of Lipid Transfer Protein in Plant Defenses

LTPs are involved in both chemical as well as physical defense mechanism against pathogens. Expression of many LTP isoforms is induced upon pathogen challenge (Van Loon and Van Strien 1999). Transgenic plants overexpressing nsLTP1 shows increased resistance to pathogens like *P. syringae* (Molina and García-Olmedo 1997). NsLTP1 can be a binding competitor of elicitors from oomycetes, and strength of interaction increases by LTP in complex with JA. Similarly, plant develops increased resistance against oomycete, *Phytophthora parasitica*. Therefore, the elicitor and nsLTP1 likely act through same receptor to modulate the plant defense responses (Buhot et al. 2004).

LTPs help to acquire resistance against pathogen through membrane permeabilization. Allen oxide precursor of 9, 10-ketol reacts with barley LTP1 to form LTP1b lipid ligand. Similarity of the adducted structure to precursors of JA suggests a role in the defense signaling. It is speculated that a signaling role may be due to trapping of oxylipins (Bakan et al. 2006). The role

of some LTPs in defense pathways have been well studied i.e. DIR1 and LTP1 (Chanda et al. 2011; Liu et al. 2011; Choi et al. 2012).

Defective in Induced Resistance 1 (DIR1) in Systemic Acquired Resistance (SAR)

Arabidopsis mutant *dir1* does not develop SAR but it develops a local resistance to pathogens at infected tissue. Similarly, transgenic plant overexpressing the DIR1 does not exhibit constitutive SAR response. It is proposed that DIR1 interacts with lipid derived molecules for the long-distance signaling (Maldonado et al. 2002). It is predicted to be member of family 2 LTPs. Interestingly, pI of the mature protein is 4.5 is lower than the most family 2 LTPs (Maldonado et al. 2002). Studies have now shown that DIR1 is involved in SAR development along with a MeSA (mobile signal) and glycerol-3-phosphate (G3P) (a SAR inducer) (Chanda et al. 2011; Liu et al. 2011).

An interconnection between MeSA and lipid based-long distance signaling during the development of SAR has been observed in *Arabidopsis* and tobacco plants. When a combined phloem/petiole exudates (PEXs) (from pathogen infected *dir1-1* mutants and *sfd1* mutants) is applied to a wild type plant, SAR develops in the wild type plants, though PEX from neither mutants alone is sufficient to induce SAR. This result suggests that at least 2 components must be coordinated to develop SAR. DIR1 may be functional in PEX from the infected *sfd1* mutant and lipid derivative may be present in PEX from the infected *dir1-1* plants. The *dir1-1* fails to develop SAR, but MeSA and AtBSMT1 transcripts are high in *P. syringae pv maculicola* (*Psm*) infected tissue and systemic tissue compared to the wild type. During an elevated expression of AtBSMT1 in the systemic tissue equilibrium between the MeSA and SA shifts toward the MeSA synthesis. This inhibits the SA accumulation in the systemic leaves and development of SAR. This research suggests that SAR in a certain condition is activated by 2 mobile signals, MeSA and a complex

formed between AtDIR1 and AtSFD1 dependent lipid or lipid derivative (Figure 3) (Liu et al. 2011).

DIR1 and G3P coordinate during long-distance signaling. G3P induces SAR. *gly1* (mutation in GLY1 that encodes glycerol-3-phosphate) and *gli1* (mutation in GLI1 that encodes glycerol kinase) mutants cannot develop SAR. When G3P is infiltrated with an *avrRpt2* into wild type *Arabidopsis* and *gly1* and *gli1* mutants, SAR is induced in all 3 plants. But, the SAR developed in the *gly1* and *gli1* mutants is weak compared to wild type plant. The SAR inducing capacity of exogenous G3P increases drastically when it is mixed with PEX from MgCl_2 (ExMgCl_2) infiltrated or a *Pseudomonas syringae* containing *avrRpt2* infiltrated plant. ExMgCl_2 and G3P induce a strong SAR when distal tissue is inoculated with a virulence pathogen after 6-12 hours of infiltration. This indicates that effectiveness of G3P conferred SAR correlated with the particular time frame within which mobile signal is transported to the distal tissue. Similarly, it also suggests that the host factor found in petiole exudates is necessary for the G3P induced SAR. DIR1 helps to shift the G3P to distal tissue. Conversely, G3P helps the DIR1 to shift it to distal tissue through a symplast (Chanda et al. 2011).

Tobacco Lipid Transfer Protein 1 (NtLTP1) in Pathogen Resistance

NtLTP1 is expressed on top of long glandular trichomes (Choi et al. 2012). It has a role in secretion of lipid from trichome heads. It is highly expressed in long trichomes but not in a short trichomes or epidermal cells. In vitro lipid binding assay using 2-p-toluidinonaphthalene-6-sulfonate probe showed that it binds to the lipid. When it is overexpressed in transgenic tobacco plants, trichome exudates including epicuticular wax increases and the plant develops an increased protection against aphids. Similarly, when the *NtLTP1* expression is knocked down, the trichome liquid secretion significantly decreases; however, epicuticular wax does not alter (Choi et al. 2012). Sterk et al. (1991) had hypothesized that LTPs are involved in the cutin synthesis by

transporting acyl chains. The hypothesis is supported by various observations i.e. LTPs are localized to cell wall; LTPs gene expression as well as the gene product accumulate to peripheral cell layers; LTPs are highly expressed in surface wax of young leaves and LTPs bind acyl chain (Pyee 1995).

Glycosylphosphatidylinositol-anchored lipid transfer protein (LTPGI) is involved directly or indirectly in cuticular lipid accumulations. It is expressed in various tissues such as pollen, mesophyll cells, vascular bundles, stem cortex, and early developing tissues. It is localized to the plasma membrane. When *LTPGI* gene is disrupted, the cuticular lipid composition alters but the total wax and cutin monomer quantity do not change. In a *ltpGI* mutant, the C29 alkane reduces by 10 % (mass), but the reduced content is overcome by an increase in C29 secondary alcohols and C29 ketones. The mutant has more diffused cuticular layer structure, and it is more susceptible to fungus *Alternaria brassicicola* compared to the wild type plant (Lee et al. 2009).

Lipid Transfer Protein in Vegetative Growth and Reproduction

Family1 LTPs may play important role in cell expansion and growth by promoting cell wall loosening. For example, tobacco family 1 LTP is involved in promoting cell wall extension. Wheat family 1 LTPs also showed the similar effect, so this appears to be common property of family 1 LTPs. The mechanism of action is not well understood, but it most likely depends on hydrophobic cavity of LTPs (Nieuwland et al. 2009). *Arabidopsis LTP5* mutant (*ltp5*) showed the defect in sexual reproduction and also growth phenotype such as delayed hypocotyl elongation, dwarfed primary shoots, abnormal tissue fusion (Chae et al. 2010). LTPs are known to involve in reproduction for example lily lipid transfer protein is involved in adhesion of pollen tube to the style transmitting tract (Park et al. 2000).

Arabidopsis LTP2 and LTP12

Arabidopsis LTP2

LTP2 belongs to family of lipid transfer protein. LTP2 is predicted to belong to pathogenesis related-14 (PR-14) proteins family. *LTP2* is highly expressed in flower, developing seeds, and leaves (Arondel et al. 2000). It is expressed in epidermis and subepidermis of the flower and embryo organs (Clark and Bohnert 1999). On the promoter region of *LTP2* conserved motifs such as Box 3 and 10 bp sequence TCATCTTCTT are present (Thoma et al. 1994). Box 3 is also conserved in *Arabidopsis* phenylalanine ammonia lyase (*PAL*), and bean chalcone synthase (*CHS*). *CHS* is involved in SA mediated defense pathway and accumulation of flavonoids and isoflavonoid phytoalexins (stress metabolite) (Dao et al. 2011). *PAL* is involved in phenylpropanoid pathway (Chen et al. 2009; Dempsey et al. 2011) and found to involved in plant defense (Bagal et al. 2012). Ten base pair sequence is present on nontranscribed region (568 bp position) of *LTP2*. This sequence is also present repeatedly in other part of the gene such as 5' proximal, 3' untranslated sequences, and exon. The 10 bp sequence is present in 30 different plant genes that are inducible by stresses (Goldsbrough 1993). Study of the *Arabidopsis* genome transcript expression using Affymetrix ATH1 microarray showed that *LTP2* is induced upon the pathogen (*P. syringae* pv. *tomato* DC3000, *P. syringae* pv. *tomato* avrRpm1, *P. syringae* pv. *tomato* DC3000 hrcC, *P. syringae* pv. *phaseolicola*) challenge (Kilian et al. 2007).

Arabidopsis LTP12

LTP12 belongs to family of lipid transfer protein. LTP12 belongs to PR-14 family. It is highly expressed in inflorescences, while in seedlings and leaf it is expressed at very low levels (Huang 2013). *LTP12* promoter is highly active in tapetum (Ariizumi et al. 2002). Study on

Arabidopsis genome transcript expression using Affymetrix ATH1 microarray showed that *LTP12* is induced upon the pathogens (*P. syringae* pv. *tomato avrRpm1*) challenge (Kilian et al. 2007).

Arabidopsis ltp2 Mutant

Arabidopsis ltp2 mutant (ABRC stock number CS736752) has Transfer DNA (T-DNA) insertion in exon of *LTP2* gene in *Arabidopsis* columbia (Col-0) plant that was transformed by *Agrobacterium* mediated transformation. Binary vector (pAC161) was used for the transformation that contains the sulfadiazine (herbicide resistance gene) open reading frame driven by a 1'-2' promoter. The mutant has a sulfadiazine resistance marker that allows selecting the transformed plant under greenhouse conditions. Phenotype of the mutant has not reported yet (Rosso et al. 2003).

Arabidopsis ltp12 Mutant

Arabidopsis ltp12 mutant (seed stock number CS736658) has T-DNA insertion in intron of *LTP12* gene of *Arabidopsis* columbia (Col-0) plant that was transformed by *Agrobacterium* mediated transformation. Binary vector (pAC161) was used for the transformation that contains the sulfadiazine open reading frame driven by a 1'-2' promoter. The mutant has a sulfadiazine resistance marker that allows selecting the transformed plant under greenhouse conditions (Rosso et al. 2003).

Gene Expression of *SBIP-470* upon Pathogen Infection

SBIP-470 Expression upon Tobacco Mosaic Virus (TMV) Infection

Gene expression of *SBIP-470* was previously carried out (Simo and Kumar unpublished). To determine *SBIP-470* expression upon viral infection, 6- to-8- week-old plants were infected with TMV. Total RNA was isolated from the TMV infected leaves as well as mock inoculated

leaves at 0, 1.5, 3, 6, 9, 12, 24, 48, and 72 Hours Post Infection (hpi). Total cDNA was made from the total RNA.

Resulting total cDNA was used as template to amplify the *SBIP-470* and *actin* where *actin* was used as an internal control. *SBIP-470* gene expression was gradually increased in C3 plant upon the TMV infection until 6 hpi then remained constant up to 48 hpi (Figure 5 A). No noticeable *SBIP-470* induction was observed in 1-2 plant upon the TMV infection (Figure 5 C).

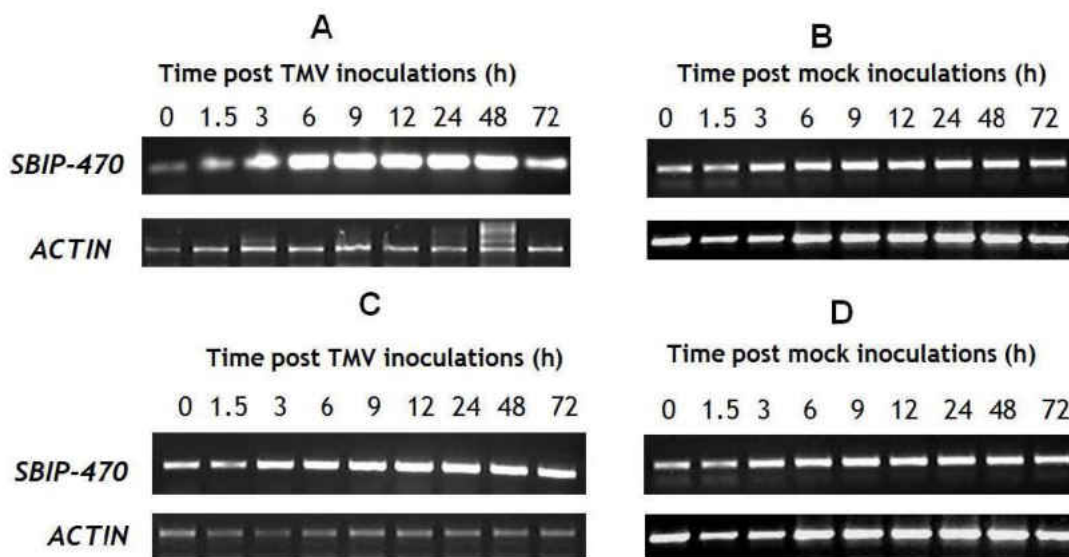


Figure 5. SBIP-470 Expression upon TMV Infection in C3 and 1-2 Plants. A. TMV infection in C3 plant. B. Mock (20 mM MgCl₂) inoculation in C3 plant. C. TMV infection in 1-2 plant. D. Mock inoculation in 1-2 plant. Total RNA was isolated from TMV infected leaves as well as mock inoculated leaves at time point mentioned above. Total cDNA was made from the total RNA. Resulting total cDNA was used as template to amplify the *SBIP-470* and *actin* where *actin* was used as an internal control.

SBIP-470 Expression upon *Pseudomonas syringae* pv. *tabaci* (*P.s. tabaci*) Infection

To determine *SBIP-470* expression upon bacterial host pathogen infection, 6- to 8-week-old C3 and 1-2 plants were infected with *P.s. tabaci*. *Actin* gene was used as internal control. *SBIP-470* gene expression was increased in C3 plant after the *P.s. tabaci* inoculation up to 6 hpi then started to decrease gradually (Figure 6 A). *SBIP-470* expression in 1-2 (SABP2 silenced

plant) plant increased after the *P.s. tabaci* inoculation then remained constant up to 12 hpi. After 12 hpi expression started to decrease (Figure 6 C).

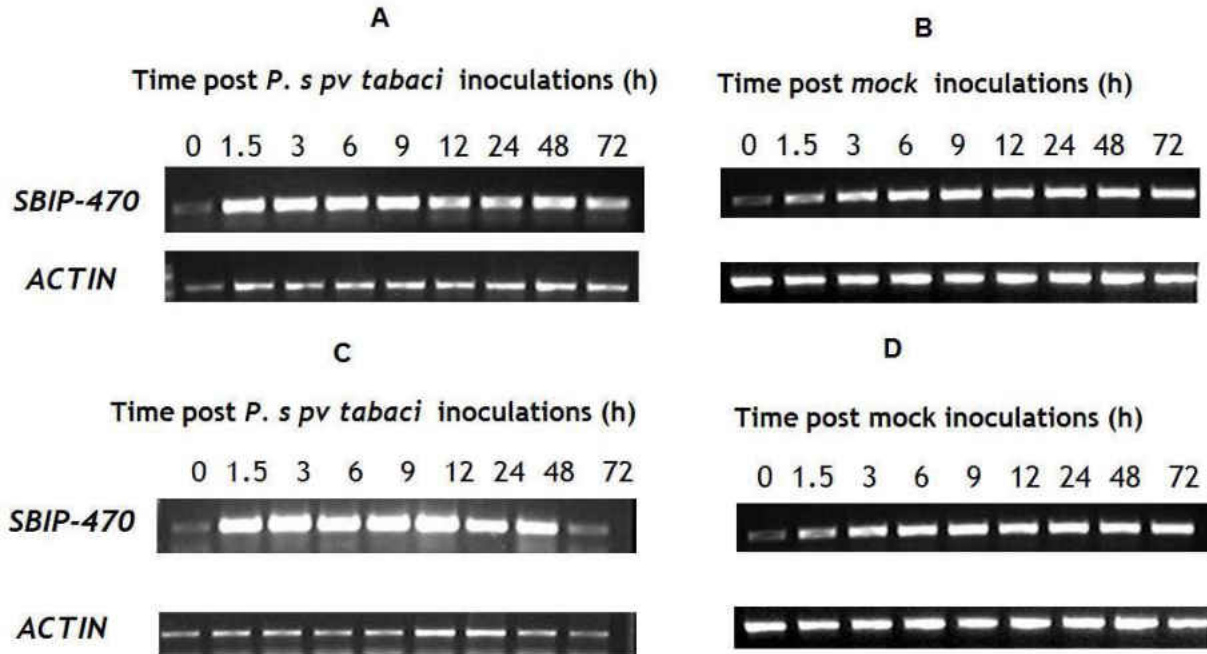


Figure 6. *SBIP-470* Gene Expression upon *P.s. tabaci* in C3 and 1-2 Plant. A. *P.s. tabaci* in C3 plant. B. Mock (20 mM $MgCl_2$) inoculation in C3. C. *P.s. tabaci* in 1-2. D. Mock inoculation in 1-2. Total RNA was isolated from *P.s. tabaci* infected leaves as well as mock inoculated leaves at time point mentioned above. Total cDNA was made from the total RNA. Resulting total cDNA was used as template to amplify the *SBIP-470* and *actin* where *actin* was used as an internal control.

SBIP-470 Expression under *Pseudomonas syringae pv. tomato DC3000 (Pst DC3000)*

To determine the *SBIP-470* expression upon the *Pseudomonas syringae pv tomato DC3000* infection, 6- to- 8-week-old C3 and 1-2 plants were infected with *Pst DC3000*. *Actin* gene was used as internal control. *SBIP-470* gene in C3 plant expression was slightly induced after the *Pst DC3000* infection until the 12 hpi then declined (Figure 7 A). *SBIP-470* expression in 1-2 plant was not observed at 0 hpi but observed at 1.5 hpi. After 1.5 hpi the expression remained constant up to 48 hpi (Figure 7 C).

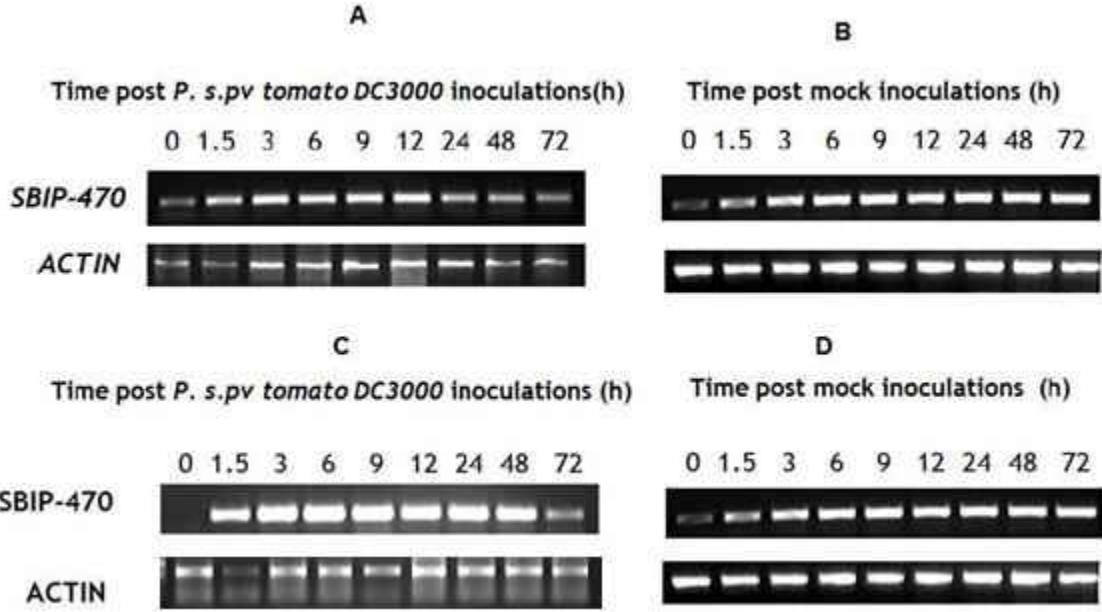


Figure 7. *SBIP-470* Gene Expression upon *Pst DC3000*. Total RNA was isolated from *Pst DC3000* infected leaves as well as mock inoculated leaves at time point mentioned above. Total cDNA was made from the total RNA. Resulting total cDNA was used as template to amplify the *SBIP-470* and *actin* where *actin* was used as an internal control.

SBIP-470 Expression under *Pseudomonas syringae pv. phaseolicola* (*P.s. pv. Phaseolicola*)

To determine the expression of *SBIP-470* during nonhost bacterial pathogen infection, 6- to 8-week-old C3 and 1-2 plants were infected with *P.s. pv. phaseolicola*. *Actin* gene was used as internal control. *SBIP-470* gene expression was almost constant in C3 plant after the *P.s. pv. phaseolicola* inoculation up to 9 hpi then decreased gradually (Figure 8 A). *SBIP-470* induced only at 9 hpi in 1-2 plant (Figure 8 C). *SBIP-470* was highly induced upon both viral as well as bacterial challenges.

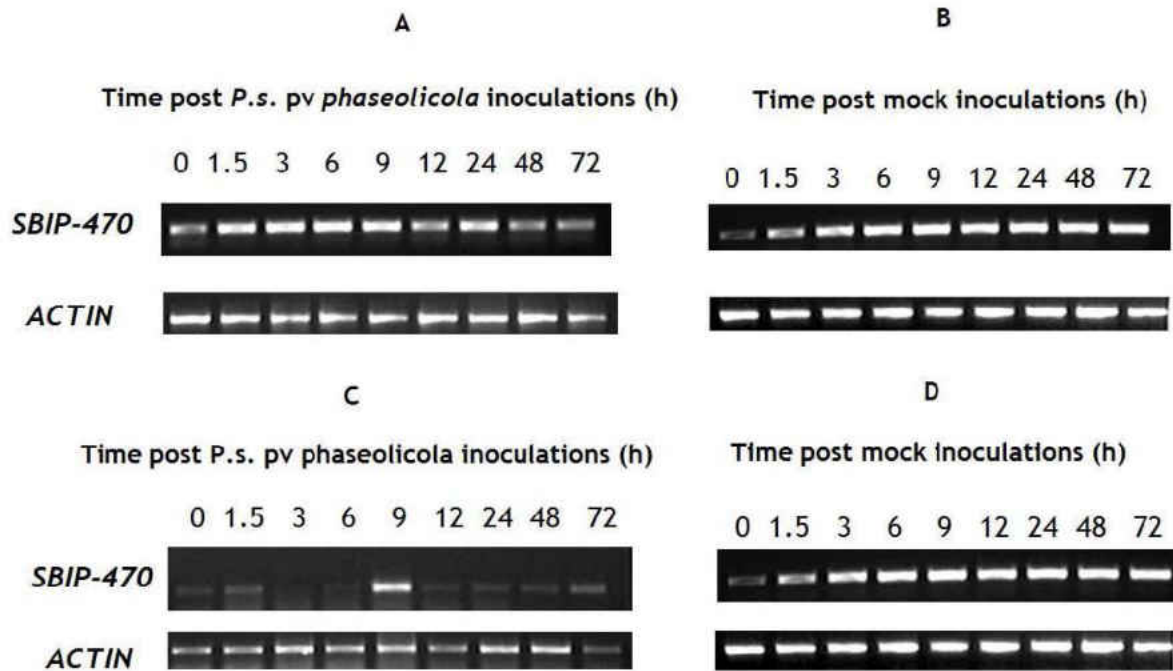


Figure 8. *SBIP-470* Gene Expression upon *P.s. pv. phaseolicola*. Total RNA was isolated from *Pst DC3000* infected leaves as well as mock inoculated leaves at time point mentioned above. Total cDNA was made from the total RNA. Resulting total cDNA was used as template to amplify the *SBIP-470* and *actin* where *actin* was used as an internal control.

Hypotheses

Hypothesis I: Tobacco SBIP-470 is a Lipid Transfer Protein

Based on *The National Center for Biotechnology Information* (NCBI) protein BLAST, SBIP-470 belongs to non-specific lipid-transfer protein type 1 (nsLTP1) subfamily. Plant nsLTP1s are small, basic, lipid binding, extracellular proteins that facilitate the transfer of fatty acids, phospholipid, glycolipid, and steroid between membranes (Cheng et al. 2004). They have important role in plant defense against pathogen (Jean and Claude Kader 1996; Maldonado et al. 2002; Chanda et al. 2011; Liu et al. 2011; Choi et al. 2014).

Bioinformatics based prediction showed SBIP-470 is a small (M.W.= 11.645 kDA) and basic (pI = 9.4) protein; it has a N-terminal signal peptide; and it likely localizes to the cell wall. nsLTPs contain an internal hydrophobic cavity that serves as lipid binding site (Jean and Claude Kader 1996; Hollenbach et al. 1997; Cameron et al. 2006; Lee et al. 2009). Feature of the hydrophobic cavity is defined by 20 amino acids that are conserved in nsLTP1 subfamily (Jean and Claude Kader 1996; Lee et al. 1998; Carvalho and Gomes 2007). Computational analysis showed the 20 conserved amino acids are also present in SBIP-470 at the similar position along the primary structure of other nsLTP1s. Tyr₇₉ is a semiconserved amino acid in nsLTP1 that is involved in hydrogen bonding to polar head group of lipid ligands (Charvolin et al. 1999). Tyr₇₉ is also present in SBIP-470. Similarly, nsLTP1s contain 8 conserved cysteine residues (Jean and Claude Kader 1996). Eight cysteine residues are engaged in disulfide bridge that stabilizes the hydrophobic cavity (Douliez et al. 2000). SBIP-470 also contains the 8 conserved cysteine residues at the similar position along the primary structure of other nsLTP1s. Previous study on gene expression of *SBIP-470* showed that its expression is induced upon viral as well as the bacterial pathogen challenge, suggesting its role in plant defense (Simo and Kumar unpublished).

Based on the bioinformatics analysis, study of similar proteins, and previous study of SBIP-470, we hypothesize that it is a lipid transfer protein.

Hypothesis II: *Arabidopsis ltp2* Mutant and *ltp12* Mutant Have Defective Growth Phenotype and are Susceptible to Pathogens

In this study SBIP470 homologs, LTP2, and LTP12 in *Arabidopsis* were studied. To assess the role of LTP2 and LTP12 in plant defense, their corresponding T-DNA insertion mutants were analyzed. LTPs have been implicated as modulators of plant vegetative growth and reproduction (Park et al. 2000; Park and Lord 2003). *LTP2* is expressed in flowering meristems, flowers, developing seeds (Clark and Bohnert 1999), and in leaves (Arondel et al. 2000). *LTP12* is highly expressed in inflorescences and also expressed in seedling and leaf at very low level (Huang et al. 2013).

Gene expression of *Arabidopsis*'s *LTP2* and *LTP12* are induced upon the bacterial pathogen challenge (Kilian et al. 2007). Both LTP2 and LTP12 are predicted as PR-14 proteins (Sels et al. 2008). Promoter region of *LTP2* contain pathogen and stress inducible motifs (Goldsbrough et al. 1993; Thoma et al. 1994). LTPs are involved in plant defense (Maldonado et al. 2002; Chanda et al. 2011; Liu et al. 2011; Choi et al. 2014). They have roles in cuticle deposition that serve as a physical barrier for pathogen entry into cells (Hollenbach et al. 1997; Cameron et al. 2006; Lee et al. 2009). Based on studies of LTP2 and LTP12, *ltp2* and *ltp12* mutants may have defective growth (vegetative and reproductive) and are susceptible to pathogens.

CHAPTER 2

MATERIALS AND METHODS

Plant Material

Arabidopsis knockout mutants i.e. CS736658 (*ltp12* mutant) and CS736752 (*ltp2* mutant) were obtained from *Arabidopsis* Biological Resource Center, OH, USA. *ltp12* mutant, *ltp2* mutant, and wild type plant (Col-0) were used for the experiment. *Arabidopsis* mutants were grown in a growth chamber (PGW 36, Conviron, Canada) at 22°C and a 16-hour light cycle at 200 $\mu\text{mol m}^{-2} \text{sec}^{-1}$ light intensity. Soil (Fafard F-15, Agawam, MA) was autoclaved for 20 minutes and put in 4 x 4 inch flats. Seeds were sown in autoclaved soil and transferred to dark room at 4°C. After 3 days of vernalization treatment, flats with seeds were transferred to the growth chamber set at 16 hours day time with 22°C temperature.

Chemicals and Reagents

Agar (Acros organics), sucrose (Bioworld), Silwet L-77, polyvinylidene fluoride (PVDF), membrane (Millipore), and ECL western blotting substrate (Thermo Scientific); Kodak developer, fixer replenisher, and toluidine blue (Sigma-Aldrich), Bradford's reagent, prestained protein marker, 10x SDS loading buffer, acrylamide, SDS dye (Bio-Rad), sodium chloride (NaCl), sodium phosphate monobasic (NaH_2PO_4), sodium phosphate dibasic (Na_2HPO_4), sodium dodecyl sulfate (SDS), β -Mercaptoethanol (β -ME), ammonium persulfate (APS), coomassie brilliant blue (R-250, G-250), ponceau-S, TRIS base, glycerol, glycine, imidazole, methanol, ethanol, tween-20, magnesium chloride (MgCl_2), tetramethylethylenediamine (TEMED), bovine serum albumen (BSA), phenylmethylsulfonyl fluoride (PMSF), chloroform, isopropanol, gellan gum, magnesium sulfate, and other chemicals were obtained from Fisher Scientific.

Other Materials

Spectrophotometer, nanodrop spectrophotometer, french press, centrifuge (Beckman, model J2-21 or Sorvall RC5B), SYNERGY HT multi-mode microplate reader (Biotek), Sonicator, AKTA purifier 10 (GE) system, One ml syringes (BD Syringes) were used.

Biochemical Characterization of SBIP-470 (Hypothesis I)

Bioinformatics Analysis

Conserved domain prediction. Translated amino acid sequence of SBIP-470 was used as a query to search for its closest relatives in *NCBI Non Redundant (NR) database* (Altschul et al. 1997). Similarly, the site was also used to find the conserved domain among the close relatives of SBIP-470.

Prediction of SBIP-470 properties. SBIP-470's properties were predicted using *ExPASy Bioinformatics research portal, ProtParam tool* (Wilkins et al. 1999).

Subcellular localization. Subcellular localization of SBIP-470 was predicted using the online software i.e. *Protein Prowler* (Bodén and Hawkins 2005) and *MultiLoc* (Höglund et al. 2006).

Signal peptide and cleavage site prediction. SBIP-470's signal peptide and signal peptide cleavage were predicted using the *Signal P* (Thomas et al. 2011). Similarly, signal peptide cleavage site of SBIP-470 similar protein was also analyzed.

3D structure prediction. The amino acid sequence of SBIP-470 in FASTA format was used to predict its 3D structure using the *Protein Structure Prediction Server of Molecular Bioinformatics Center National Chiao Tung University* (Chen et al. 2006).

Phylogenetic analysis. Full-length SBIP-470 protein sequence was used as a query to search for its similar or closest relatives in the *NCBI* (Altschul et al. 1997). Then, LTPs from tobacco, potato, *Arabidopsis*, sweet orange, and *Plasmodium* were aligned using the *Molecular Evolutionary Genetics Analysis (MEGA)* software. Finally, the aligned sequences were used to construct a phylogeny tree.

Cloning of SBIP-470 without the Signal Peptide (SBIP-470-25)

Full-length *SBIP-470* was cloned using gateway cloning to make N-terminal 6xHis tagged SBIP-470 protein. However, recombinant protein could not be expressed in soluble form. Studies have shown that the removal of a transmembrane or signal peptide helps in expression and solubility of protein (Raina and Missiakas 1997; Gopal and Kumar 2013). To increase the solubility of the protein, SBIP-470 without the signal peptide (SBIP-470-25) was cloned into pDEST17 (Gateway cloning) as well as pET28a. Then, the pDEST17-SBIP-470-25 and pET28a-SBIP-470-25 constructs were transformed to competent *E. coli* and *E. coli* BL21 cell lines respectively. Only, recombinant SBIP-470-25 (recSBIP-470-25) obtained from *E. coli* Magic cell line (with pDEST17-SBIP-470-25 construct) was expressed in soluble form. Cloning of *SBIP-470-25* using gateway cloning is explained later in this thesis.

cDNA Synthesis

To amplify *SBIP-470-25*, forward (5'GGGGACAAGTTTGTACAAAAAAGCAGGCTCACTGAGCTGCGGCCAGGTT-3') and reverse (3'GGGGACAAGTTTGTACAAAAAAGCAGGCTAGGCACTGAGCTGCGGCCAG-5') primers were used. PCR mix {(1.5 µl of 10 mM dNTP, 37.1 µl sterile distilled water, 0.4 µl Platinum Pfx DNA polymerase (1 unit), 5 µl of 10X Pfx amplification buffer, 1 µl of 50 mM MgSO₄, 1.5 µl of 10 µM forward primer, 1.5 µl of 10 µM reverse primer and 2 µl template (74.43 ng/µl)} was added to a 0.2 ml PCR tube on ice. The template used was pDONR221*SBIP-470*

construct that was already verified by sequencing. Tube contents were mixed and centrifuged briefly. The mixture was heated for 2 minutes at 94°C, then PCR cycle consisting 94°C for 30 seconds (denaturation), 50°C for 30 seconds (annealing), and 68°C for 1.5 minute (extension) was repeated 35 times. The amplified product was then stored in -20°C.

Agarose Gel Electrophoresis

Agarose gel (1.2%) was prepared. Agarose (0.6 g) was mixed with 50 ml 1x TAE buffer that was heated to dissolve the agarose. After 2-3 minutes of cooling down, 2.5 µl (10 mg/ml) of ethidium bromide was added to the solution. Then, the solution was poured onto a gel tray. A mixture (5 µl of PCR product and 1 µl of 6X DNA loading dye) was loaded in the wells of an agarose gel. 100 base pairs DNA ladder (NEB) (25 ng/ml) was also loaded. Then, the gel was run for 20 minutes at 130 volts. Finally, the gel was visualized using a UV trans-illuminator.

PCR Purification

Purification of the PCR product was carried out using the PureLink PCR Purification Kit (Invitrogen). Fifty microliter of PCR amplified product was added to 200 µl PureLink binding buffer with isopropanol and was mixed well. The mixture was then added to PureLink spin column and centrifuged at 10,000xg for 1 minute at room temperature. Flow through was discarded and spin column was placed in a collection tube. The column was washed with 650 µl of wash buffer with ethanol and centrifuged at 10,000xg for 1 minute at room temperature. Flow through from the collection tube was discarded and the column was placed into a tube. To remove any residual wash buffer, the column was centrifuged at maximum speed at room temperature for 2-3 minutes. The collection tube was discarded. The spin column was then placed in a clean 1.7 ml tube. 50 µl of elution buffer (10 mM Tris-HCL, pH 8.5) was added to the center of the column and incubated for 1 minute at room temperature. The column was centrifuged at maximum speed for 2 minutes. Eluted fraction contained the purified *SBIP-470-25*.

Quantitation of SBIP-470

Purified *SBIP-470-25* was quantified using Nanodrop following manufacturer's instructions. Nanodrop software was opened and nucleic acid module was selected. Both optical surfaces were cleaned with a kimwipe. One microliter of water was placed on the lower optical surface and then "initialize" in the Nanodrop software was selected. Two microliter of elution buffer were loaded as a blank. Two microliter of purified *SBIP-470-25* were loaded as a sample and then concentration was measured.

Agarose Gel Electrophoresis

Agarose gel electrophoresis of purified *SBIP-470-25* was carried as previously mentioned.

BP Recombination Reaction

BP recombination reaction was carried out following the manufacturer's instructions (Invitrogen). PCR product equivalent to ng 50 femtomoles (fmol) was calculated using formula $\{\text{ng} = (\text{fmol}) (\# \text{ of DNA bp}) (660 \text{ fg/fmol}) (1\text{ng}/10^6 \text{ fg})\}$. About 0.9 μl of purified *SBIP-470-25* (12.3 ng/ μl), 1 μl pDONR222 vector (150 ng/ μl), 6.101 μl of TE buffer pH 8.0 was added to a 1.5 μl micro centrifuge tube at room temperature and mixed well. BP Clonase II enzyme was removed from -20°C and thawed on ice for approximately 2 minutes. The enzyme was mixed briefly twice by vortexing. One microliter of the enzyme was added to the samples and mixed well by vortexing. The mixture was incubated for 1 hour at 25°C. After 1 hour of incubation, 1 μl of Proteinase K solution was added to each reaction and incubated for 10 minutes at 37°C.

Transformation to Competent *E. coli* Cells

One vial of one shot chemically competent cells (*E. coli* Topo10) was thawed on ice. One microliter of the BP recombination reaction was added into a vial of one shot chemically competent cells and mixed gently. The vial was incubated on ice for 30 minutes and heat shocked

for 30 seconds at 42°C. Then, the vial was placed on ice for 2 minutes. Two hundred fifty microliter of Super Optimal broth with Catabolite repression (SOC) medium was added to the vial under the hood. The vial was then incubated in a shaker at 37°C, 250 rpm for 1 hour. Twenty microliter of the transformation mix was added to 180 µl of LB medium. Then, 20 µl and 100 µl were plated on LB plates containing 50 µg/ml of kanamycin. The plates were incubated overnight at 37°C.

Plasmid Isolation

The transformed plasmid (pDONR221-*SBIP-470-25*) was isolated and purified using the QIAprep Spin MiniPrep Kit (Qiagen). Three milliliter of bacterial culture was grown at 37°C and 250 rpm overnight in 3 ml LB medium containing 50 µg/ml kanamycin. One milliliter culture was placed in 1.5 ml tube and then centrifuged at 8,000 rpm for 3 minutes at room temperature. Pellet was collected and suspended in 250 µl of buffer P1. 250 µl of buffer P2 was added and mixed by inverting 4-6 times. Three hundred fifty microliter of buffer N3 was added and mixed immediately by inverting 4-6 times then centrifuged for 10 minutes at 13,000 rpm at room temperature. Supernatant was applied to the QIAprep spin column then centrifuged for 1 minute. Flow through was discarded. Spin column was washed with 0.75 ml buffer PE. Column was centrifuged for 1 minute, then flow through was discarded. Again, column was centrifuged for additional 1 minute. The column was added to a clean 1.5 ml tube Fifty microliter of buffer EB was added to column, incubated for 1 minute, and centrifuged for 1 minute. Again, 50 µl of buffer EB was added to column, incubated for 1 minute, and centrifuged for 1 minute. Purified plasmid DNA was quantified and also analyzed by 0.8% agarose gel electrophoresis as mentioned before.

Sequencing

Ten microliter of purified plasmid DNA (~500 ng) in PCR tube was sent to DNA Analysis Facility at Yale University for sequencing. The Sanger Sequencing method was used for

sequencing the pDONR221-*SBIP-470-25* construct. M13 forward and reverse primers were used to sequence the construct.

LR Recombination Reaction

LR recombination reaction was carried out as described by the manufacturer (Invitrogen). One micro liter of pDONR222-*SBIP-470-25* DNA construct (or entry clone) (60 ng/μl), 1 μl pDEST17 vector (150 ng/μl), and 5.5 μl TE buffer pH 8.0 were added to a 1.5 μl micro centrifuge tube at room temperature and mixed well. LR Clonase enzyme was removed from -20°C and thawed on ice for about 2 minutes. One microliter of the enzyme was added to the samples and mixed well by vortexing. The mixture was incubated at 25°C for 1 hour. After 1 hour of incubation, 1 μl of Proteinase K solution was added to the reaction and incubated at 37°C for 10 minutes.

Transformation of Competent *E. coli* (DH5α)

One hundred microliter of chemically competent cells (*E. coli* DH5α) in micro centrifuge tube were thawed on ice. One microliter of LR recombination reaction was added into micro centrifuge tube and mixed gently. The tube was incubated on ice for 30 minutes and heat shocked for 30 seconds at 42°C. Then, the tube was placed on ice for 2 minutes. Nine hundred microliter of LB medium was added to the vial under the hood. The tube was then shaken horizontally at 37°C for 1 hour. Then, 100 μl and 200 μl of the culture were spread on plates containing 10 μg/ml of kanamycin and 100 μg/ml of ampicillin. The plates were incubated at 37°C overnight.

Plasmid Isolation

Transformed plasmid from *E. coli* DH5α cell was isolated and purified using QIAprep Spin MiniPrep Kit as mentioned before. Purified plasmid DNA was quantified and also ran on 0.8%

agarose gel as mentioned before. Then, purified plasmid DNA was transformed to the *E. coli* magic cell line.

Transformation of Competent *E. coli* Magic Cell (BL21De3)

One hundred microliter of chemically competent cells (*E. coli* magic cell) in the micro centrifuge tube were thawed on ice. One microliter of pDEST17-SBIP-470-25 construct (12.3 ng/ μ l) was added and mixed gently. The tube was incubated on ice for 30 minutes and heat shocked at 42°C for 30 seconds. Then, the tube was placed on ice for 2 minutes. LB medium (900 μ l) was added to the tube. The tube was shaken at 37°C for 1 hour. Then, 100 μ l and 200 μ l of the culture were spread on LB plates containing 10 μ g/ml of kanamycin and 100 μ g/ml of ampicillin. The plates were incubated at 37°C overnight.

Expression of Recombinant SBIP-470 in *E. coli*

An overnight culture from a single colony was grown at 37°C in 1 ml LB media containing 100 μ g/ml ampicillin and 10 μ g/ml kanamycin. Overnight culture was diluted 100 times into fresh LB media containing 100 μ g/ml ampicillin and 10 μ g/ml kanamycin then incubated at 37°C until the $OD_{600} = 0.6$ (OD = optical density). The protein expression was induced by adding 10 μ M Isopropyl β -D-1-Thiogalactopyranoside (IPTG) to the bacterial culture as a final concentration and then was incubated at 17°C overnight in a shaker. Bacterial pellet was collected by centrifugation at 13,000 rpm for 3 minutes at room temperature. Pellet was then suspended into 2X SDS dye. Expression of recSBIP-470-25 was confirmed by Sodium Dodecyl Sulfate Polyacrylamide Gel Electrophoresis (SDS-PAGE), and western blotting using monoclonal anti-polyHistidine antibody (Sigma).

Solubility Test of Recombinant SBIP-470 in *E. coli*

An overnight culture from a single colony was grown at 37°C in 1 ml LB media containing 100 µg/ml ampicillin and 10 µg/ml kanamycin. The overnight culture was diluted 100 times into fresh LB media containing 100 µg/ml ampicillin and 10 µg/ml kanamycin and then was incubated at 37°C until the OD₆₀₀ = 0.6 (OD = Optical Density). The protein expression was induced by adding 10 µM IPTG and 100 µM IPTG to the bacterial culture as a final concentration and then incubated at 17°C overnight in a shaker. Similarly, the protein expression was induced by adding 10 µM IPTG and 100 µM IPTG to the bacterial culture as final concentration and then incubated at 37°C for 3 hours in a shaker. Bacterial pellet was collected by centrifugation at 13,000 rpm for 3 minutes at room temperature. The pellet was suspended into 1X Ni-NTA binding buffer (50 mM sodium phosphate monobasic, 300 mM sodium chloride, 10 mM imidazole, pH 8.0). Bacterial cells were broken by sonication with 20% amplitude for 15 seconds. Process was repeated 3 times. The supernatant (soluble) and pellet (insoluble) were separated by centrifugation at 13,000 rpm for 15 minutes in 4°C. The pellet was resuspended in 1X Ni-NTA binding buffer. Proteins from both soluble and insoluble fractions were run on SDS gel and western blotting was performed to determine the solubility of recSBIP-470-25.

Purification of Recombinant SBIP-470

Ni-NTA column chromatography. An overnight culture from a single colony was grown at 37°C in 5 ml LB media containing 100 µg/ml ampicillin and 10 µg/ml kanamycin. Then, the overnight culture was diluted 100 times into fresh LB media containing 100 µg/ml ampicillin and 10 µg/ml kanamycin and then incubated at 37°C until the OD₆₀₀ = 0.6. The bacterial culture was induced with 10 µM IPTG as a final concentration and then incubated at 17°C overnight in a shaker. Bacterial pellet was collected by centrifugation at 8,000 rpm for 15 minutes at 4°C and

then resuspended in 1X Ni-NTA buffer. Protease Inhibitor (PI) (10 µl/ml) was added to the suspended bacterial pellet. Bacterial cells were lysed with a French press (Thermo Electron Corporation; cell type 20 K) and the soluble fraction (supernatant) was collected by centrifugation at 13,000 rpm for 15 minutes at 4°C. The soluble fraction was then incubated with 1x Ni-NTA resin (Qiagen) at 4°C overnight. The unbound proteins were removed by washing with washing buffer containing 10 mM Imidazole in 1x Ni-NTA buffer. The bound recSBIP-470-25 was then eluted with elution buffer containing 250 mM Imidazole in 1x Ni-NTA buffer at room temperature. Presence of recSBIP-470-25 was confirmed by western blotting using monoclonal anti-polyHistidine antibody.

Q-Sepharose column chromatography. RecSBIP-470-25 purified by Ni-NTA column chromatography was further purified by anion exchange column chromatography. Purified fractions from Ni-NTA chromatography containing SBIP470 were collected and desalted against 50 mM Tris-Cl, pH 8. The desalted fractions containing protein were applied to a Q Sepharose column pre-equilibrated with buffer (50 mM Tris-Cl, pH 8). The bound protein was eluted with linear gradient of 1M NaCl in 50 mM Tris-Cl, pH 8. The presence of recSBIP470-25 was confirmed by western blotting using monoclonal anti-polyHistidine antibody.

Ni-NTA column chromatography. The protein fractions containing recSBIP-470-25 were further purified using Ni-NTA column chromatography. The protein fractions from Q-sepharose chromatography were mixed and incubated with 1x Ni-NTA resin overnight at 4°C. The unbound proteins were removed by washing with washing buffer (10 mM imidazole in 1x Ni-NTA buffer). The bound SBIP-470 was then step eluted with elution buffer containing various concentrations (50, 100, 150, and 250 mM) of an imidazole in 1x Ni-NTA buffer at room temperature. Presence of recSBIP-470-25 was confirmed by western blotting.

SDS PAGE

Each protein samples was mixed with 6X SDS sample buffer containing β -Mercaptoethanol (β -ME) and was boiled for 4 minutes, and centrifuged at 13,000 rpm for 1 minute at room temperature. The SDS-PAGE was run at 20 mA constant current for ~55 minutes. The buffers were prepared as mentioned in Appendix B.

Western Blot Analysis

Western blot analysis was performed using a standard protocol after the protein from SDS gel was transferred to the PVDF membrane. The PVDF membrane was first soaked in 100% methanol for 15 seconds and was then rinsed with deionized water for 2 minutes followed by 1x transfer buffer (Appendix B) for 10-15 minutes. Then, the SDS gel and PVDF membrane were sandwiched between the sponge and 3mm Whatman papers. Protein transfer was carried at ~94V for 1 hour at 4°C. The PVDF membrane following the proteins transfer was taken out and soaked in 100% methanol for 10 seconds and then allowed to air dry. Once the membrane was dried, it was again soaked in 100% methanol for 10 seconds. The membrane was stained with ponceau S (0.1% ponceau S and 5% acetic acid) for 2 minutes and was subsequently rinsed with deionized water. To verify the protein transfer and equal loading, a picture was taken for record. The membrane was washed with 1X PBS. The membrane was then incubated with monoclonal anti-polyHistidine antibody (1:3,000) in 5 ml of blocking buffer (1% dry milk, 3% BSA in 1X PBS) at 4°C on a platform shaker for overnight. Next morning, the membrane was washed 3 times for 5 minutes each with 1x PBS first, then with 1x PBS containing 3% tween 20, and finally rinsed with 1x PBS. The membrane was incubated in anti-mouse IgG peroxidase conjugate (1:10,000 in 5 ml of blocking buffer) at room temperature for 1 hour on a shaker. Membrane was subjected to washing as described above. The membrane was incubated in the ECL substrate (Thermo

Scientific) as described by the manufacturer. The signal on the membrane was captured on X-ray film.

Dialysis of recSBIP-470

Recombinant SBIP-470-25 purified using Ni-NTA column chromatography was pooled (~4 ml) and dialyzed (Molecular weight cutoffs = 100-3000 Da) against 1X PBS buffer at 4°C with gentle stirring. The buffer was changed at least 2 times. Finally, dialyzed samples were collected and stored at 4°C. Then, the dialyzed protein was used for in vitro lipid binding assay. To use for in vitro lipid transfer assay, recSBIP-470-25 purified using Ni-NTA column chromatography was pooled (3.5 ml) and then dialyzed against the PLTP buffer (Appendix B) as described above.

Quantification of recSBIP-470

Pierce BCA Protein Assay Kit (Thermo Scientific) was used to quantify the dialyzed recSBIP-470-25. Recombinant SBIP-470-25 was quantified following the manufacture's instruction. Ten microliter of dialyzed recSBIP-470-25 and Bovine Serum Albumin (BSA) with various concentrations (2,000 µg/ml, 1,500 µg/ml, 1,000 µg/ml, 750 µg/ml, 500 µg/ml, 250 µg/ml, 125 µg/ml, 25 µg/ml, and 0 µg/ml) were added into microplate wells. Same amount of sample and individual standard were also added into microplate wells as a replicate. BSA was used as a standard. Two hundred microliter of working solution (50 parts of BCA reagent A with 1 part of BCA reagent B) was added to each well and then mixed thoroughly on a plate shaker for 30 seconds. The plate was covered and incubated at 37°C for 30 minutes. The plate was cooled and then absorbance was measured at 562 nm on a SYNERGY HT Multi-Mode Microplate Reader. The average absorbance of the blank standard was subtracted from all other samples and individual standard replicates. The standard curve was prepared by plotting the average blank corrected absorbance of each BSA standard to the concentration (µg/ml). The standard curve was used to determine the concentration of sample (recSBIP-470-25).

Biochemical Characterization

In Vitro Lipid Binding Assay

In vitro lipid binding assay was performed using the PIP Strip membrane (Echelon Biosciences Inc.) following the manufacturer's instructions. The PIP Strip is a nitrocellulose membrane that has several phospholipids spotted on it. Two different PIP Strip membranes were used i.e. PIP Strips (Catalog # P-6001) and PIP Strips (Catalog # P-6002). Each strip has 15 different phospholipids (Table 1). Each strip was covered with 5 ml of blocking buffer {PBS-T (0.1% V/V Tween-20) + 3% BSA} and gently shaken at 4°C overnight. The blocking buffer was discarded and then recSBIP-470-25 (18.75 µg/ml) in blocking buffer was added to the strips. The strips were then incubated for 1 hr at room temperature with gentle shaking.

Table 1

Various Phospholipids Spotted on PIP Strip

	Nomenclature	Phospholipid
1	Lysophosphatidic acid (LPA)	Triglyceride
2	Lysophosphocholine (LPC)	Phosphatidylinositol (PtdIns)
3	Phosphatidylinositol (PtdIns)	Phosphatidylinositol (4)-phosphate (PtdIns(4)P)
4	Phosphatidylinositol (3) phosphate (PtdIns(3)P)	Phosphatidylinositol (4,5)-bisphosphate (PtdIns(4,5)P ₂)
5	Phosphatidylinositol (4) phosphate (PtdIns (4)P)	Phosphatidylinositol (3,4,5)-trisphosphate (PtdIns(3,4,5)P ₃)
6	Phosphatidylinositol (5) phosphate (PtdIns(5)P)	Phosphatidylserine (PS)
7	Phosphatidylethanolamine (PE)	Phosphatidylethanolamine (PE)
8	Phosphatidylcholine (PC)	Phosphatidic acid (PA)
9	Sphingosine 1-Phosphate (S1P)	Diacylglycerol (DAG)
10	Phosphatidylinositol (3,4) bisphosphate (PtdIns(3,4)P ₂)	Cholesterol
11	Phosphatidylinositol (3,5) bisphosphate (PtdIns(3,5)P ₂)	Phosphatidylcholine (PC)
12	Phosphatidylinositol (4,5) bisphosphate (PtdIns(4,5)P ₂)	Sphingomyelin
13	Phosphatidylinositol (3,4,5) trisphosphate (PtdIns(3,4,5)P ₃)	Phosphatidylglycerol (PG)
14	Phosphatidic acid (PA)	3-sulfogalactosylceramide (Sulfatide)
15	Phosphatidylserine (PS)	Cardiolipin

The protein solution was discarded and the strips were washed with 5 ml PBS-T 3 times with gentle shaking for 6 minutes each. The wash solution was discarded and then the strips were incubated with monoclonal anti-polyHistidine antibody (diluted 1:3,000 in blocking buffer). The strips were then incubated for 1 hr at room temperature with gentle shaking. The strips were washed again with 5 ml PBS-T 3 times with gentle shaking for 6 minutes each. The wash solution was discarded and then the strips were covered with anti-mouse IgG (diluted 1:10,000 in blocking buffer). The strips were incubated for 1 hour at room temperature with gentle shaking. The strips were washed again 3 times with 5 ml PBS-T with gentle shaking for 6 minutes each. The signal on the strips was developed on X-ray film using Pierce ECL reagent (Thermo Scientific) as described by the company. To check the sensitivity of experimental procedure, 10 μ l (18.75 μ g/ml) recSBIP-470-25 and BSA were spotted on nitrocellulose membrane and allowed to dry for 15 minutes. Then, the same steps as mentioned above were followed.

In Vitro Lipid Transfer Assay

In vitro lipid transfer assay was performed using Phospholipid Transfer Protein (PLTP) Activity Assay kits. Kits were obtained from Roar Biomedical (New York, NY, USA). The assay was performed following the manufacturer's instruction. Recombinant SBIP-470-25 in 1X PLTP buffer was used for the assay. The buffer and acceptor were chilled on ice and the donor was stored at room temperature. A microplate was chilled on ice and the components (Table 2) were added while chilling. The components were mixed by aspiration with the pipette and then incubated at 37°C for 3 hours. Florescence reading was taken at excitation wavelength 485 nm (Ex 485nm) and emission wavelength 528 nm (Em 528 nm) every 10 minutes.

Table 2

PLTP Activity Assay Kit Work Flow

	Donor	Acceptor	SBIP-470	Buffer	Total
1	4 μ l	4 μ l	10 μ l	182 μ l	200 μ l
2	4 μ l	4 μ l	20 μ l	172 μ l	200 μ l
3	4 μ l	4 μ l	40 μ l	152 μ l	200 μ l
4	4 μ l	4 μ l	0 μ l	192 μ l	200 μ l

Characterization of *Arabidopsis* Mutants (Hypothesis II)*Arabidopsis* Mutant Screening

Leaf samples (~4 mg) were collected in a 1.5 ml micro-centrifuge tubes and homogenized in 200 μ l of extraction buffer {10 times diluted Edward solution (200mM Tris-CL pH 7.5, 250mM NaCl, 25mM EDTA, 0.5% SDS) in TE buffer pH 8}. Homogenized samples were then centrifuged at 14,000 rpm for 5 minutes. Supernatant was collected and 1 μ l supernatant used for PCR (20 μ l) to confirm the T-DNA insertions. *Arabidopsis* knockout mutants i.e. CS736658 (*ltp12 mutant*) and CS486424 (*ltp2 mutant*) were obtained from Arabidopsis Biological Resource Center. CS736658 and CS486424 have a T-DNA insertion in intron of *LTP12* and exon of *LTP2* gene respectively. Homozygous T-DNA insertion mutants were obtained by screening using PCR using a T-DNA left border primer and gene specific primer. To screen the *ltp12*, gene specific primer (DK462: 5'-TTAGTTTCTTTTCAATCGCCG-3') and T-DNA left border prime (DK463: 3'-ATAATAACG CTGCGGACATCTACATTTT-5') were used. To screen the *ltp2*, gene specific

primer (DK470: 5'-TCTCCAAATGTTTGTTC AAGC-3') and T-DNA left border primer (DK463: 3'-ATAATAACGCTGCGGACATCTACATTTT-5') were used.

Mutant screening using cDNA. Leaves from Col-0, *ltp12* and *ltp12* mutant were collected. One microliter of TRI reagent (Sigma) was added to powdered leaf samples using liquid nitrogen and incubated at room temperature for 5 minutes. Then, 200 μ l of chloroform was added and mixed by inverting 2-3 times (~15 seconds) then incubated at room temperature for 2-3 minutes. Samples were centrifuged at 12,000x g for 15 minutes at 4°C. Supernatant was collected and then transferred to new tubes. After transferring the supernatant, 0.5 ml of isopropanol was added to the tubes then incubated at 15-30°C for 10 minutes. After 10 minutes of incubation, samples were again centrifuged at 12,000x g for 10 minutes at 4°C and the pellet was collected. One milliliter of cold 75% ethanol was added to the pellet and mixed. Again, the samples were centrifuged at 7,500x g for 5 minutes at 4°C. Resulting pellet was air dried for 10-20 minutes then suspended in 43 μ l depc treated water (Appendix B). Five microliter of 10X DNase buffer and 2 μ l of DNase were added to the resuspended samples that were then incubated at 37°C for 20 minutes.

The same steps mentioned above were repeated with half the amount of chemicals until resuspending pellet in 23 μ l depc treated water. Samples were heated for 10 minutes at 55-60°C. Finally, the RNA concentration (ng/ μ l) was measured by Nanodrop spectrophotometer at 260 nm.

Reverse transcriptase (RT)-PCR. To make first stranded cDNA, MMLV reverse transcriptase and oligo dT18 were used following manufacturer's instructions. Two microliter of oligo-dT18 (0.5 μ g/ μ l) was added to 8 μ l (1 μ g) of RNA in PCR tubes then incubated at 75°C for 10 minutes in a thermocycler. A mix (1 μ l of reverse transcriptase, 1 μ l of RNAsin, 4 μ l of 5X reverse transcriptase buffer, 1 μ l of 10 mM dNTP mix, and 3 μ l of depc treated water) was added to 10 μ l of oligo dT-RNA mix in PCR tubes. After brief mixing the tubes were incubated at 42°C

for 60 minutes and then at 70°C for 10 minutes in a thermocycler. The newly synthesized cDNA was stored in -20°C until used.

cDNA synthesis. Total RNA was prepared from leaves of *Arabidopsis* plants (*ltp12* mutant, *ltp2* mutant, and Col-0). Then, first stranded cDNA was synthesized as mentioned above. Gene specific primers were used to determine the loss of transcription. The loss of *LTP12* transcription was determined by RT-PCR using forward (DK461: 5'-ATGGCGTTTACTCCGAAG-3') and reverse (DK462: 3'-TCACACGGCAGTCGATAT-5') primers. Similarly, the loss of *LTP2* transcription was determined by RT-PCR using forward (DK469: 5'-GTCTTGGCTTGCATGATTG-3') and reverse (DK470: 3'-GTTGTACTGGCCATGTTTTT-5') primers.

PCR mix (1µl 10x dNTP, 6 µl sterile water, 0.2 µl Taq DNA polymerase, 1µl Taq DNA polymerase buffer, 0.4 µl 10 µM forward primer, 0.4 µl 10 µM reverse primer, and 1µl cDNA) was made and mixed by vortexing. Then, the PCR mix was incubated in a thermo cycler. The mixture was heated for 2 minutes at 94°C, then a cycle consisting 94°C for 30 seconds (denaturation), 55°C for 30 seconds (annealing), and 72°C for 30 seconds (extension) was repeated 35 times for *LTP12* and *LTP2* and *EF1-α*. The amplified product was then stored in -20°C until analysis by agarose gel electrophoresis (as described earlier).

Phenotype Analysis

Mutant *ltp12*, *ltp2*, and Col-0 seeds were sown in autoclaved soil. After 3 days of vernalization treatment, flats with seeds were transferred to a growth chamber. The plants were monitored visually after 1, 2, 3, 4, and 5 weeks. The plants were fertilized with a liquid fertilizer (nitrogen-phosphate-potassium fertilizer). The flowering, siliques formation times, and overall height were recorded. The overall height of plants was measured at 15, 22, 30, and 39 days after germination (DAG). Photographs of growing seedlings were taken to record any differences.

Toluidine Blue (TB) Test

The TB test was carried out as described by Tanka et al. (2004). Mutants *ltp12*, *ltp2* mutant and Col-0 seeds were incubated in 70% ethanol for 5 minutes followed by 20% (v/v) commercial bleach containing 0.1% tween 20. After 5 minutes of incubation the seeds were washed with sterile water for 5-6 times. Then, the seeds were sown on plates of Murashige and Skoog's medium solidified with 0.4% (w/v) gellan gum (Fisher Scientific). Plants were transferred to a growth chamber (22°C, continuous light) after 3 days of vernalization treatment. An aqueous solution of 0.05 % (w/v) toluidine blue (TB) (Sigma-Aldrich) was filtered using a 0.2 µm filter. The aqueous solution was poured onto the plates that had plants until the plants were completely submerged. The TB solution was removed after 10 minutes and plants were washed with sterile water.

Pathogen Growth Assay

To determine the pathogen growth in mutant plants, seedling flood-inoculation method was performed as described by Ishiga et al. (2011). *Pseudomonas syringae* pv. *tomato* DC3000 (*Pst* DC3000) and *Pseudomonas syringae* pv. *tomato* DC3000 *AvrRpt2* (*Pst* DC3000 *AvrRpt2*) were made in sterile 0.025% Silwet L-77. The diluted bacterial suspension (5×10^6 cfu/ml) was added to the 2-week-old plants on plates. After 3 minutes of incubation at room temperature, the

bacterial suspension was decanted and the plates were sealed with surgical micropore tape. Then, the plates were incubated at 24°C with 150-200 $\mu\text{E m}^{-2}\text{sec}^{-1}$ light intensity and a 12-hour dark/light period. In each experiment 2 independent set of plants were used. The leaves from the inoculated seedling were collected and the weight of the leaves was measured. The leaves were surface sterilized by 3% H_2O_2 (1 ml) for 3 minutes and then washed 3 times with sterile water (1 ml). The leaves (~12.5 mg) were then homogenized in 200 μl of sterile water. The leaves were then ground using the Fastprep-24 3 times with 5 minutes of interval. Ground samples were then diluted in sterile water. The diluted samples (20 μl) were then plated on Kings B media containing 20 $\mu\text{g/ml}$ of rifampicin and 25 $\mu\text{l/ml}$ of kanamycin as a final concentration. Bacterial colony forming units (cfu) were counted. The cfu was normalized based on the total weight of leaves used. The bacterial growth was evaluated in 2 independent experiments.

CHAPTER 3

RESULTS

Biochemical Characterization of SBIP-470 (Hypothesis I)

Computational Analysis of SBIP-470

Yeast two-hybrid screening using SABP2 as bait and tobacco leaf proteins as prey has resulted in identification of several interacting proteins including SBIP-470. SBIP-470 DNA was sent for sequencing. DNA sequence (Figure 9) was then translated to corresponding amino acid sequence (Figure 10) using *ExPASy Bioinformatics Research Portal*.

```
5' ATGGAAATGGTTGGCAAGATTGCGTGCTTTGTGTTACTTTGCATGGTGGTGGTTG  
CACCCCATGCAGAGGCACTGAGCTGCGGCCAGGTTTCAGTCTGGCCTGGCTCTTTGCC  
TCCCTTATCTGCAGAGTCGCGGCCCTCTAGGGAGGTGTTGTGGCGGCGTTAAAGGTG  
TGTTGGGTGCTGCCCCGACCCAGCTGACCGCAAGACTGCATGCACTTGCCTGAAAT  
CAGCTGCTTATGCTATTAAGGGTATTAATATGGGCAAAGCCGCTGGACTTCCTAGTG  
CTTGTGGCGTTAACATTCCCTACAAGATCAGTCCCTCTACTGACTGCTCCAGGGTCC  
AGTGA 3'
```

Figure 9. SBIP-470 DNA Sequence (345 Bases) Obtained from Y2H Screening.

```
MEMVGKIACFVLLCMVVVAPHAELSCGQVQSGLALCLPYLQSRGPLGRCCGGVK  
GVLGAARTPADRKTACTCLKSAAYAIAKGINMGKAAGLPSACGVNIPYKISPSTDC  
SRVQ
```

Figure 10. SBIP-470 Amino Acid Sequence (114 aa) Translated from Nucleotide Sequence by ExPASy Bioinformatics Research Portal.

Predicted Properties of SBIP-470

SBIP-470's properties were predicted using *ExPASy Bioinformatics Research Portal*, ProtParam (Table 3).

Table 3

Predicted Properties of SBIP-470

Categories	Predicted Values	Remarks
Molecular weight	11645.9 Dalton	
Extinction coefficients	5095 M ⁻¹ cm ⁻¹ measured at 280 nm in water	Assuming all pair of cysteine forms cysteine's
Extinction coefficients	4470 M ⁻¹ cm ⁻¹ measured at 280 nm in water	Assuming all cysteine are reduced
Theoretical pI	9.14	

Conserved Domain

SBIP-470 amino acid sequence was used as query to determine the presence of conserved domain using *NCBI Non Redundant (NR) Database*. SBIP-470 was predicted to be a member of nsLTP1 subfamily (Figure 11). A hydrophobic cavity is present in nsLTP1 subfamily, which is defined by 20 conserved amino acids. These amino acids also present in SBIP-470 are Valine 30, Leucine 34, Leucine 41, Valine 54, Valine 57, Leucine 58, Arginine 62, Alanine 65, Cysteine 73, Leucine 74, Alanine 77, Alanine 89, Leucine 92, Proline 93, Isoleucine 100, Proline 101, Tyrosine 102, Isoleucine 104, and Serine 105 (Figure 12).

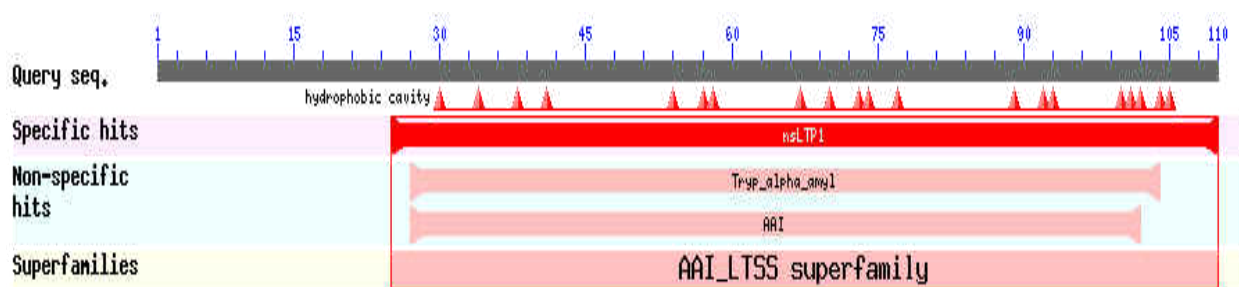


Figure 11. Result Showing Protein BLAST of SBIP-470

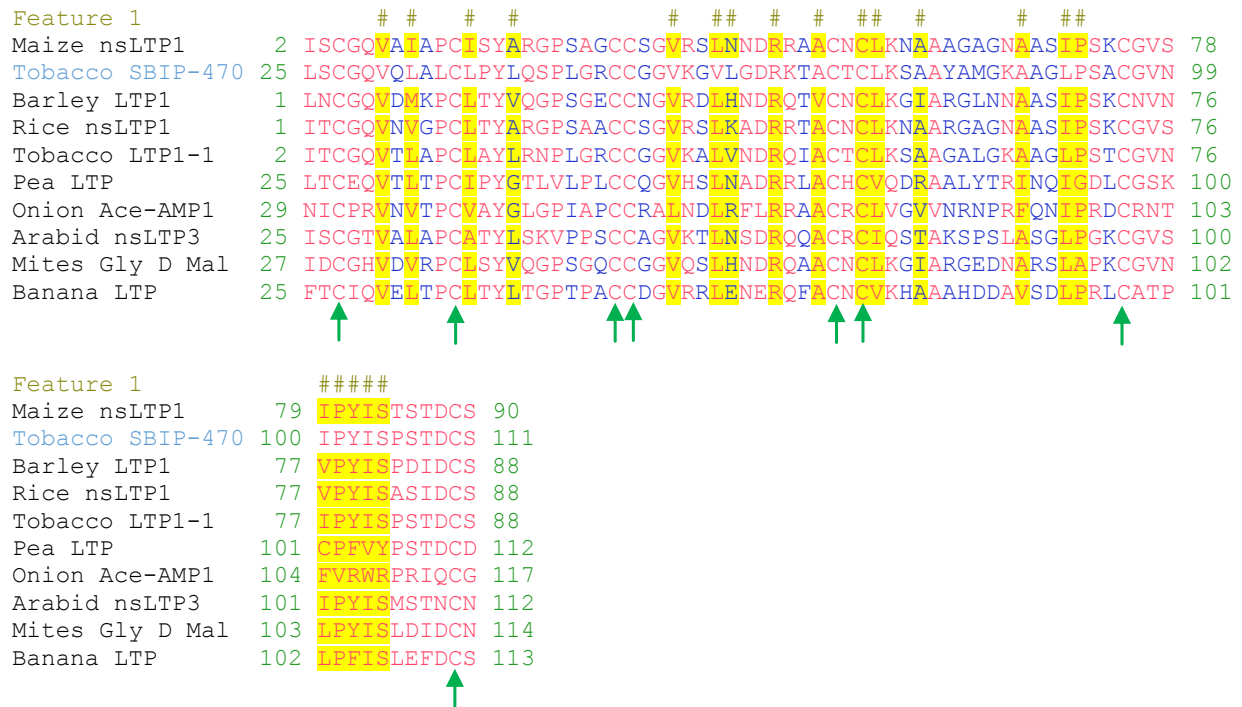


Figure 12. Conserved Domain of nsLTP1. The highly conserved amino acid is shown in red and the least conserved amino acid is shown in blue. Eight conserved cysteine (C) residues are shown with arrows. 20 conserved amino acids indicated with hash marks (#) define the hydrophobic feature of hydrophobic cavity. Name of protein and data base accession numbers are shown as follows: maize nsLTP1 (1MZM), barley LTP1 (1JTB), rice nsLTP1 (1UVB_A), tobacco LTP1-1 (1T12_A), pea LTP precursor (gi 7381207), onion Ace-AMP1 (gi 2497758), *Arabidopsis* nsLTP3 (gi 18424225), mites Gly d Mal d 3-like protein (gi 33772604), and banana LTP (gi 102139791).

Subcellular Localization

Online prediction software such as *Protein Prowler* and *MultiLoc* were used to predict subcellular localization of SBIP-470. The *Protein Prowler* predicted that SBIP-470 likely enters the secretory pathway (Figure 13). *MultiLoc* calculates scores for each predictable location were based on amino acid composition. For instance, nuclear protein tends to get a positive nuclear output score and a negative score otherwise (Höglund et al. 2006). *MultiLoc* predicted 3 possible places for localization such as extracellular (most probable), vacuole (second most probable), and endoplasmic reticulum (least probable) (Table 4). Among them, scores for extracellular location are highest, which indicates that SBIP-470 is an extracellular protein (Table 4).

Sequence	PProwler				PTS1Prowler
	SP	MTP	CTP	OTHER	Peroxisome
SBIP-470	1.00	0.00	0.00	0.00	0.00

Figure 13. Subcellular Localization of SBIP-470. SBIP-470 is predicted to enter secretory pathway after its synthesis.

Table 4

Subcellular Localization of SBIP-470

Rank	Location	Score
1	extracellular	0.99
2	Vacuolar	0.01
3	ER	0.00

Signal Peptide Cleavage Site

Signal peptide cleavage site of SBIP-470 was predicted using *SignalP* online software. The predicted signal peptide cleavage site of SBIP-470 is between 24th and 25th amino acids (Figure 14). To cleavage signal peptide by a protease the amino acid residues at -3 and -1 relative to signal peptide cleavage site must be small and uncharged (so they can fit into protease pocket), and large amino acid might be at -2 position (Von, 1985). SBIP-470 also has small and uncharged (i.e. Alanine) at both -3 and -1 positions, and large amino acid (i.e. Glutamic acid) at position -2 relative to predicted signal peptide cleavage site (Figure 14). Same amino acid pattern at signal peptide cleavage site is also found in tobacco lipid transfer protein (LTP) (Accession number BAK19150) (Choi et al. 2012) (Figure 15).

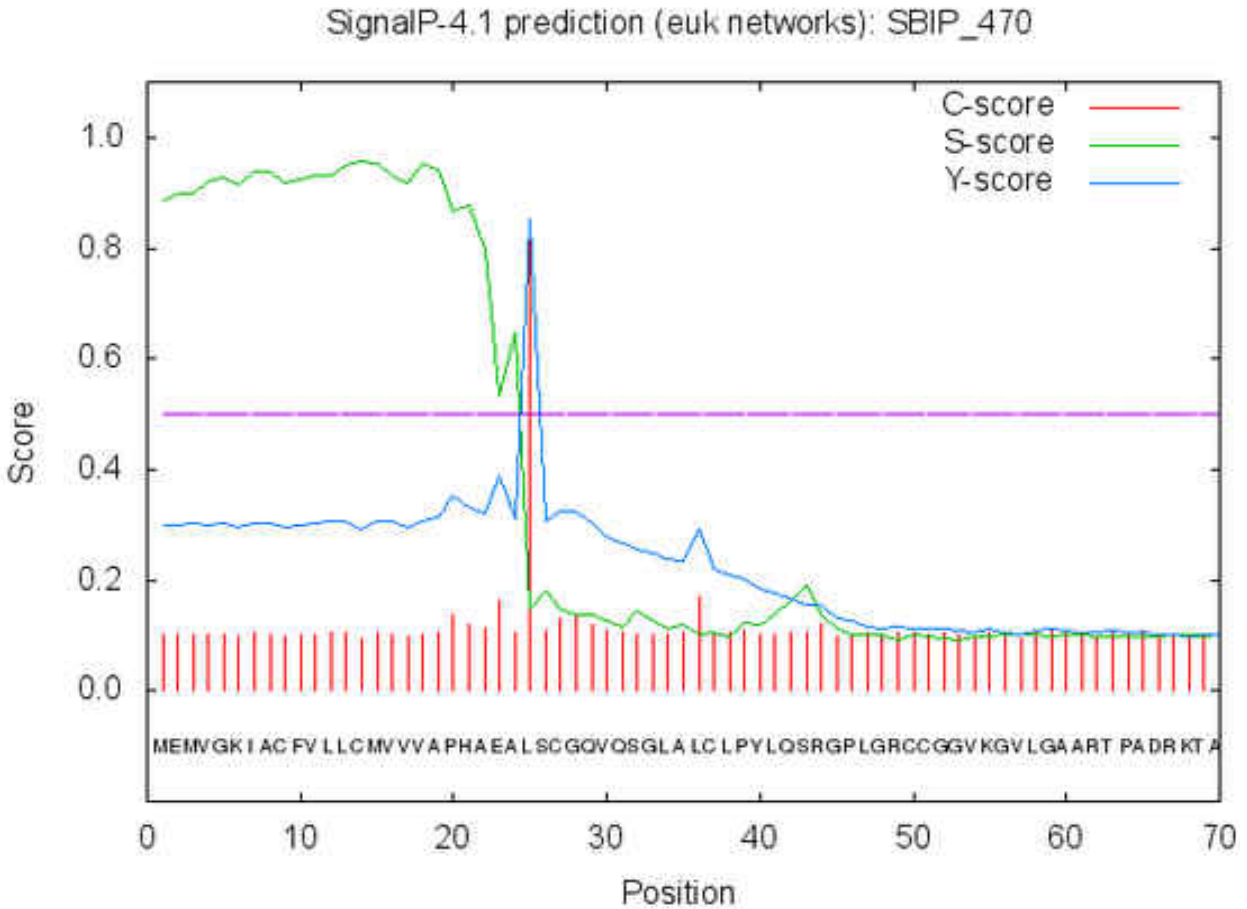


Figure 14. SBIP-470 Signal Peptide Cleavage Site Prediction. The predicted signal peptide cleavage site is between 24th and 25th amino acids. C-score is a raw cleavage site score, which distinguishes the signal peptide from the mature part of the protein. S-score is a signal peptide score, which distinguishes the position within signal peptides from the position in the protein both without signal peptide and with the signal peptide. Y-score is the geometric average of the C-score and the slope of the S-score. For the non- secretory proteins, all the scores on *SignalP* output are close to 0.1 (Thomas et al. 2011).

-4 -3 -2 -1

Nt_SBIP-470 **MEMV**G**KIACFVLL**C**MVVV**A**PH**A**E**A****-LSCGQV 30
 Nt-LTP **MEMV**S**KIACFV**V**L**C**MVVV**A**PH**A**E**A****-LT**C**GQV 30

Nt_SBIP-470 Q**S**GLALCLPYLQ**S**RGPLGRCCGGVKGVLGA 60
 Nt-LTP Q**S**SLAPCVPYLL**G**RGPLGGCCGGVKRLLGA 60

Nt_SBIP-470 ART**P**ADRKTACTCL**K**SAAYAIKGINMGKAA 90
 Nt-LTP ART**P**ADRKTAC**N**CL**K**SAANTFKGIDMGNAA 90

Nt_SBIP-470 AGL**P**SACGVNIPYKISPSTDCSRVQ 114
 Nt-LTP ARL**P**GT**C**GVNIPYKISPSTDCSKVQ 114

Figure 15. Analysis of Amino Acid Residues at Signal Peptide Cleavage Site of Tobacco SBIP-470 and Tobacco LTP. Number with negative sign (i.e. -1,-2,-3, and -4) refers to position of amino acid relative to signal peptide cleavage site. The signal peptide cleavage site of tobacco LTP is between 24th and 25th amino acids (shown in blue triangle). The predicted signal peptide cleavage site of the tobacco SBIP-470 is also between 24th and 25th amino acids (shown in blue triangle). SBIP-470 has Alanine, Glutamic acid and Alanine at -1, -2 and -3 relative to predicted signal peptide cleavage site respectively. Same amino acid pattern at signal peptide cleavage site is also found in the tobacco LTP.

SBIP-470 Arabidopsis Homolog

Tobacco SBIP-470 translated protein sequence was used as query to find the most similar *Arabidopsis* proteins using *The Arabidopsis Information Resource Database*. *Arabidopsis*. LTP2 (Accession number: NP_181387) has highest 53% identity while the *Arabidopsis* LTP12 (Accession number: NP_190727) has second highest 46% identity with tobacco SBIP-470 respectively. Amino acid sequences of tobacco SBIP-470, *Arabidopsis* LTP12, *Arabidopsis* LTP2 were then aligned using ClustalW (Figure 16).

```

At_LTP2      MAGVMK-IACMVLACMIVAGPITANALMSCGTVNGNLAGCIAYLTRGAPLTQGCCNGVIN 59
Nt_SBIP-470 MEMVVGK-IACFVLLCMVVVAP-HAEALS-CGQVQSGLALCLPYLQSRGPLGR-CCGGVKG 56
At_LTP12     MAFTPKEIITCLIVLTIYMASP--TESTIQCGTSTLAQCLTYLTNSGPLPSQCCVGVKS 58
          * . * ::*::: : :..* ::: ** * . ** *:.** .** ** **..

At_LTP2      LKNMASTTFDRQQACRCLQSAAKAVGPGINTARAAGLPSACKVNIPYKISASTNCNTVR- 118
Nt_SBIP-470  VLGAARTPADRKTACTCLKSAAYAIAK-GINMGKAAGLPSACGVNIPYKISFSTDCSRVQ- 114
At_LTP12     LYQLAQITTFDRKQVCECLKLAGKEIK-GLNTDLVAALPTTCGVSIPIYPIISFSTNCDSIST 117
          : * *..** : * ** : * : *:* .*.***:* *.* ** ** **:* :

At_LTP2      --
Nt_SBIP-470  --

```

Figure 16. Multiple Sequence Alignment between tobacco SBIP-470, *Arabidopsis* LTP12, and *Arabidopsis* LTP2. *Arabidopsis* LTP2 has highest 53% identity while the *Arabidopsis* LTP12 has second highest 46% identity with tobacco SBIP-470 respectively. Different signs are shown at bottom of sequence alignment such as star, dot, colon, and gap. Star shows the identity, dot shows preserved substitution, colon shows semi preserved substitution between two proteins, and gap shows dissimilarities between proteins. Sequence alignment was carried out by ClustalW.

Predicted 3D Structure

3D structure of tobacco SBIP-470, *Arabidopsis* LTP12 and *Arabidopsis* LTP2 were predicted using *Protein Structure Prediction Server of Molecular Bioinformatics Center National Chiao Tung University*. Solution structure of tobacco Lipid Transfer Protein (LTP1_1) (Protein Data Base ID: 1T12) was used as template. 3D structure was created to analyze the structural similarity between tobacco SBIP-470, *Arabidopsis* LTP12, *Arabidopsis* LTP2 and solution structure of tobacco LTP1_1. Comparison between the 3D structures showed that all 3 proteins have 4 alpha helixes connected by 4 disulfide bridge as tobacco LTP1-1 has. Like in the tobacco LTP1_1, a tunnel like cavity is also found in tobacco SBIP-470, *Arabidopsis* LTP12 and *Arabidopsis* LTP2 (Figure 17).

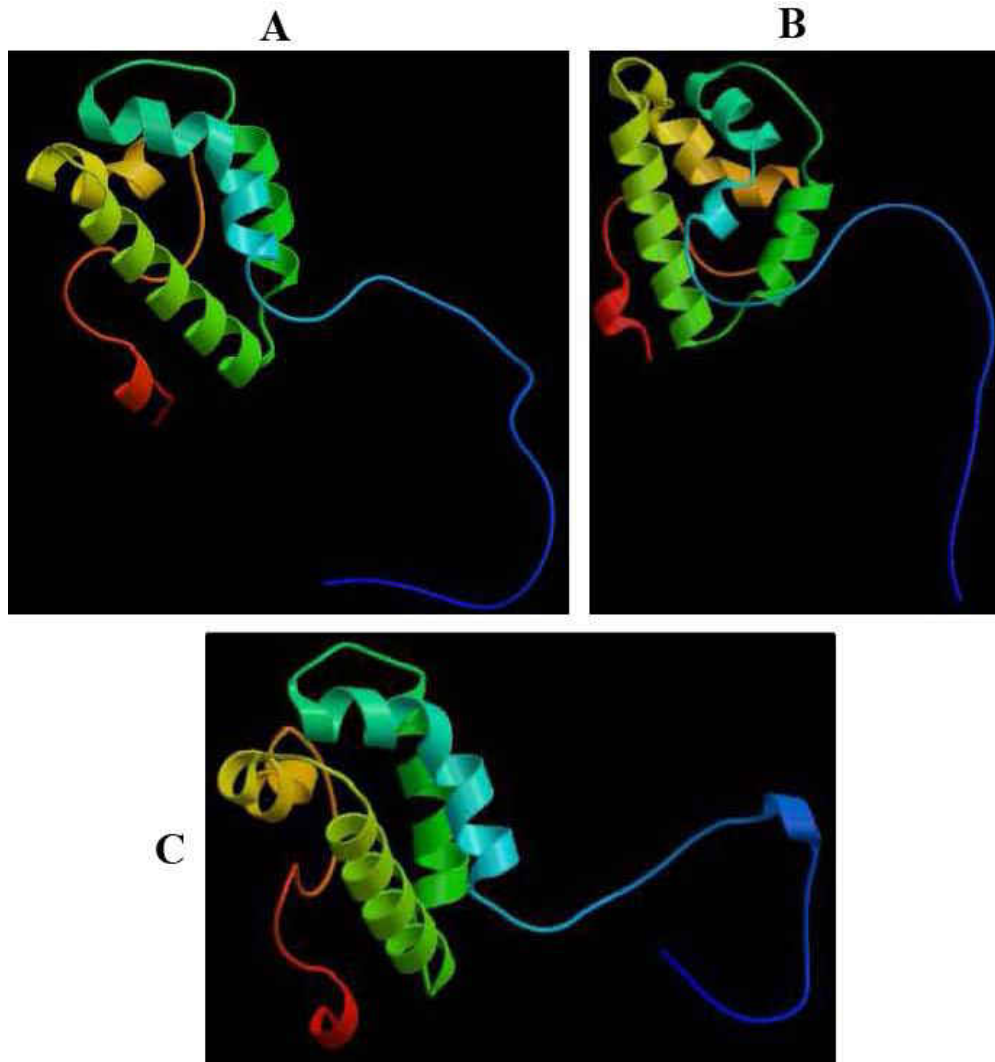


Figure 17. Predicted Protein Model of *Arabidopsis* LTP12, *Arabidopsis* LTP2, and Tobacco SBIP-470. A. 3D structure of *Arabidopsis* LTP12, B. 3D structure of *Arabidopsis* LTP2, and C. 3D structure of tobacco SBIP-470.

Phylogeny Tree

A phylogeny tree was constructed to determine how SBIP-470 is evolutionary related to the LTPs from tobacco, potato, *Arabidopsis*, and sweet orange. Full-length sequences of 16 LTPs were aligned using ClustalW2 then manually refined. Based on the constructed phylogeny tree, SBIP-470 is closely related to other tobacco LTPs i.e. LTP and nsLTP2 (Figure 18). Other than tobacco LTPs, SBIP-470 is closely related to potato nsLTP2 (Figure 18). *Arabidopsis* DIR

proteins make separate clade (Figure 18). *Arabidopsis* LTP2 is more closely related to *Arabidopsis* LTP1 (Figure 18).

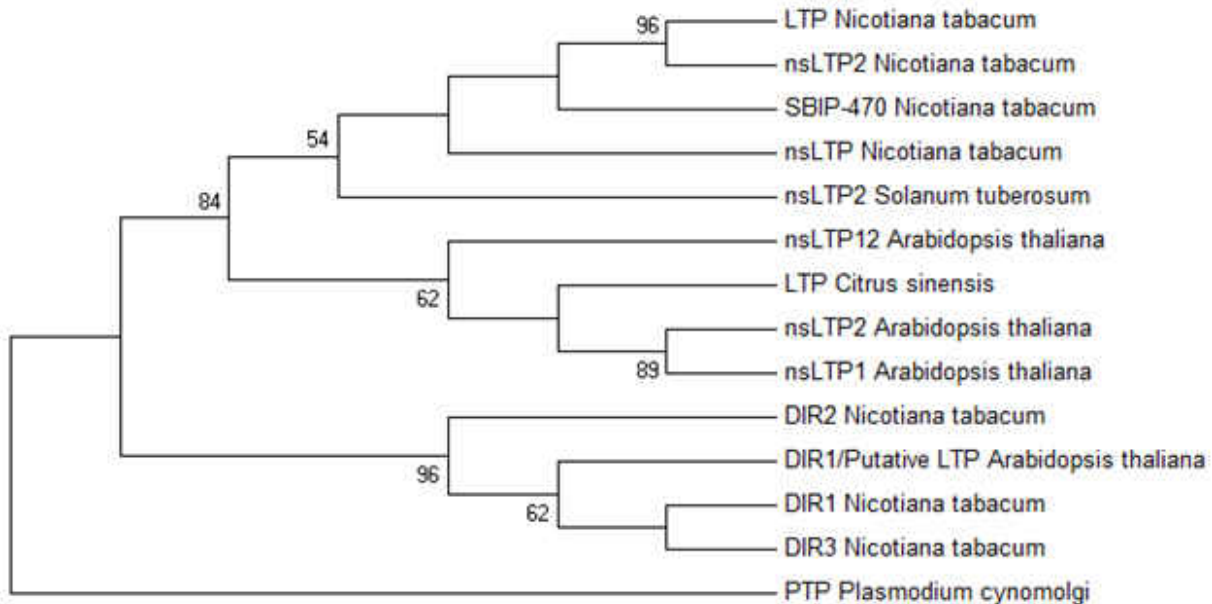


Figure 18. Rooted Phylogeny Tree (Maximum Likelihood, Character State Method) between Tobacco, Potato, *Arabidopsis*, *Citrus sinensis*, and *Plasmodium cynomolgi* LTP Protein Family. Number of Bootstrap Replications used was 500. The number for each interior branch shows the percentage of the bootstrap values. In the tree the bootstrap value above the 50 is shown. Out group: Simian malaria parasite (*Plasmodium cynomolgi* stain B). The phylogeny tree shows that SBIP-470 is closely related to other tobacco LTPs. Other than tobacco LTPs, SBIP-470 is closely related to potato nsLTP2.

Cloning of SBIP-470

cDNA Synthesis

Three hundred thirty five base pairs long *SBIP-470-25* with attb sites (*SBIP-470-25* are flanked by attB1 and attB2 sites) was amplified using the verified clone (pDONR221-*SBIP-470* construct) as a template. PCR was performed using the Platinum Pfx DNA polymerase. Result showed that the successful amplification of the *SBIP-470-25* with attb sites (Figure 19).

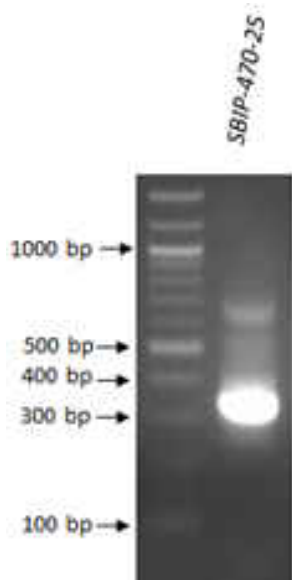


Figure 19. 1.2% Agarose Gel Picture of *SBIP-470-25* Amplified from Verified Clone, pDONR221-*SBIP-470* Construct.

PCR Purification

SBIP-470-25 was purified using the PureLink PCR purification kit. The quality of the purified *SBIP-470-25* was analyzed by agarose gel electrophoresis (Figure 20).

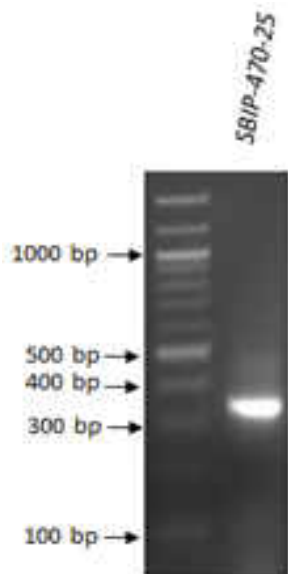


Figure 20. 1.2% Agarose Gel Picture of Purified *SBIP-470-25*.

pDONR221-SBIP-470-25 Entry Clone Validation

Gateway cloning allows one to select the positive clone by replacing the *ccdB*, toxic gene. *ccdB* gene is replaced by gene of interest if a recombination between attB PCR product and entry clone occurs. Cells that carry the unreacted entry clone carrying the toxic *ccdB* gene cannot grow. Transformed bacterial cells were grown in LB plates containing kanamycin to validate the pDONR221-SBIP-470-25 entry clone. The presence of SBIP-470-25 was further validated by colony PCR using M13 forward and reverse primers, M13 forward and *SBIP-470-25* reverse primers, and *SBIP-470-25* forward and M13 reverse primers (data not shown).

The entry clone was isolated and purified from transformed bacterial cells (*E. coli* Topo 10) using QIAprep Spin MiniPrep Kit (Figure 21). Purified entry clone DNA was sequenced. Result showed that the entry clone has *SBIP-470-25* in proper reading frame (Figure 22). After sequence verification the entry clone was used for LR recombination reaction.

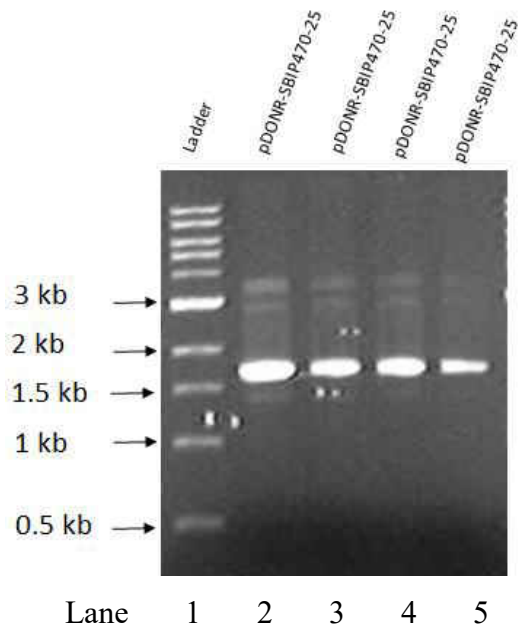


Figure 21. Agarose Gel Showing Purified pDONR221-SBIP-470-25 Entry Clone by QIAprep Spin MiniPrep Kit. 6 μ l of entry clone was loaded in the gel. Entry clone was eluted twice with buffer EB during purification. Lane 1: 1 KB ladder, Lane 2: Entry clone from colony 1 (first elution), Lane 3: Entry clone from colony 1 (second elution), Lane 4: Entry clone from colony 2 (first elution), and Lane 5: Entry clone from colony 2 (second elution).

```

470_attBs -----
ENC      AGGCCAGTCTTCTGAATGAACTTTTCGTATTATTAGAAAGCCTGGCAGGTCCGTA CTCTC 60

470_attBs -----
ENC      GCGTTAACGAGAGCATGGATGTTTTCCAGTCATGACGTAGTAAAACGACGGCCAGTGTT 120

470_attBs -----
ENC      AAGCTCGGGCCCCAAATAATGATTTTATTTTGACTGATAGTGACCTGTTCGTTGCAACAA 180

470_attBs -----
ENC      ATTGATGAGCAATGCTTTTTTATAATGCCAACTTTGTACAAAAAGCAGGCTCACTGAGC 25
                                     GTACAAAAAGCAGGCTCACTGAGC 25
                                     GTACAAAAAGCAGGCTCACTGAGC 240
                                     *****

470_attBs TCGCGCCAGGTTTCAGTCTGGCCTGGCTCTTTGCCTCCCTTATCTGCAGAGTCGCGGCCCT 85
ENC      TCGCGCCAGGTTTCAGTCTGGCCTGGCTCTTTGCCTCCCTTATCTGCAGAGTCGCGGCCCT 300
                                     *****

470_attBs CTAGGGAGGTGTTGTGGCGGCGTTAAAGGTGTGTTGGGTGCTGCCCGGACCCAGCTGAC 145
ENC      CTAGGGAGGTGTTGTGGCGGCGTTAAAGGTGTGTTGGGTGCTGCCCGGACCCAGCTGAC 360
                                     *****

470_attBs CGCAAGACTGCATGCACTTGCCTGAAATCAGCTGCTTATGCTATTAAGGTATTAATATG 205
ENC      CGCAAGACTGCATGCACTTGCCTGAAATCAGCTGCTTATGCTATTAAGGTATTAATATG 420
                                     *****

470_attBs GGCAAAGCCGCTGGACTTCCTAGTGCTTGTGGCGTTAACATTCCCTACAAGATCAGTCCC 265
ENC      GGCAAAGCCGCTGGACTTCCTAGTGCTTGTGGCGTTAACATTCCCTACAAGATCAGTCCC 480
                                     *****

470_attBs TCTACTGACTGCTCCAGGGTCCAGTGA TACCCAGCTTTCT----- 305
ENC      TCTACTGACTGCTCCAGGGTCCAGTGA TACCCAGCTTTCTTGTACAAAGTTGGCATTATA 540
                                     *****

470_attBs -----
ENC      AGAAAGCATTGCTTATCAATTTGTTGCAACGAACAGGTCACTATCAGTCAAAATAAAATC 600

470_attBs -----
ENC      ATTATTGCCATCCAGCTGAATCCCTATCGAATC 633

```

Figure 22. Sequence Alignment of *SBIP-470-25* with attB Sites (#470-attBs) and pDONR221-*SBIP-470-25* Entry Clone (#ENC). Sanger sequencing method was used for sequencing the pDONR221-*SBIP-470-25* entry clone using M13 forward and reverse primers. *SBIP-470-25* is shown in yellow color, sequence from attB1 is shown in blue and sequence from attB2 is shown in red. Result showed that entry clone has *SBIP-470-25* in proper reading frame.

pDEST17-*SBIP-470-25* Validation

pDEST17-*SBIP-470-25* plasmid DNA was isolated and purified from *E. coli* DH5α cells using QIAprep Spin MiniPrep Kit as described earlier in the material and methods section. Quality of purified plasmid DNA was analyzed by agarose gel (Figure 23).

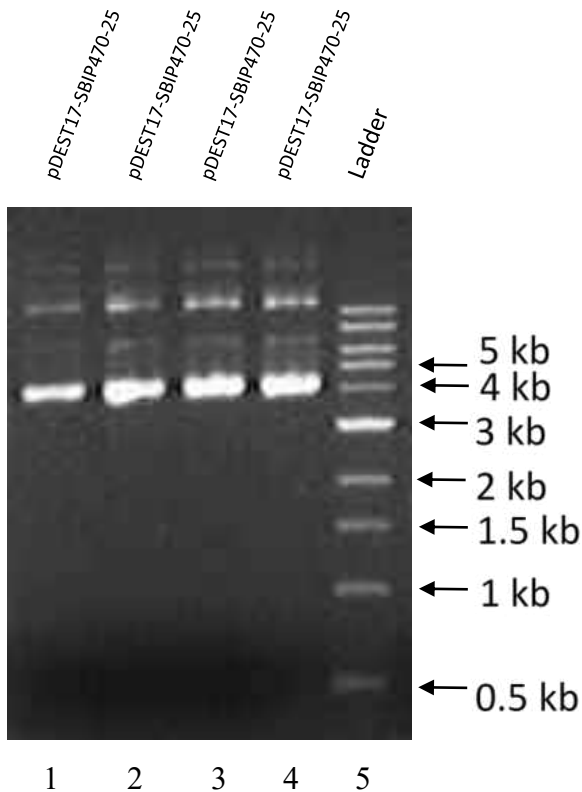


Figure 23. Agarose Gel Showing Purified pDEST17-SBIP-470-25 DNA Construct by QIAprep Spin MiniPrep Kit. Two micoliter of plasmid DNA was loaded in the gel. The plasmid DNA was eluted twice with buffer EB during purification. Lane 1: Plasmid DNA from colony 1 (second elution), Lane 2: Plasmid DNA from colony 1 (first elution), Lane 3: Plasmid DNA from colony 2 (second elution), Lane 4: Plasmid DNA from colony 2 (first elution), and Lane 5: 1 KB ladder.

Quantity of purified plasmid DNA was determined using Nanodrop. One microliter of purified plasmid DNA (12.3 ng/ μ l) was used to transform to the *E. coli* Magic cell line. The construct was confirmed by colony PCR using T17 forward and reverse primers (data not shown).

Expression of Recombinant SBIP-470

Expression

Expression of recSBIP-470-25 was performed as described in materials and methods section. Expression of recSBIP-470 was confirmed by SDS-PAGE and western blotting analysis using monoclonal anti-polyHistidine antibody.

Solubility Test

Solubility test of recSBIP-470-25 was performed as described in Materials and Methods section. Pellet collected from 1 ml culture was suspended in 1X Ni-NTA binding buffer. Bacterial cells were broken by sonication and then centrifuged. The supernatant (soluble) and pellet (insoluble) were collected. Resulting pellet was suspended in 1X Ni-NTA buffer. Proteins from both soluble and insoluble fractions were run on SDS gel and western blotting was performed to determine the presence of recSBIP-470-25. RecSBIP-470-25 was expressed in insoluble form (Figure 24). Based on western result recSBIP-470-25 grown at 37°C culture was expressed more in insoluble form compared to recSBIP-470-25 culture grown at 17°C.

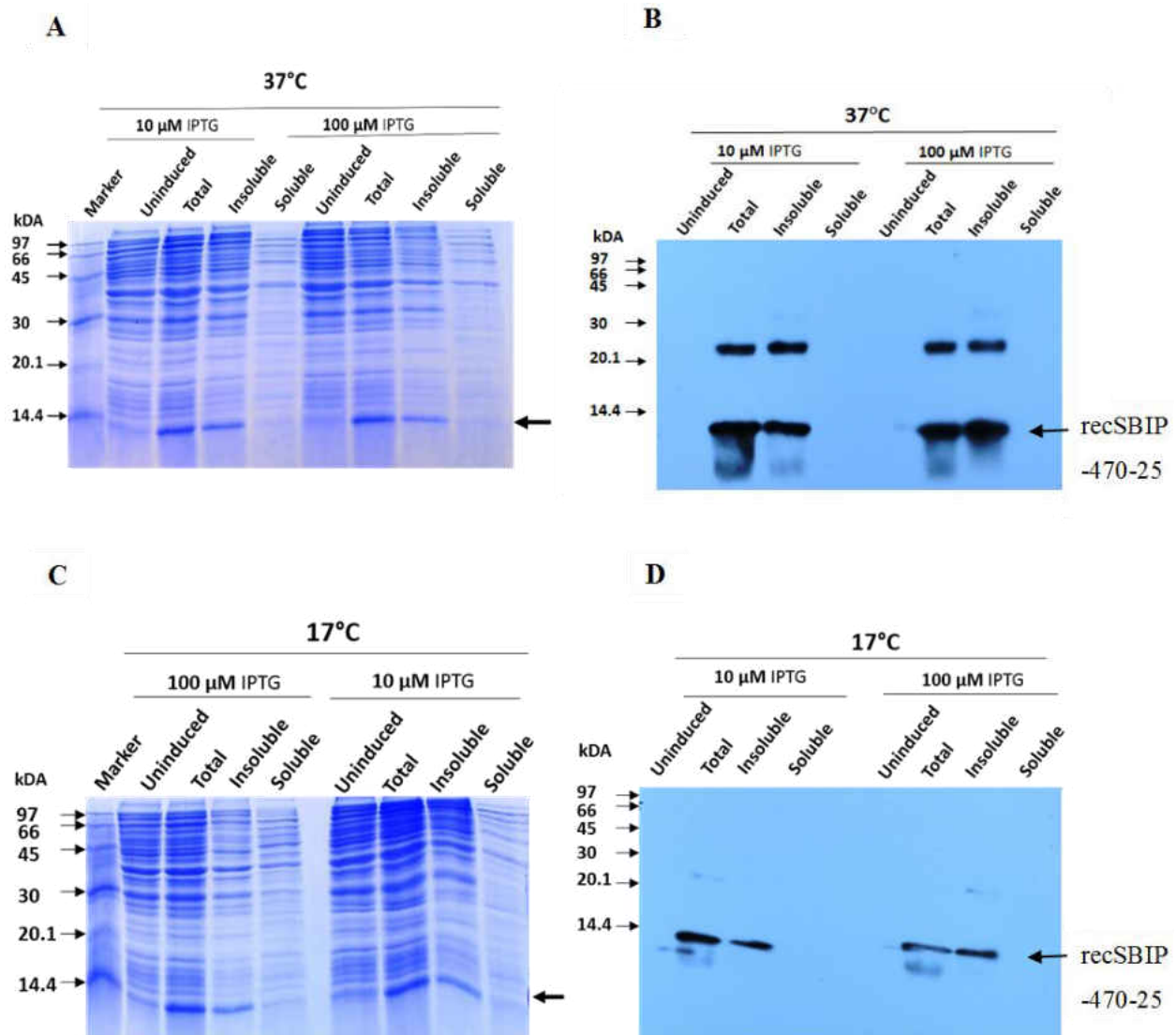


Figure 24. Solubility Test of recSBIP-470-25 Obtained from 37°C and 17°C Culture. A. SDS page analysis of the protein from 37°C culture. B. Western blotting of protein from 37°C using monoclonal polyhistidine antibody. C. SDS page analysis of the protein from 17°C culture. C. Western blot analysis of protein from 17°C detected using monoclonal poly-Histidine antibody. RecSBIP-470-25 (condition mentioned above) was mostly expressed in insoluble condition.

Expression of SBIP-470 under Soluble Condition

Ni-NTA Column Chromatography

Based on solubility test, recSBIP-470 was mostly expressed in insoluble condition, but it was also detected in soluble condition when concentrated from large culture.

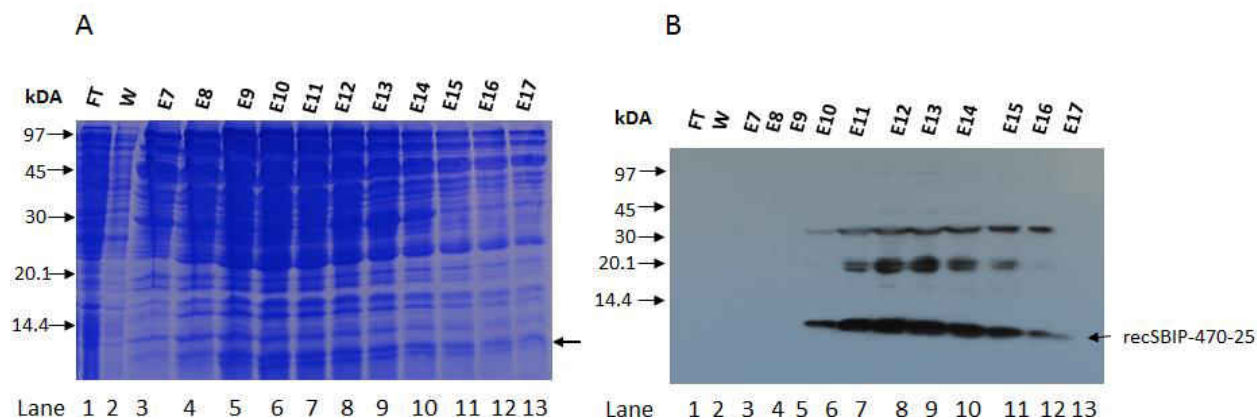


Figure 25. Purification of recSBIP-470-25 using Ni-NTA Column Chromatography. A. 15 % SDS gel of purified recSBIP-470-25 with eluted fraction (E7-E17). B. Western blot analysis of eluted fractions (E7 to E17). Flow through (FT) and Wash (W) loaded on first and second lanes respectively. 2 μ l ‘FT’ and ‘W’ were loaded while 10 μ l of E7 to E17 were loaded on gel. The eluted fractions (E10 to E16) were detected by western blot using monoclonal poly-Histidine antibody (Figure 14 B).

To find the best condition for soluble protein expression, expression of recSBIP-470-25 was carried at various temperature and IPTG concentration (data not shown). RecSBIP-470-25 was expressed in soluble condition when induced with 10 μ M IPTG and grown at 17°C for overnight or 37°C for 4 hours. More soluble recSBIP-470-25 was detected when induced with 10 μ M IPTG and grown at 17°C for overnight than at 37°C. Then, recSBIP-470-25 was expressed in *E. coli* and purified using Ni-NTA column chromatography. SDS and western blotting were performed to confirm the purification of recSBIP-470-25. Samples were mixed with 6X SDS loading dye, boiled for 5 minutes, and centrifuged at 13,000 rpm for 1 minute. Supernatant was loaded on the gel (data not shown).

Q-Sepharose Column Chromatography

Ni-NTA column purified fractions (# E10 to E16) containing recSBIP-470-25 were pooled and desalted then purified using a Q Sepharose column chromatography (detail on Materials and Methods section). In Q Sepharose chromatography, the 2 peaks were observed (Figure 26). Based on the chromatogram, most of proteins eluted in fractions 35 to 60. Fractions (#40-57) were

analyzed by SDS and western blotting (Figure 27). RecSBIP-470-25 (11.6 kDA) was detected in fractions (# 40 to 51) by western blotting (Figure 27 D). SDS page analysis showed that there were other proteins that eluted along with the recSBIP-470-25 (Figure 27 B).

Chromatogram

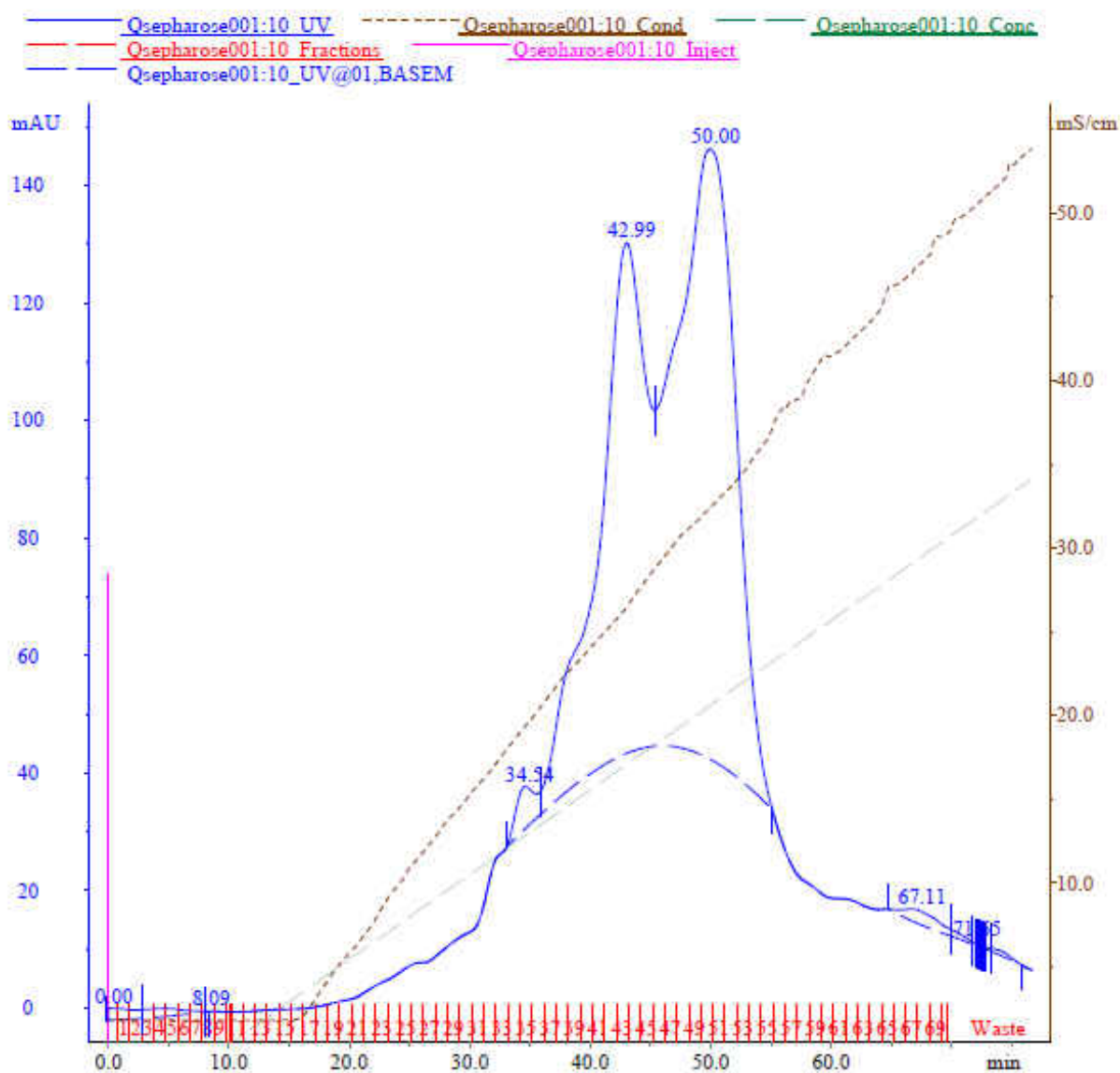


Figure 26. Chromatography Profile of Protein in Q Sepharose Column Chromatography. Absorbance of protein at 280 nm (brown line), collected fraction (1 ml) (red line), and salt conductivity (red line). Fractions # (40-57) was ran on gel for SDS and western blotting.

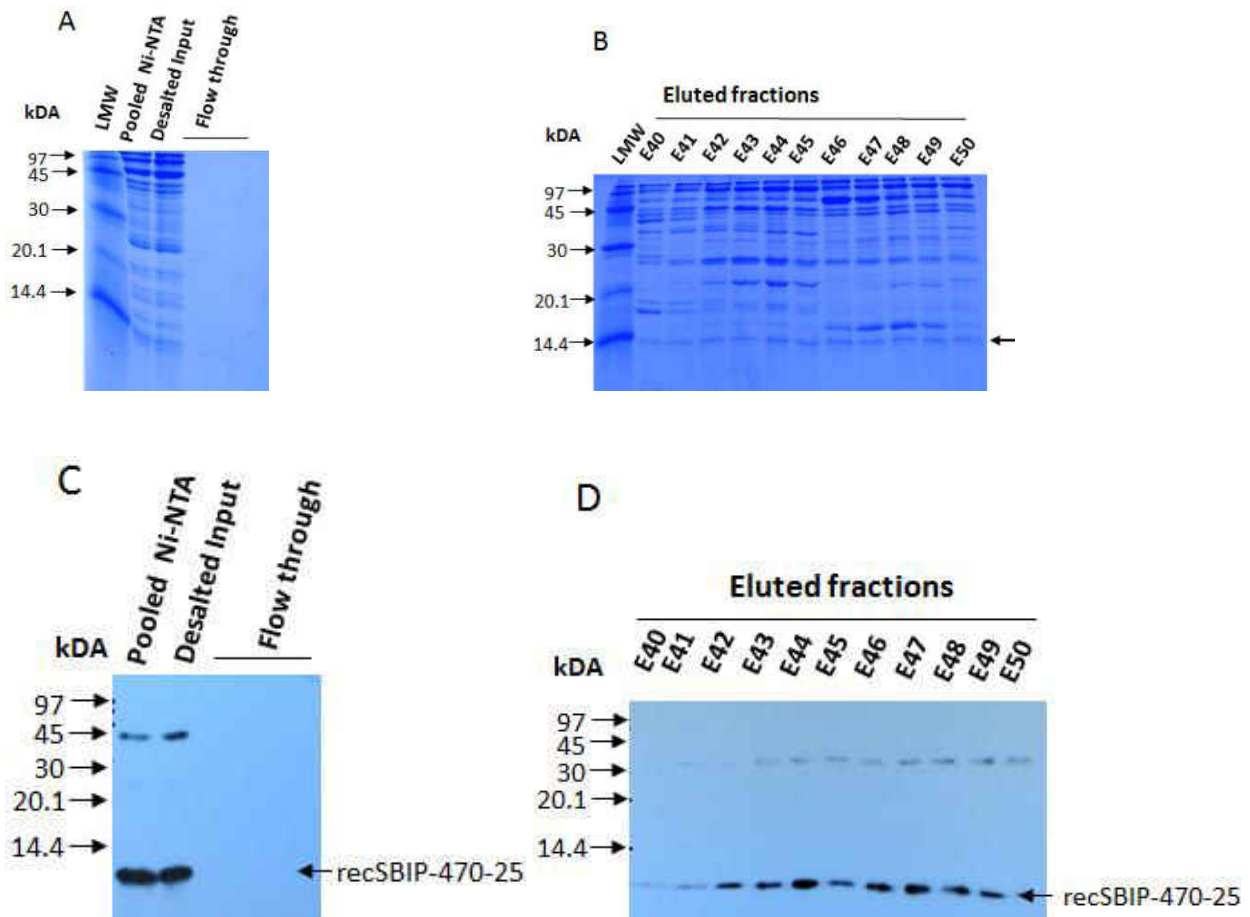


Figure 27. Purification of recSBIP-470-25 using Q Sepharose Column Chromatography. A. 15% SDS gel showing pooled protein from Ni-NTA purification, desalted protein, and flow through. B. 15% SDS gel of purified recSBIP-470-25 with eluted fraction (E40-E50). C. Western blot analysis of pooled protein from Ni-NTA purification, desalted protein, and flow through. D. Western blot analysis of eluted fractions (E40 to E50). The eluted fractions (E40 to E50) were detected by western blot using monoclonal poly-Histidine antibody (Figure 24 B).

Ni-NTA Column Chromatography

In Q-Sepharose column chromatography some other proteins copurified with recSBIP-470-25. Fractions (E42-50) were pooled and incubated with Ni-NTA column. Unbound proteins were washed with 1X Ni-NTA buffer containing 10 mM of imidazole. Then, the bound proteins were step eluted with 1X Ni-NTA elution buffer containing various concentrations of Imidazole. Fractions E1-E3, E4-E6, E7-E9, and E10-E12 were eluted with elution buffer containing 50 mM, 100 mM, 150 mM, and 250 mM of imidazole respectively.

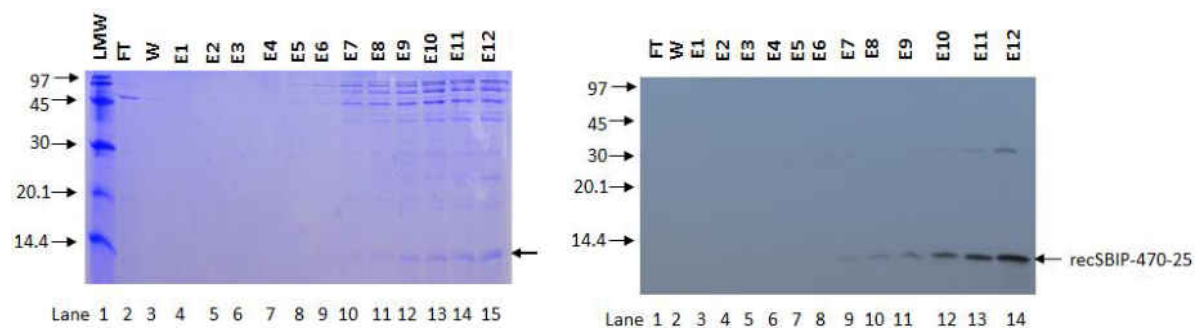


Figure 28. Purification of recSBIP-470-25 using Ni-NTA Column Chromatography. Protein purified by the Q-Sepharose was purified again using the Ni-NTA column chromatography. A. 15% SDS gel of purified recSBIP-470-25 with eluted fraction (E1-E12). B. Western blot analysis of eluted fractions (E1 to E12). Flow through (FT) and Wash (W) were loaded on first and second lanes respectively. The eluted fractions (E7 to E12) were detected by western using monoclonal poly-Histidine antibody (Figure 14 B).

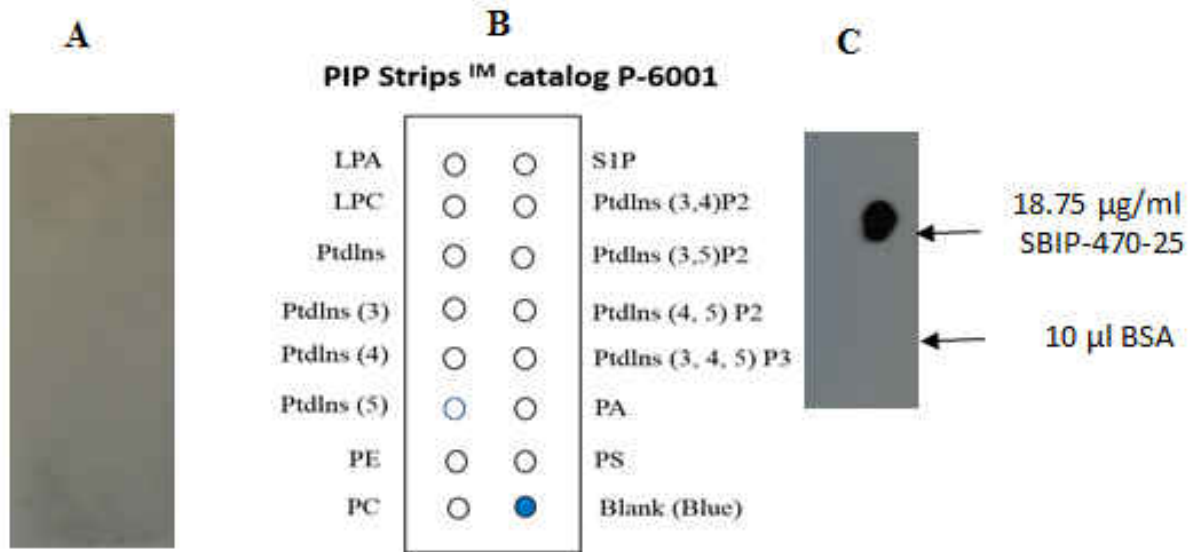
Partially purified recSBIP-470-25 by Ni-NTA column chromatography was pooled and dialyzed against 1X PBS buffer, and 1x PLTP buffer as mentioned in materials and methods section. Dialyzed recSBIP-470-25 quantified using BCA Protein Assay Kit as mentioned in materials and methods section.

Biochemical Characterization

Lipid Binding Assay

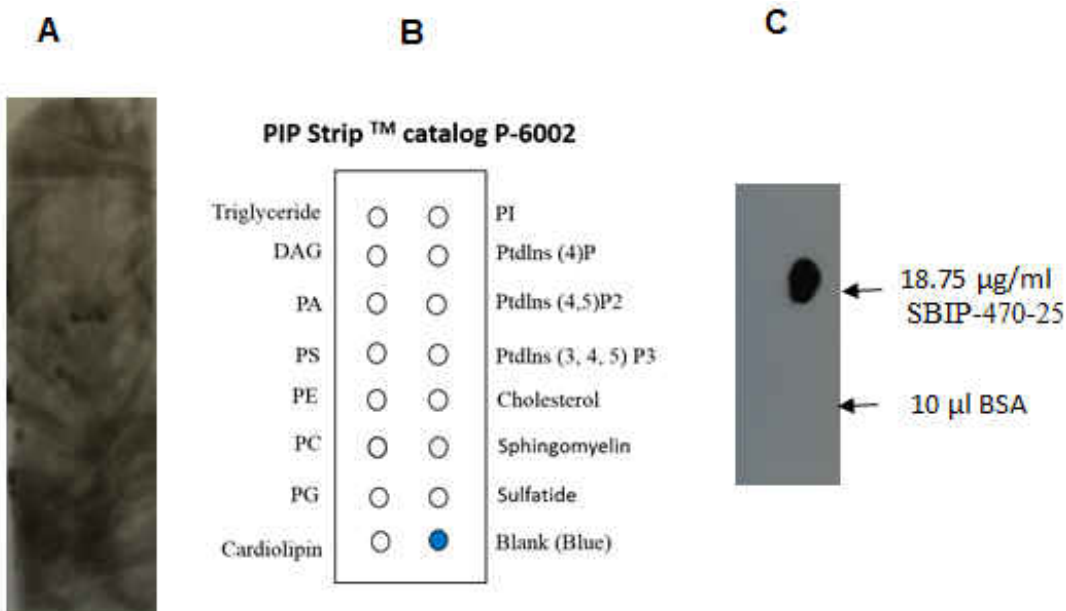
In vitro lipid binding assay was performed to determine whether the recSBIP-470-25 interacts with one or more lipids. Well established protein-lipid overlay assay was used to find recSBIP-470-25 target. Dialyzed recSBIP-470-25 (18 $\mu\text{g/ml}$) was applied to membranes that were spotted with various phospholipids (Figure 16 B and Figure 17 B). After the extensive washing the membranes, the monoclonal polyhistidine antibody was applied to membranes and revealed the bound recSBIP-470-25 with secondary horseradish peroxidase antibody. To check the sensitivity of the antibody to the His tagged SBIP-470-25, 10 μl of recSBIP-470-25 (18 $\mu\text{g/ml}$) was blotted. Result showed that antibody under the same condition used for PIP Strip perfectly recognizes the His tagged SBIP-470-25 (recSBIP-470-25) (Figure 29 C and Figure 30 C). Under the experimental

condition (mentioned in material and methods section), recSBIP-470-25 did not bind the lipids spotted on the PIP Strip or if it does, its binding is very weak and undetectable (Figure 30 A and Figure 30 A).



18 µg/ml recSBIP-470-25

Figure 29. Lipid Binding Assay of recSBIP-470-25 using PIP Strips™ (Catalog P-6001). His tagged bacterially purified SBIP-470-25 (recSBIP-470-25) was applied to the PIP Strips™ spotted with various phospholipids (100 pmol per spot) then revealed with anti his tag antibody (detail mentioned in Materials and Methods sections). A. recSBIP-470-25 on the strip. B. Nomenclature of various phospholipids spotted on the strip (detail mentioned in materials and methods sections). C. recSBIP-470-25 spotted on nitrocellulose membrane.



18 µg/ml
RecSBIP-470-25

Figure 30. Lipid Binding Assay of recSBIP-470-25 using PIP Strips™ (Catalog P-6002). His6 tagged bacterially purified SBIP-470-25 (recSBIP-470-25) was applied to the strip spotted with various phospholipids (100 pmol per spot) then revealed with anti his tag antibody. A. recSBIP-470-25 (18 µg/ml) on strip. B. Nomenclature of various phospholipids spotted on strip (detail mentioned in materials and methods sections). C. recSBIP-470-25 spotted on nitrocellulose membrane.

In Vitro Lipid Transfer Assay

Phospholipid transfer activity was carried out using a PLTP activity assay kit following the manufacturer's instruction (detail in Materials and Methods section). PLTP assay include donor containing fluorescent phospholipid (nitrobenzoxadiazole labelled phospholipid) and acceptor molecule. Fluorescent phospholipid is present in a self-quench state when it is associated with donor particle. Incubation of the donor, acceptor, and the PLTP source results in transfer of fluorescent labeled phospholipid from donor to the acceptor, and that is determined by increase in fluorescent intensity. Briefly, dialyzed recSBIP-470-25 was incubated with the donor, acceptor, and PLTP buffer at 37°C for 3 hours. Changes in fluorescence were measured every 10 minutes (following 3 hours of incubation) using a SYNERGY HT Multi-Mode Microplate Reader (Biotek)

at Ex 485 nm and Em 528 nm wavelength. Fluorescence intensity units that transferred during the incubation time were obtained by subtracting the fluorescence intensity values of blank (control) to the sample. Fluorescence unit over time decreased so recSBIP-470-25 failed to transfer phospholipid (Figure 31).

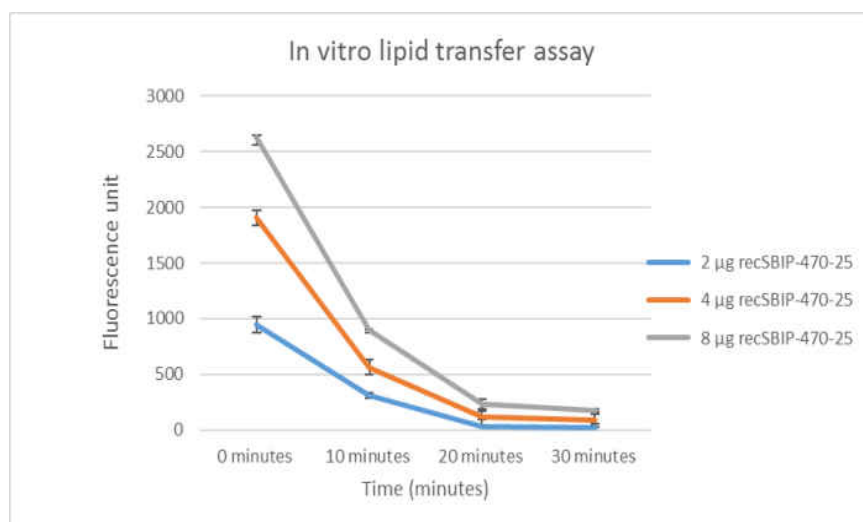


Figure 31. Time Dependent Phospholipid Transfer Activity of recSBIP-470-25. RecSBIP-470-25 was incubated with donor containing fluorescent self-quenched phospholipid, acceptor, and PLTP buffer at 37°C in 96 well micro plates for 3 hours. Changes in fluorescence were measured every 10 minutes as described in Materials and Methods section. Vertical bar represents the standard error for the triplicate samples.

Phenotype Analysis of *Arabidopsis* Mutants (Hypothesis II)

T-DNA Based Mutant Screening

Arabidopsis knockout mutants i.e. CS736658 (*ltp12* mutant), and CS736752 (*ltp2* mutant) have a T-DNA insertion in the intron of *LTP12* and exon of *LTP2* gene respectively. Mutant plants were screened by PCR based screening using a T-DNA left border primer and gene specific primer. DNA bands ~500 bp were detected confirming that both mutants were homozygous (Figure 32 A and 32 B) (band between 410 bp to 710 bp is expected for a homozygous mutant).

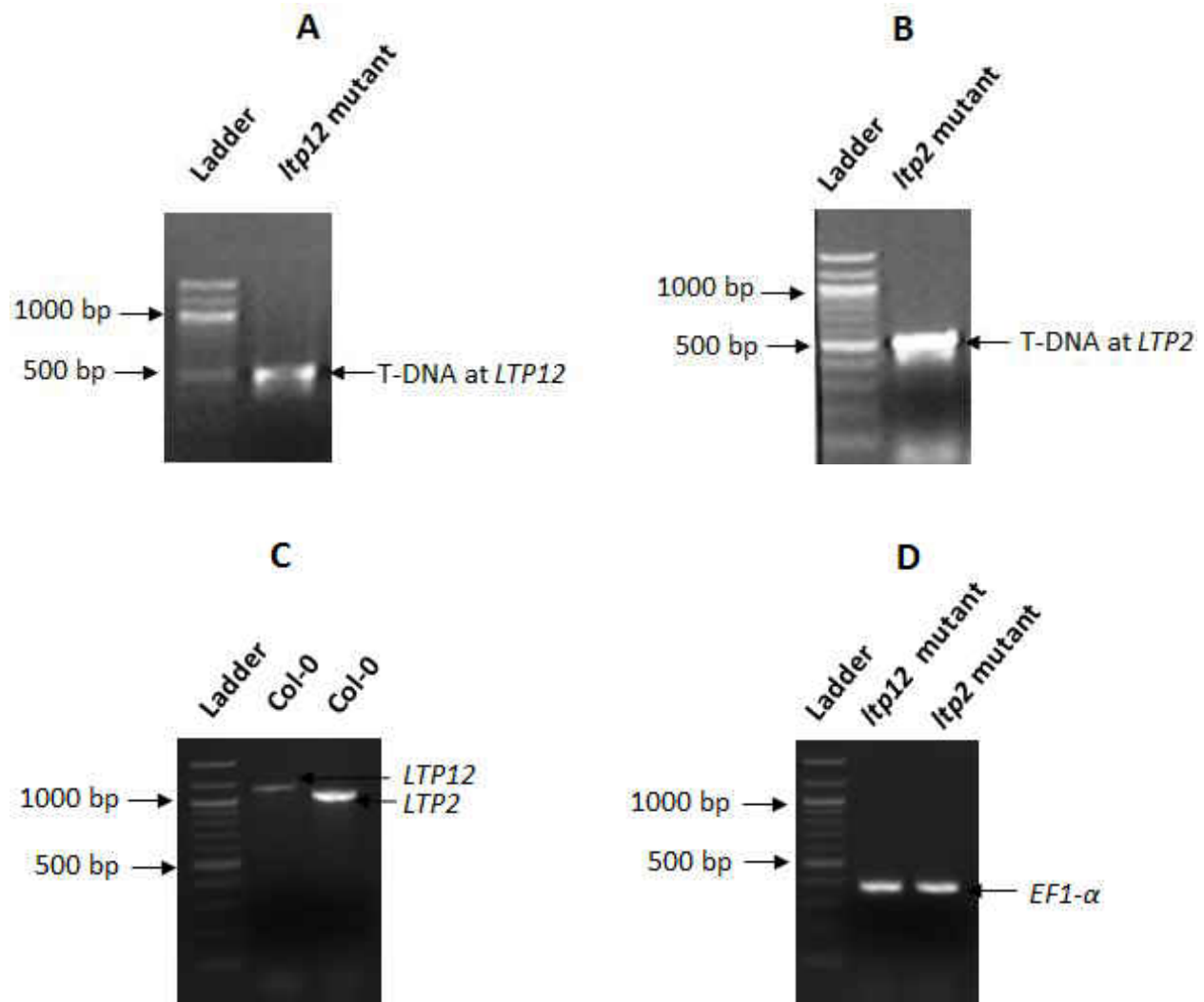


Figure 32. Confirmation of T-DNA Insertion at *LTP12* and *LTP2* Gene. (A) T-DNA on *LTP12* of *ltp12* Mutant, (B) T-DNA on *LTP12* of *ltp2* Mutant, (C) Genomic DNA of *LTP12* and *LTP2* of parental Line (Col-0), (D) Genomic DNA of *EF1-α* of *ltp12* (Second Lane), and *ltp2* Mutant (Third Lane). Result showed that both mutants were homozygous.

RT-PCR Based Mutant Screening

LTP12 and *LTP2* RNA expression was analyzed in *ltp12* and *ltp2* mutants respectively (Figure 33 A). As control the *LTP12* and *LTP2* expression was analyzed in parental line (Col-0) (Figure 33 B). Total RNA and cDNA was synthesized as described earlier. Finally, the cDNA of *LTP12*, *LTP2* (partial *LTP2*) and *EF1- α* was amplified (Figure 33 C). Very low levels of expression of *LTP12* were observed in Col-0. So, *LTP12* was re-amplified using the amplified PCR product obtained from *ltp12* mutant as well as Col-0.

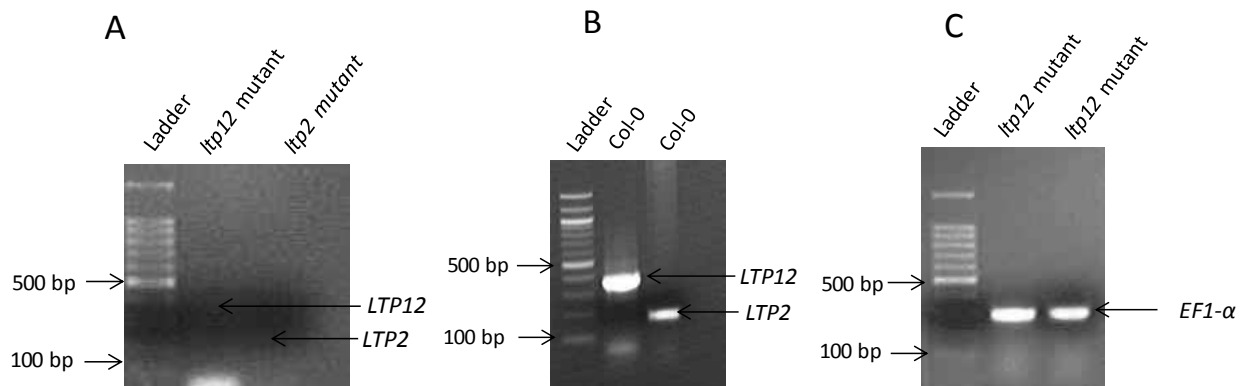


Figure 33. RT-PCR Analysis of *Arabidopsis* *LTP12* and *LTP2* (Partial) Genes. (A) RNA expression of *LTP12* and *LTP2* in *ltp12* and *ltp2* mutants respectively. (B) RNA expression of *LTP12* and *LTP2* in Col-0. (C) RNA expression of housekeeping gene (*EF-1 α*) in mutants (Lane 2: *ltp12* mutant, Lane 3: *ltp2* mutant). DNA ladder (100 bp) was loaded on first lanes. Result showed that *ltp12* mutant and *ltp2* mutant were unable to make *LTP12* and *LTP2* RNA respectively.

Growth Phenotype of *ltp12* and *ltp2* Mutant

To compare the growth phenotype of *ltp12* mutant (CS736658) and *ltp2* mutant (CS486424) with their corresponding wild type parental line (Col-0), 5 to 6 seeds of each mutant and control plants were sown in autoclaved soil. After 3 days of vernalization treatment, flats containing seeds were transferred to the growth chamber. Growing plants were inspected visually after 1, 2, 3, 4, and 5 weeks. The height of plants was measured at 15, 30, and 39 days after germination (DAG). Similarly, numbers of leaf, and length of the longest leaf were determined at 30 DAG. Height of inflorescence was measured at 39 DAG. Moreover, inflorescence emergence

and time of silique formation was also noted. Additionally, leaf morphology and other abnormalities were visually inspected (Figure 34).

Average height of *ltp12* and *ltp2* mutant compared to Col-0 at 15 DAG was 0.876 cm, 0.88 cm, and 0.884 cm respectively (Figure 35). At 22 DAG, average height of *ltp12*, *ltp2*, and Col-0 was 0.98 cm, 0.96 cm, and 1.06 cm respectively (Figure 35). At 15 DAG and 22 DAG no significant difference in height was observed between *ltp12*, *ltp2* mutants, and Col-0. At 30 DAG, average height of *ltp12*, *ltp2*, and Col-0 was 3.68 cm, 6.5 cm, and 15.9 cm respectively (Figure 35). Average height of *ltp12*, *ltp2*, and Col-0 at 39 DAG was 23.3 cm, 29.7 cm, and 34 cm respectively (Figure 35). Height of plant at 30 DAG showed significant difference between *ltp12* mutants and Col-0 and *ltp2* mutants and Col-0. The height of plant at 39 DAG showed significant difference only in *ltp12* mutant with respect to Col-0. Average numbers of leaves at 30 DAG in *ltp12* mutants, *ltp2* mutants, and Col-0 was 19.4, 25.4, and 29.2 respectively (Figure 36). Average numbers of leaf at 30 DAG showed significant difference between *ltp12* mutants and Col-0, but no significant difference was shown between *ltp2* mutant and Col-0. Average length of longest leaf at 30 DAG in *ltp12* mutants, *ltp2* mutants, and Col-0 was 5.3 cm, 5.54 cm, and 5.7 cm respectively (Figure 37). There was no significant difference observed in length of longest leaf between *ltp12*, *ltp2* mutant and Col-0. Average time of bolting in *ltp12* mutant, *ltp2* mutant, and Col-0 was 30.6 DAG, 27.8 DAG, 23.4 DAG respectively (Figure 38). Average time of inflorescence emergence in *ltp12* mutant, *ltp2* mutant, and Col-0 was 33 DAG, 30 DAG, 26 DAG respectively (Figure 39). Time of inflorescence emergence showed significant difference (Figure 39). Average time of silique formation in *ltp12* mutants, *ltp2* mutant, and Col-0 plant was 38.2 DAG, 34.6 DAG, and 30.4 DAG respectively (Figure 40). Time of silique formation showed significant difference between *ltp12* mutant and Col-0, but did not show in *ltp2* mutants and Col-0.



Figure continued

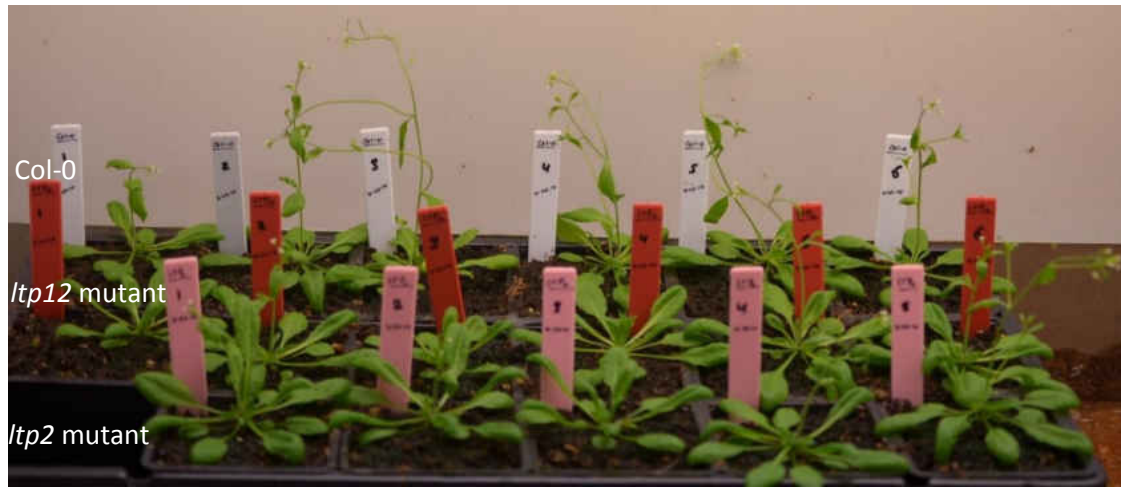


*Figure 34. Growth Phenotype Analysis of *ltp12* Mutant, *ltp2* Mutant, and Col-0. A. 2-week-old plants (15 DAG). B. 3-week-old plants (22 DAG), C. 3-week-old plants (28 DAG). D. 4-week-old plants (30 DAG). *ltp2* mutant (with pink label), *ltp12* mutant (with red label), and Col-0 (with white label).*

No visual difference in flower and leaf morphology was observed between *ltp12*, *ltp2* mutant and Col-0. Significant difference in growth phenotype was observed in *ltp12* mutant and *ltp2* mutant with respect to Col-0; additionally, significant difference in the overall growth phenotype of mutants with respect to Col-0 was also observed in a previous experiment where 18 plants from each mutants and Col-0 were analyzed.

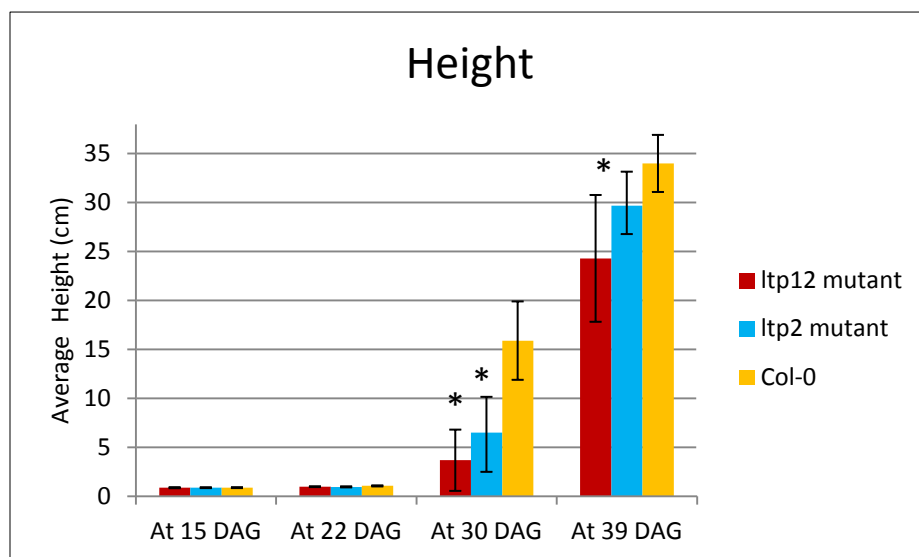


Figure 35. Height of *Arabidopsis* Plant at 15, 22, 30, and 39 DAG. At 15 DAG and 22 DAG, no significant difference between the height of *ltp12* mutant and Col-0 and *ltp2* mutant and Col-0 was observed (Student t test, $p > .05$). At 30 DAG, significant difference between the height of *ltp12* mutant and Col-0 and *ltp2* mutant and Col-0 was observed (Student t test, $p < .05$). At 39 DAG, significant difference between the height of *ltp12* mutant and Col-0 was observed (Student t test, $p < .05$). No significant difference between the height of *ltp2* mutant and Col-0 was observed (Student t test, $p > .05$). Asterisk shows the significant difference from the parental line, Col-0 (* = $p < .05$).

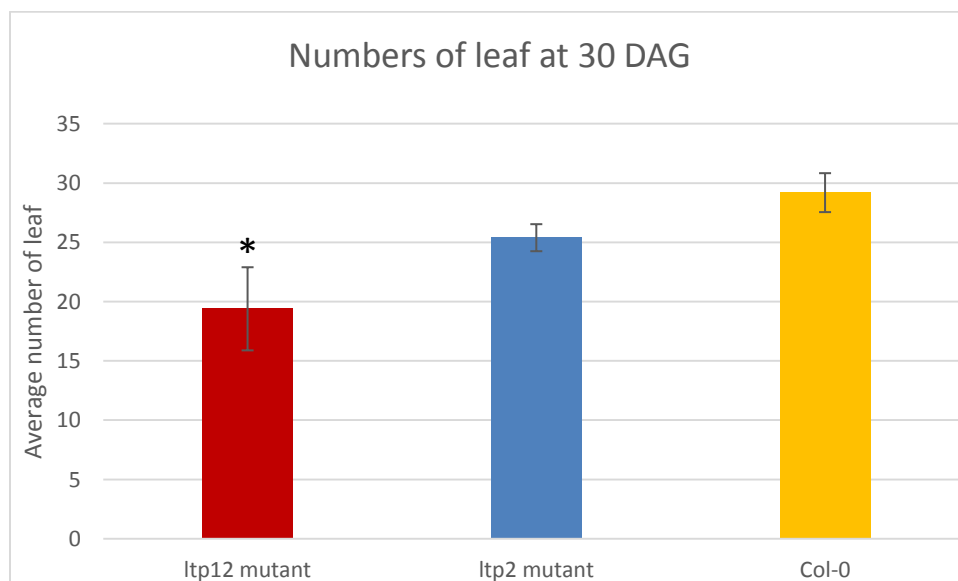


Figure 36. Numbers of Leaf of *ltp12* Mutant, *ltp2* Mutant, and Col-0 at 30 DAG. Significant difference in numbers of leaf between *ltp12* mutant and Col-0 was observed (Student t test, $p < .05$). No significant difference in numbers of leaf between *ltp2* mutant and Col-0 plants was observed (Student t test, $p > .05$).

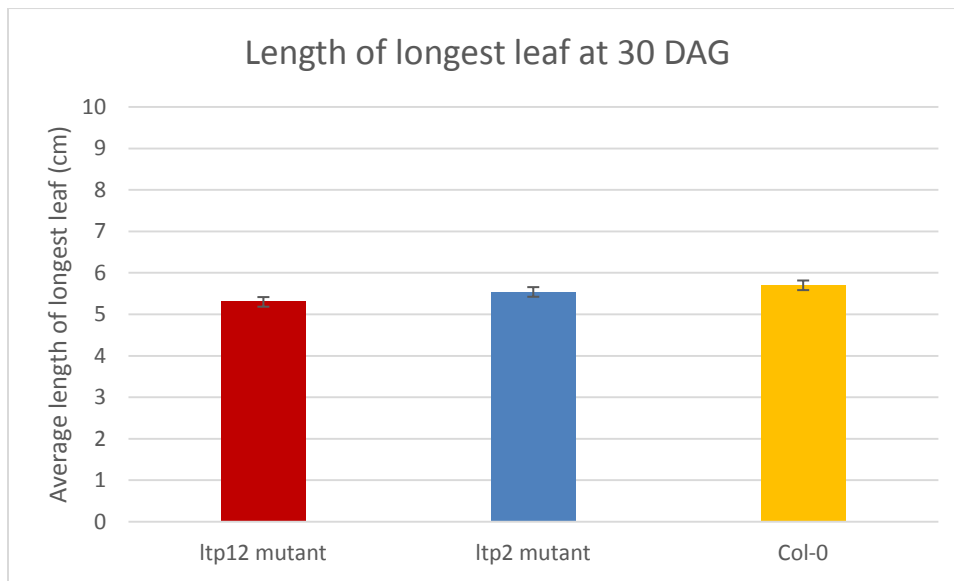


Figure 37. Length of Longest Leaf in *ltp12* Mutant, *ltp2* Mutant, and Col-0. No significant difference in length of longest leaf at 30 DAG between *ltp12* mutant and Col-0 plant was observed (Student t test, $p > .05$). No significant difference in length of longest leaf at 30 DAG between *ltp2* mutant and Col-0 plant was observed (Student t test, $p > .05$).

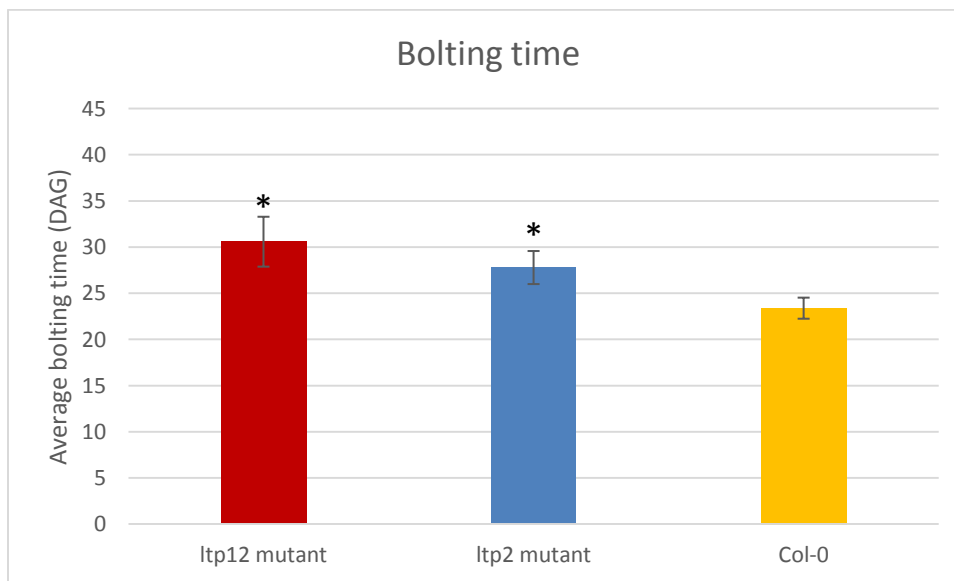


Figure 38. Bolting Time of *ltp12* Mutant, *ltp2* Mutant, and Col-0. Significant difference in bolting time between *ltp12* mutant and Col-0 plant was observed (Student t test, $p < .05$). Similarly, significant difference in bolting time between *ltp2* mutant and Col-0 plant was observed (Student t test, $p < .05$).

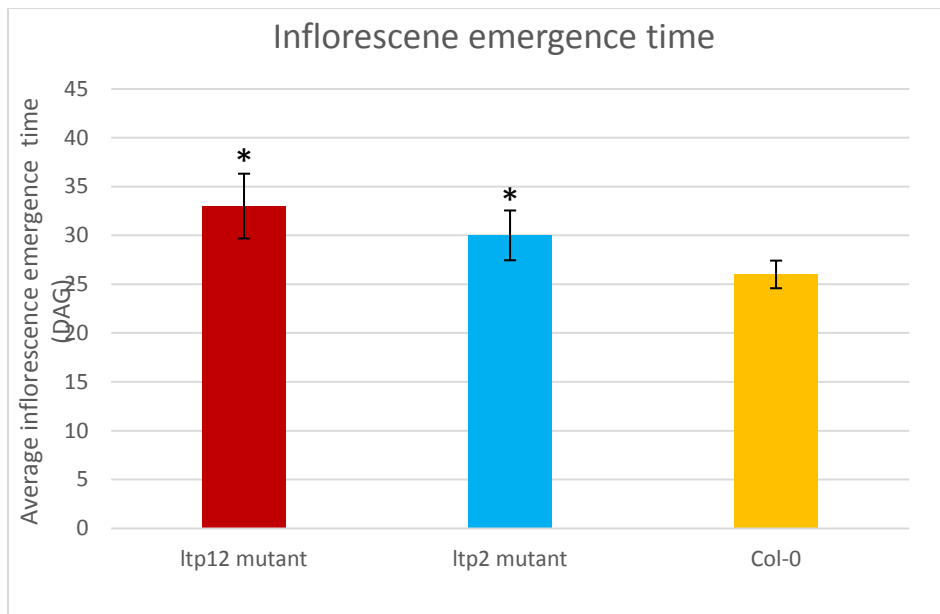


Figure 39. Time of Inflorescence Emergence in *ltp12* Mutant, *ltp2* Mutant, and Col-0. Significant difference in inflorescence emergence time between *ltp12* mutant and Col-0 plant was observed (Student t test, $p < .05$). Similarly, significant difference in inflorescence emergence time between *ltp12* mutant and Col-0 plant was observed (Student t test, $p < .05$).

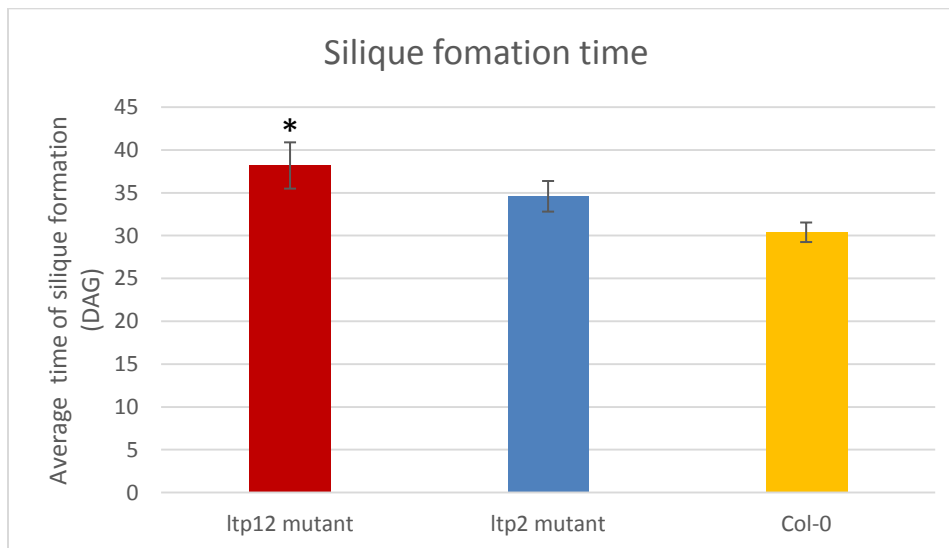


Figure 40. Time of Silique Formation in *ltp12* Mutant, *ltp2* Mutant, and Col-0. There was a significant difference of silique formation time between *ltp12* mutant and Col-0 (Student t test, $p < .05$). No significant difference of silique formation time between *ltp2* mutant and Col-0 was observed (Student t test, $p > .05$).

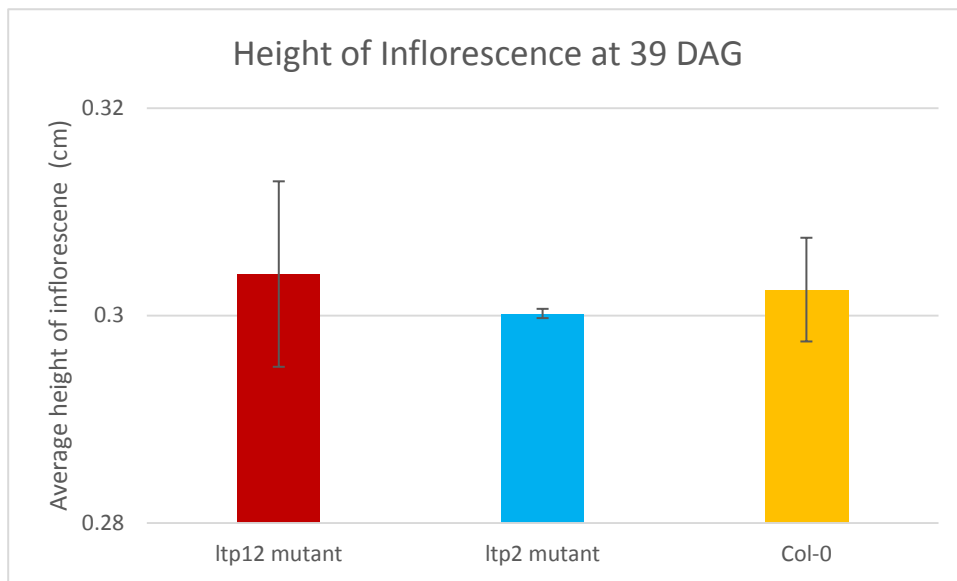


Figure 41. Height of Inflorescence at 39 DAG in *ltp12* Mutant, *ltp2* Mutant, and Col-0. No significant difference in height of inflorescence in *ltp12* mutant and Col-0 plants was observed (Student t test, $p > .05$). Similarly, no significant difference in length of inflorescence between *ltp12* mutant and Col-0 plants was observed (Student t test, $p > .05$).

Toluidine Blue (TB) Test

Surface sterilized *ltp12* mutant, *ltp2* mutant, and Col-0 seeds were sown on Murashige and Skoog's medium solidified with gellan gum (0.4%). After vernalization treatment for 3 days at 4°C, plates were transferred to a growth chamber (22°C, continuous light). For TB staining, 0.05% (w/v) of Toluidine Blue (TB) was poured onto plates containing growing plants (18 days old). After the 10 minutes of TB staining, TB solution was decanted and plates were washed with water to remove the TB. No TB staining on any part of the plant was observed (Figure 42 B).

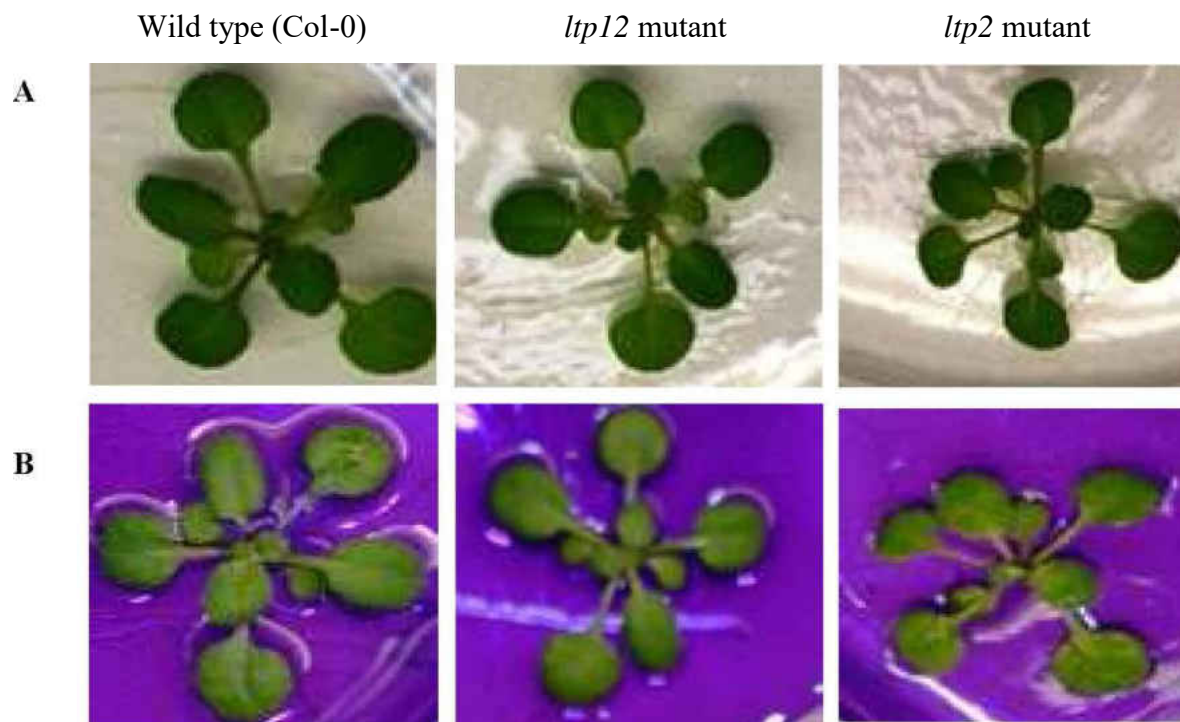


Figure 42. Application of Toluidine Blue on Plant Surface to Detect Permeable Epidermal Surface. (A) Plants before TB treatment. (B) Plants after TB treatment.

Pathogen Growth Assay

A seedling flood inoculation method was carried out to analyze gene for gene mediated resistance response in *ltp12* mutant, *ltp2* mutant, and Col-0. *Arabidopsis* Col-0 has 'R' protein that recognizes *AvrRPT2*. *Pst DC3000* or *Pst DC3000 AvrRpt2* at 5×10^6 cfu/ml in 0.025% silwet L-77 was added to the plates containing 2-week-old plants and incubated for 3 minutes at room temperature. Plants were rinsed with sterile water, and then incubated at 24°C with 150-200 $\mu\text{E m}^{-2}\text{sec}^{-1}$ light intensity and a 12-hour dark/light period. Symptoms were recorded at 1 days post infection (dpi) and 4 dpi for *Pst DC3000* inoculated plants. Symptoms were recorded at 3 and 4 dpi for *Pst DC3000 AvrRPT2* inoculated plants. Leaf samples (12.5 mg) were collected and their surface was sterilized with 3% H_2O_2 , and then washed 3 times with sterile water. The leaves samples were homogenized in 200 μl of sterile water, and then the samples were serially diluted. The diluted samples were plated on Kings B media containing 20 $\mu\text{g/ml}$ of rifampicin and 25 $\mu\text{l/ml}$

of kanamycin. Bacterial colony forming units (cfu) were counted. *ltp12* and *ltp2* mutant showed more susceptibility to both pathogens compared to control, Col-0. Results show that *ltp12* mutants are more susceptible to *Pst DC3000* at 1 dpi (Figure 43) and 4 dpi (Figure 44) compared to control. Similarly, *ltp2* mutant was also found to be more susceptible to *Pst DC3000* at 1 dpi (Figure 45) and 4 dpi (Figure 46) compared to control. In another experiment the growth of avirulent *Pst DC3000 AvrRpt2* was quantified at 3 dpi and 4 dpi. *ltp12* mutant was found to be more susceptible at 3 dpi (Figure 47) and 4 dpi (Figure 48) compared to control plants. Likewise, *ltp2* mutant showed more susceptibility to *Pst DC3000 AvrRpt2* at 3 dpi (Figure 49) and 4 dpi (Figure 50) compared to control.

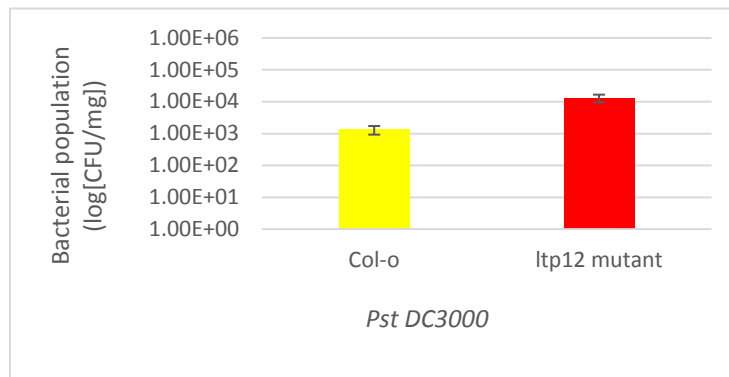


Figure 43. Bacterial Population of *Pst DC3000* in Col-0 and *ltp12* Mutant at 1 dpi (Days after Post Inoculation). Seedlings were flood inoculated with *Pst DC3000* (5×10^6 cfu/ml) in 0.025% silwet L-77.

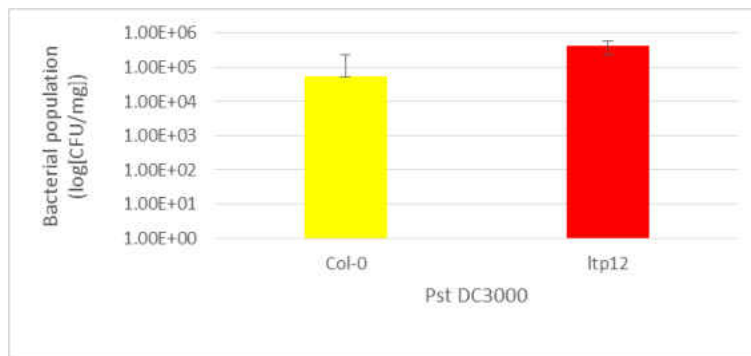


Figure 44. Bacterial Population of *Pst DC3000* in Col-0 and *ltp12* Mutant at 4 dpi. Seedlings were flood inoculated with *Pst DC3000* (5×10^6 cfu/ml) in 0.025% silwet L-77.

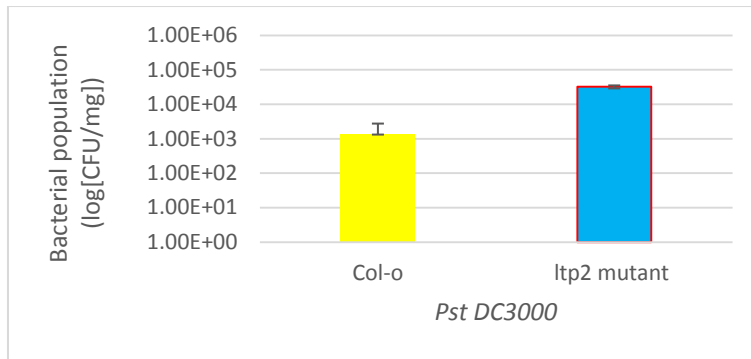


Figure 45. Bacterial Population of *Pst DC3000* in Col-0 and *ltp2* Mutant at 1 dpi. Seedlings were flood inoculated with *Pst DC3000* (5×10^6 cfu/ml) in 0.025% silwet L-77.

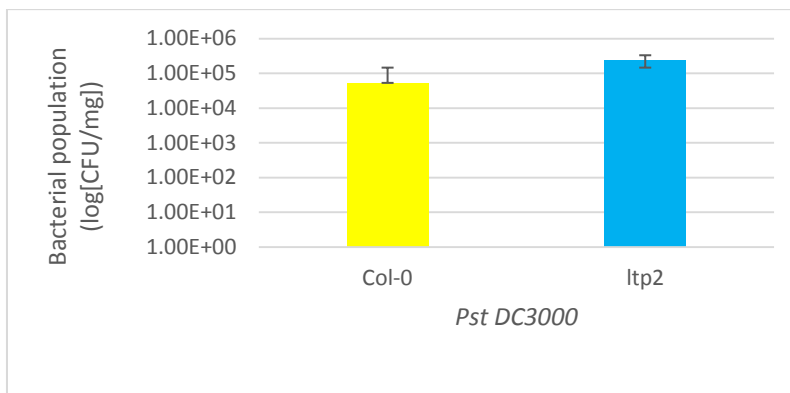


Figure 46. Bacterial Population of *Pst DC3000* in Col-0 and *ltp2* Mutant at 4 dpi. Seedlings were flood inoculated with *Pst DC3000* (5×10^6 cfu/ml) in 0.025% silwet L-77.

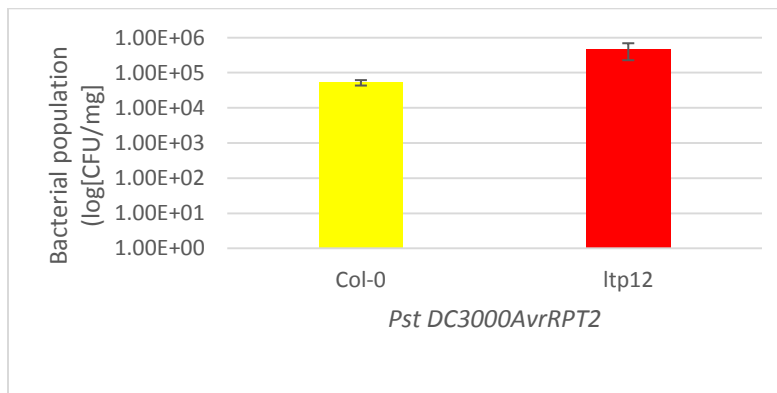


Figure 47. Bacterial Population of *Pst DC3000 AvrRPT2* in Col-0 and *ltp12* Mutant at 3 dpi. Seedling were flood inoculated with *Pst DC3000 AvrRPT2* containing 0.025% Silwet L-77 at a concentration of 5×10^6 cfu/ml.

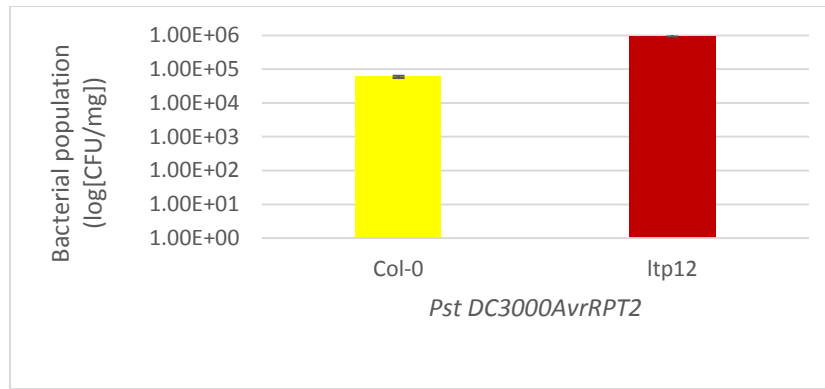


Figure 48. Bacterial Population of *Pst DC3000 AvrRPT2* in Col-0 and *ltp12* Mutant at 4 dpi. Seedling were flood inoculated with *Pst DC3000 AvrRPT2* (5×10^6 cfu/ml) in 0.025% silwet L-77.

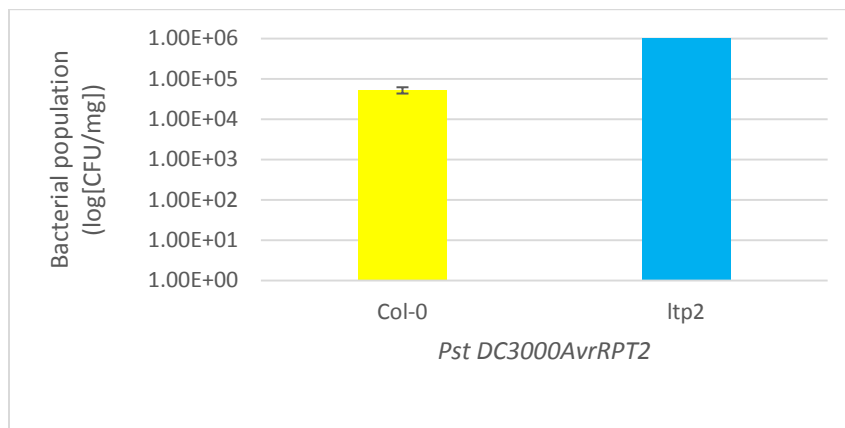


Figure 49. Bacterial Population of *Pst DC3000 AvrRPT2* in Col-0 and *ltp2* Mutant at 3 dpi. Seedling were flood inoculated with *Pst DC3000 AvrRPT2* (5×10^6 cfu/ml) in 0.025% silwet L-77.

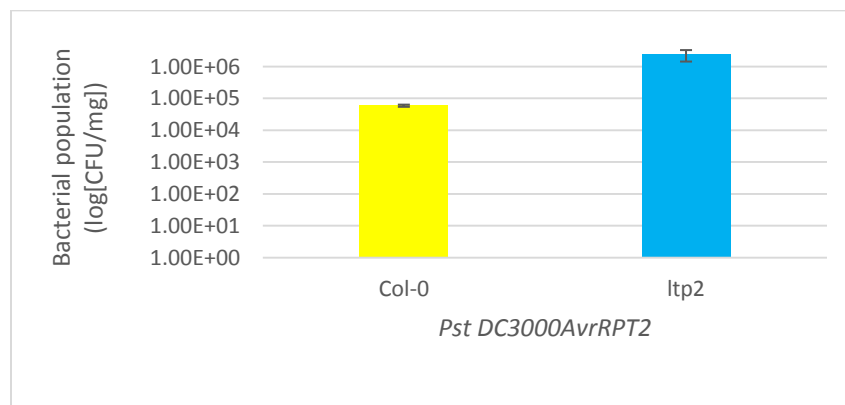


Figure 50. Bacterial Population of *Pst DC3000 AvrRPT2* in Col-0 and *ltp2* Mutant at 4 dpi. Seedling were flood inoculated with *Pst DC3000 AvrRPT2* (5×10^6 cfu/ml) in 0.025% silwet L-77.

CHAPTER 4

DISCUSSION

SA mediated defense pathway is an extensively studied pathway in plants. Various studies have shown that SA is critical for activation of both local as well as systemic acquired resistance. SABP2 has esterase activity that converts lipid soluble MeSA to SA in order to increase cytosolic concentration for activation of the signaling network through NPR1. To learn more about the network, Y2H screening was performed using SABP2 as a bait and tobacco leaf proteins as prey. Y2H screening has identified several SBIPs and SBIP-470 is one of the interacting proteins. *Arabidopsis* LTP2 is the most similar and *Arabidopsis* LTP12 is the second most similar protein to tobacco SBIP-470. Characterization of SBIP-470 and its corresponding *Arabidopsis* knockout mutants (*ltp2* and *ltp12* mutant) are the main focus of the present study. Computational analysis predicted that SBIP-470 belongs to the nsLTP1 subfamily (Figure 11). NsLTP1s have internal hydrophobic cavity and SBIP-470 is predicted to have the hydrophobic cavity (Figure 11). Hydrophobic cavity is involved in lipid binding and lipid transfer (Sodano et al. 1997). Members of nsLTP1 subfamily are small, soluble proteins that are potentially involved in the transfer of fatty acids, glycolipids, phospholipids, and sterols between membranes (Jean and Claude Kader 1996; Charvolin et al. 1999; Renan et al. 2003; Cheng et al. 2004). Based on computation analysis, Tyr₇₉, a conserved amino acid in nsLTP1 subfamily, is also conserved in SBIP-470. Tyr₇₉ stabilizes the bonding between LTP and hydrophobic molecules by a hydrogen bond that is formed between the hydroxyl group of Tyr and carboxyl group of polar head of lipid (Cheng et al. 2004). Studies have shown that nsLTP1s have a role in physical as well as chemical defense mechanism against pathogens (Molina and García-Olmedo 1997; Van Loon and Van Strien 1999; Maldonado et al. 2002; Lee et al. 2009; Liu et al. 2011; Choi et al. 2012). Previous study on gene expression of *SBIP-470* showed that its expression is induced upon viral as well as the bacterial pathogen

challenge suggesting its role in plant defense (Simo and Kumar unpublished). Based on the bioinformatics analysis study of similar proteins and previous study of SBIP-470, we hypothesize that it is a lipid transfer protein.

LTPs have been implicated as modulators of plant vegetative growth and reproduction (Park et al. 2000; Park and Lord 2003). *LTP2* is expressed in flowering meristems, flowers, developing seeds (Clark and Bohnert 1999), and in leaves (Arondel et al. 2000). On promoter region of *LTP2*, pathogen and stress inducible motifs are present (Goldsbrough et al. 1993; Thoma et al. 1994). *LTP2* belongs to Pathogenesis Related-14 (PR-14) protein family (Sels et al. 2008). Study on *Arabidopsis* genome transcript expression using Affymetrix ATH1 microarray showed that *LTP2* is induced upon bacterial pathogen challenge (Kilian et al. 2007). *LTP12* is highly expressed in inflorescences during early stages of flower development but also expressed in seedling and leaf at very low level (Huang et al. 2013). *LTP12* promoter is highly active in tapetum (Ariizumi et al. 2002). *LTP12* belongs to the PR-14 protein family (Sels et al. 2008). The study on *Arabidopsis* showed that *LTP12* transcript is induced upon the bacterial pathogen challenge (Kilian et al. 2007). LTPs are involved in plant defense (Maldonado et al. 2002; Chanda et al. 2011; Liu et al. 2011; Choi et al. 2012) and also have roles in cuticle deposition that serve as a physical barrier for pathogens (Hollenbach et al. 1997; Cameron et al. 2006; Lee et al. 2009). All of this information has raised questions about *ltp12* and *ltp2* mutant. Do *ltp12* and *ltp2* mutant have normal growth phenotypes? Do *ltp12* and *ltp2* mutant exhibit altered resistance to pathogens? To answer these questions we hypothesized that *ltp12* and *ltp2* mutant have altered growth phenotypes and that mutants are susceptible to pathogens.

Characterization of SBIP-470

Full length *SBIP-470* with the signal peptide was cloned using gateway cloning to make N terminal 6xhis tagged recombinant protein. However, full length recombinant SBIP-470 protein in soluble form could not be expressed and purified (data not shown). Removal of the transmembrane signal peptide helps in the expression and solubility of protein (Raina and Missiakas 1997; Gopal and Kumar 2013). In order to increase the solubility of the protein, the *SBIP-470* was cloned without signal peptide. Then, recombinant protein (recSBIP-470-25) was expressed in *E. coli* and purified under soluble form. In vitro lipid binding assay was performed using the Membrane Lipid Strips (Echelon). Purified recSBIP-470-25 was used as a binding site for the different biologically important phospholipids found in cell membranes. Result showed recSBIP-470-25 does not bind the lipids represented on the available PIP Strip under present experimental conditions (mentioned in Materials and Methods), or if it does, its binding is very weak and is undetectable using this technique (Figure 29 A and Figure 30 B). In vitro Lipid transfer assay was performed using Phospholipid Transfer Protein (PLTP) assay kit (Roar Biomedical). Purified recSBIP-470-25 was incubated with donor containing fluorescent labelled phospholipid, acceptor, and PLTP buffer. Result showed that recSBIP-470-25 fail to transfer the phospholipid from donor to acceptor (Figure 28). Phospholipid used in this study may not be right substrate for the recSBIP-470-25.

SBIP-470 Gene Expression upon Pathogen Infection

Study on *SBIP-470* gene expression has shown that it is highly induced upon TMV infection in C3 plant expressing SABP2 (Figure 5 A) while its expression is compromised in 1-2 plant lacking SABP2 (Figure 5 C). SABP2 restricts the TMV replication and movement in TMV inoculated leaves (Kumar and Klessig 2003). *SBIP-470* gene expression is compromised in C3 plant upon the *P.s. Phaseolicola* (nonhost pathogen) inoculation (Figure 8 A) while highly induced in 1-2 plant only at 9 hpi (Figure 8 C). *SBIP-470* gene expression is slightly induced in C3 plant

(Figure 7 A) while highly induced in 1-2 plant (Figure 7 C) upon the *Pst DC3000*, host pathogen, inoculation. *SBIP-470* gene expression is highly induced in both C3 (Figure 6 A) and 1-2 (Figure 6 C) plant upon the *P.s. tabaci* (host pathogen) inoculation. But, *SBIP-470* gene induction is higher in 1-2 plant compared to C3 plant (Simo and Kumar Unpublished).

Hence, *SBIP-470* is highly inducible to viral as well as bacterial pathogens. Induction of *SBIP-470* gene expression upon the TMV infection most likely depends upon the SABP2 while its (*SBIP-470*) expression upon nonhost pathogen most probably inhibited by the SABP2. LTPs have antimicrobial activity (Wang et al. 2004; Zottich et al. 2011) and they have antiviral activity too (Ooi et al. 2008). High expression of the *SBIP-470* upon the viral and bacterial pathogen challenge might be to suppress the pathogen growth.

Mutant Analysis

In our present study the *Arabidopsis* knockout mutant lacking the *SBIP-470* homolog gene were studied. *ltp12* and *ltp2* mutant showed differences in growth phenotypes compared to their parental line (Col-0). *ltp12* and *ltp2* mutant showed a significant difference in bolting time (Figure 38). Similarly, *ltp12* and *ltp2* mutant showed significant differences in height at 30 DAG and 39 DAG compared to Col-0 (Figure 35). However, the height of *ltp12* and *ltp2* mutant was almost same at 15 DAG and 22 DAG compared to Col-0 (Figure 35). Total numbers of leaf in *ltp12* mutant at 30 DAG was significantly lower than in Col-0 (Figure 20). But, total numbers of leaf in *ltp2* mutant at 30 DAG was not significantly different from Col-0 (Figure 36). The delayed time of inflorescence emergence (Figure 39), and silique formation (Figure 40) was observed in both *ltp12* and *ltp2* mutant respect to Col-0. The height of inflorescence in *ltp12* and *ltp2* mutant at 39 DAG was not significantly different than Col-0 (Figure 41). The collected data showed no significant differences in growth phenotypes until bolting. But after bolting, the differences in phenotype were observed. This suggests the developmental specific expression of *LTP12* and *LTP2*. Result

showed that *ltp12* and *ltp2* mutant have defective growth phenotype. *ltp12* mutant showed more defective growth phenotype than *ltp2* mutant with respect to Col-0. LTP12 might have more dominant role in growth and reproduction than the LTP2. Taken all together, LTP12 and LTP2 have role in plant growth and reproduction, and the mutation on their genes might have affected their role.

Pathogen Growth Assay

In order to determine the effect of mutation on effector triggered immunity upon the pathogen attack, *ltp12* and *ltp2* mutant were inoculated with host pathogens i.e. *Pst DC3000* and *Pst DC3000 AvrRpt2* (5×10^6 cfu/ml). *Pst DC3000 AvrRpt2* is an avirulent pathogen, whereas the *Pst DC3000* is a virulent pathogen to *Arabidopsis* Col-0. Resistance exerted by plant against host pathogen could be associated with gene for gene resistance and involves the SA mediated defense followed by the *PR* gene expression. In the absence of R proteins, plants may still exert some resistance called as basal resistance. The resistance exerted by the plant against non-host pathogen is associated with inducible and constitutive defense mechanism (Dangl and Jones 2001). *Pst DC3000* (virulent) population was found to higher than the *Pst DC3000 AvrRpt2* (avirulent) when Col-0 was inoculated with these pathogens (Ishiga et al. 2011). Result showed that *ltp12* and *ltp2* mutants are more susceptible to the both pathogens compared to wild type, Col-0 (Figure 43, Figure 44, Figure 45, Figure 46, Figure 47, Figure 48, Figure 49, and Figure 50). *Pst DC3000* population in Col-0 was found higher than *Pst DC3000 AvrRpt2* (Figure 43, Figure 44, Figure 45, Figure 46, Figure 47, Figure 48, Figure 49, and Figure 50). In agreement with that, *ltp12* mutant was found to more susceptible to *Pst DC3000* compared to *Pst DC3000 AvrRpt2* (Figure 43, Figure 44, Figure 47, and Figure 48). Similarly, *ltp2* mutant is also found to more susceptible to *Pst DC3000* compared to *Pst DC3000 AvrRpt2* (Figure 45, Figure 46, Figure 49, and Figure 50). Result showed that both *ltp2* and *ltp12* mutant has weaker ETI against both pathogen compared to

Col-0. This suggests that *LTP2* and *LTP12* have role in both basal and gene for gene resistance in plants.

Toluidine Blue Test

Studies have shown that LTPs are involved in cuticle deposition (Hollenbach et al. 1997; Cameron et al. 2006; Lee et al. 2009). Toluidine blue test was performed in order to check any changes in permeability of cuticular surface due to mutations. There was no toluidine staining on any parts of *ltp12*, *ltp2* mutant, and Col-0 (Figure 42), which suggests that the cuticular surface of those plants were not altered.

Lipid Binding and Transfer Test

The research was conducted to characterize the SBIP-470 and *Arabidopsis* knockout mutants lacking the *SBIP-470* homolog genes. Result showed that SBIP-470 does not bind the select lipids. SBIP-470 fails to transfer the phospholipid.

Gene Expression and Pathogen Growth

Study on gene expression analysis showed that *SBIP-470* is highly inducible upon pathogen challenge. *Arabidopsis ltp12* and *ltp2* mutant showed differences in growth phenotypes with respect to Col-0. *ltp12* mutant showed the more noticeable differences in growth phenotype than *ltp2* mutant with respect to Col-0. *ltp12* and *ltp2* mutant showed susceptibility to the pathogen with respect to Col-0.

Future Direction

Further biochemical characterization of SBIP-470 needs to be pursued. In vitro lipid transfer assay showed that SBIP-470 fails to transfer phospholipid under present experimental

conditions. Lipid transfer assay needs to be carried out using other substrates to determine its lipid transfer activity. Roles of *SBIP-470* in SA mediated defense pathway need to be studied. Both *ltp12* and *ltp2* mutant have shown the growth phenotype and *ltp12* and *ltp2* mutant showed susceptibility to pathogens. Complementation of *Arabidopsis* mutants with functional tobacco *SBIP-470* could be carried out to determine if mutant phenotype is complemented. The complementation assay would be another way to characterize the SBIP-470.

REFERENCES

- Altschul SF, Madden TL, Schäffer AA, Zhang J, Zhang Z, Miller W, Lipman DJ. 1997. Gapped BLAST and PSI-BLAST: a new generation of protein database search programs. *Nucleic Acids Res.* 25:3389–3402.
- Ariizumi T, Amagai M, Shibata D, Hatakeyama K, Watanabe M, Toriyama K. 2002. Comparative study of promoter activity of three anther-specific genes encoding lipid transfer protein, xyloglucan endotransglucosylase/hydrolase and polygalacturonase in transgenic *Arabidopsis thaliana*. *Plant Cell Rep.* 21:90–96.
- Arondel V, Vergnolle C, Cantrel C, Kader J. 2000. Lipid transfer proteins are encoded by a small multigene family. *Plant Sci.* 157:1–12.
- Bagal UR, Leebens-Mack JH, Lorenz WW, Dean JFD. 2012. The phenylalanine ammonia lyase (PAL) gene family shows a gymnosperm-specific lineage. *BMC Genomics* 13: 1-9.
- Bakan B, Hamberg M, Perrocheau L, Maume D, Rogniaux H, Tranquet O, Rondeau C, Blein JP, Ponchet M, Marion D. 2006. Specific adduction of plant lipid transfer protein by an allene oxide generated by 9-lipoxygenase and allene oxide synthase. *J. Biol. Chem.* 281:38981–38988.
- Bodén M, Hawkins J. 2005. Prediction of subcellular localization using sequence-biased recurrent networks. *Bioinformatics* 21:2279–2286.
- Buhot N, Gomès E, Milat M. 2004. Modulation of the biological activity of a tobacco LTP1 by lipid complexation. *Mol. Biol. Cell* 15:5047–5052.
- Cameron KD, Teece MA, Smart LB. 2006. Increased accumulation of cuticular wax and expression of lipid transfer protein in response to periodic drying events in leaves of tree tobacco 1. *Plant Physiol.* 140:176–183.
- Chae K, Gonong BJ, Kim SC, Kieslich CA, Morikis D, Balasubramanian S, Lord EM. 2010. A multifaceted study of stigma/style cysteine-rich adhesin (SCA)-like *Arabidopsis* lipid transfer proteins (LTPs) suggests diversified roles for these LTPs in plant growth and reproduction. *J. Exp. Bot.* 61:4277–4290.
- Chanda B, Xia Y, Mandal MK, Yu K, Sekine KT, Gao Q, Selote D, Hu Y, Stromberg A, Navarre D, et al. 2011. Glycerol-3-phosphate is a critical mobile inducer of systemic immunity in plants. *Nat. Genet.* 43:421–427.
- Charvolin D, Douliez JP, Marion D, Cohen-Addad C, Pebay PE. 1999. The crystal structure of a wheat nonspecific lipid transfer protein (ns-LTP1) complexed with two molecules of phospholipid at 2.1 Å resolution. *Eur. J. Biochem.* 264:562–568.
- Chen CC, Hwang JK, Yang JM. 2006. (PS)2: protein structure prediction server. *Nucleic Acids Res.* 34:152–157.

- Chen Z, Zheng Z, Huang J, Lai Z, Fan B. 2009. Biosynthesis of salicylic acid in plants. *Plant Signal. Behav.* 4:493–496.
- Cheng H, Cheng P, Peng P, Lyu P. 2004. Lipid binding in rice nonspecific lipid transfer protein-1 complexes from *Oryza sativa*. *Protein Science* 13:2304–2315.
- Choi YE, Lim S, Kim HJ, Han JY, Lee M-H, Yang Y, Kim JA, Kim Y-S. 2012. Tobacco NtLTP1, a glandular-specific lipid transfer protein, is required for lipid secretion from glandular trichomes. *Plant J.* 70:480–491.
- Clark AM, Bohnert HJ. 1999. Cell-specific expression of genes of the lipid transfer protein family from *Arabidopsis thaliana*. *Plant Cell Physiol.* 40:69–76.
- Clarke JD, Volko SM, Ledford H, Ausubel FM, Dong X. 2000. Roles of salicylic acid, jasmonic acid, and ethylene in cpr-induced resistance in *Arabidopsis*. *Plant Cell* 12:2175–2190.
- Dao TTH, Linthorst HJM, Verpoorte R. 2011. Chalcone synthase and its functions in plant resistance. *Phytochem. Rev.* 10:397–412.
- Dempsey DA, Klessig DF. 2012. SOS - too many signals for systemic acquired resistance? *Trends Plant Sci.* 17:538–545.
- Dempsey DA, Vlot AC, Wildermuth MC, Klessig DF. 2011. Salicylic acid biosynthesis and metabolism. Rockville, MD: American Society of Plant Biologists. 1-24.
- De Vos M, Van Zaanen W, Koornneef A, Korzelius JP, Dicke M, Van Loon LC, Pieterse CMJ. 2006. Herbivore-induced resistance against microbial pathogens in *Arabidopsis*. *Plant Physiol.* 142:352–363.
- Dong X. 2001. Genetic dissection of systemic acquired resistance Xinnian Dong. *Curr. Opin. Plant Biol.* 4:309–314.
- Felix G, Duran JD, Volko S, Boller T. 1999. Plants have a sensitive perception system for the most conserved domain of bacterial flagellin. *Plant J.* 18:265–276.
- Goldsbrough AP, Albrecht HSR. 1993. Salicylic acid-inducible binding of a tobacco nuclear protein to a 10 bp sequence which is highly conserved amongst stress-inducible genes. *Plant J.* 3:563–571.
- Han GW, Lee JY, Song HK, Chang C, Min K, Moon J, Shin DH, Kopka ML, Sawaya MR, Yuan HS, et al. 2001. Structural basis of non-specific lipid binding in maize lipid-transfer protein complexes revealed by high-resolution X-ray crystallography. *J. Mol. Biol.* 308:263–278.
- Höglund A, Dönnes P, Blum T, Adolph HW, Kohlbacher O. 2006. MultiLoc: prediction of protein subcellular localization using N-terminal targeting sequences, sequence motifs and amino acid composition. *Bioinformatics* 22:1158–1165.

- Hollenbach B, Schreiber L, Hartung W, Dietz KJ. 1997. Cadmium leads to stimulated expression of the lipid transfer protein genes in barley: Implications for the involvement of lipid transfer proteins in wax assembly. *Planta*, 203 (1) 9-19.
- Huang MD, Chen TLL, Huang AHC. 2013. Abundant type III lipid transfer proteins in *Arabidopsis* tapetum are secreted to the locule and become a constituent of the pollen exine. *Plant Physiol.* 163:1218–1229.
- Jones JDG, Dangl JL. 2006. The plant immune system. *Nature* 444:323–329.
- Kilian J, Whitehead D, Horak J, Wanke D, Weinl S, Batistic OD, Angelo C, Bornberg BE, Kudla J, Harter K. 2007. The AtGenExpress global stress expression data set: protocols, evaluation and model data analysis of UV-B light, drought and cold stress responses. *Plant J.* 50:347–363.
- Kinkema M, Fan W, Dong X. 2000. Nuclear localization of NPR1 is required for activation of PR gene expression. *Plant Cell* 12:2339–2350.
- Kumar D, Klessig DF. 2003. High-affinity salicylic acid-binding protein 2 is required for plant innate immunity and has salicylic acid-stimulated lipase activity. *Proc. Natl. Acad. Sci. U. S. A.* 100:16101–16106.
- Lee SB, Go YS, Bae HJ, Park JH, Cho SH, Cho HJ, Lee DS, Park OK, Hwang I, Suh MC. 2009. Disruption of glycosylphosphatidylinositol-anchored lipid transfer protein gene altered cuticular lipid composition, increased plastoglobules, and enhanced susceptibility to infection by the fungal pathogen *Alternaria brassicicola*. *Plant Physiol.* 150:42–54.
- Liu PP, Von Dahl CC, Park SW, Klessig DF. 2011. Interconnection between methyl salicylate and lipid-based long-distance signaling during the development of systemic acquired resistance in *Arabidopsis* and tobacco. *Plant Physiol.* 155:1762–1768.
- Malamy J, Carr JP, Klessig DF, Raskin I. 1990. Salicylic Acid : A likely endogenous signal in the resistance response of tobacco to viral infection. *Science* 250:1002–1004.
- Maldonado AM, Doerner P, Dixon RA. 2002. A putative lipid transfer protein involved in systemic resistance signalling in *Arabidopsis*. *Nature* 16:399–403.
- Mauch-Mani B, Mauch F. 2005. The role of abscisic acid in plant-pathogen interactions. *Curr. Opin. Plant Biol.* 8:409–414.
- Métraux AJP, Signer H, Ryals J, Ward E, Gaudin J, Schmid E, Blum W, Inverardi B. 1990. Increase in salicylic acid at the onset of systemic acquired resistance in cucumber. *Science* 4983:23–26.
- Molina A, García-Olmedo F. 1997. Enhanced tolerance to bacterial pathogens caused by the transgenic expression of barley lipid transfer protein LTP2. *Plant J.* 12:669–675.

- Nieuwland J, Feron R, Huisman BAH, Fasolino A, Hilbers CW, Derksen J, Mariani C. 2009. Lipid transfer proteins enhance cell wall extension in tobacco. *Plant cell* 17:2009–2019.
- Oerke EC. 2005. Crop losses to pests. *J. Agric. Sci.* 144(01), 31-43
- Ooi LSM, Tian L, Su M, Ho WS, Sun SSM, Chung HY, Wong HNC, Ooi VEC. 2008. Isolation, characterization, molecular cloning and modeling of a new lipid transfer protein with antiviral and antiproliferative activities from *Narcissus tazetta*. *Peptides* 29:2101–2109.
- Park AS, Kaimoyo E, Kumar D, Mosher S, Klessig D F. 2007. Methyl salicylate is a critical systemic signal for plant resistance acquired. *Science* 318(5847), 113–116.
- Park SY, Jauh GY, Mollet JC, Eckard KJ, Nothnagel EA, Walling LL, Lord EM. 2000. A lipid transfer-like protein is necessary for lily pollen tube adhesion to an in vitro stylar matrix. *Plant Cell* 12:151–164.
- Park SY, Lord EM. 2003. Expression studies of SCA in lily and confirmation of its role in pollen tube adhesion. *Plant Mol. Biol.* 51:183–189.
- Pyee J, Kolattukudy PE. 1996. The gene for the major cuticular wax-associated protein and three homologous genes from broccoli (*Brassica oleracea*) and their expression patterns. *Plant J.* 7:49–59.
- Raina S, Missiakas D. 1997. Making and breaking disulfide bonds. *Annu. Rev. Microbiol.* 51:179–202.
- Rosso MG, Li Y, Strizhov N, Reiss B, Dekker K, Weisshaar B. 2003. An *Arabidopsis thaliana* T-DNA mutagenized population (GABI-Kat) for flanking sequence tag-based reverse genetics. *Plant Mol. Biol.* 53:247–259.
- Ryals JA, Neuenschwander UH, Willits MG, Molina A, Steiner HY, Hunt MD. 1996. Systemic acquired resistance. *Plant Cell* 8:1809–1819.
- Sels J, Mathys J, De Coninck BM, Cammue BP, De Bolle MFC. 2008. Plant pathogenesis-related (PR) proteins: a focus on PR peptides. *Plant Physiol. Biochem.* 46:941–950.
- Shah J. 2003. The salicylic acid loop in plant defense. *Curr. Opin. Plant Biol.* 6:365–371.
- Shah J. 2009. Plants under attack: systemic signals in defence. *Curr. Opin. Plant Biol.* 12:459–464.
- Thoma S, Hecht U, Kippers A, Botella J, De Vries S, Somerville C. 1994. Tissue-specific expression of a gene encoding a cell wall-localized lipid transfer protein from *Arabidopsis*. *Plant Physiol.* 105:35–45.
- Thomma BP, Eggermont K, Penninckx IA, Mauch-Mani B, Vogelsang R, Cammue BP, Broekaert WF. 1998. Separate jasmonate-dependent and salicylate-dependent defense-response pathways in *Arabidopsis* are essential for resistance to distinct microbial pathogens. *Proc. Natl. Acad. Sci. U. S. A.* 95:15107–15111.

- Von HG. 1985. Signal sequences the limits of variation. *J. of Mol. Biol.* 184(1) 99-105.
- Wang KL, Li H, Ecker JR. 2002. Ethylene biosynthesis and signaling networks. *Plant cell* 14 :131–151.
- Wang SY, Wu JH, Ng TB, Ye XY, Rao PF. 2004. A non-specific lipid transfer protein with antifungal and antibacterial activities from the mung bean. *Peptides* 25:1235–1242.
- Wilkins MR, Gasteiger E, Bairoch A, Sanchez JC, Williams KL, Appel RD, Hochstrasser DF. 1999. Protein identification and analysis tools in the ExPASy server. *Methods Mol. Biol.* 112:531–552.
- Yang SF, Hoffman NE. 1984. Ethylene biosynthesis and its regulation in higher plants. *Annu. Rev. Plant Physiol.* 35:155 –189.

APPENDICES

APPENDIX A – Abbreviations

1-2 – transgenic plant *Nicotiana tabacum* cv Xanthi nc in which *SABP2* gene expression was silenced by RNA interference

ABA – Abscisic Acid

Avr – Avirulence

BT – *Bacillus thuringiensis*

C3 – Control plants (*N.t.* cv Xanthi nc containing empty gene silencing vector)

cfu – Colony forming units

DIR1 – Defective in Induced Resistance 1

EFalpha1 – Elongation Factor alpha 1

Em 528 – Emission wavelength 528

ET – Ethylene

ETS – Effector-Triggered Susceptibility

Ex485 – Excitation wavelength 485

HR – Hypersensitive Response

ICS 1 – Isochorismate Synthase 1

JA – Jasmonic Acid

KBM – King's B Medium

KDa – Kilo Dalton

LTP12 – Lipid Transfer Protein 12

LTP2 – Lipid Transfer Protein 2

MeSA – Methyl Salicylate

ml – Milli litre

mM – Milli molar

MSE – MeSA Esterase

NO – Nitric Oxide

NPR1 – Non-Expresser of Pathogenesis-Related protein 1

OD – Optical Density

PAMPs – Pathogen-Associated Molecular Patterns

PCR – Polymerase Chain Reaction

PLTP – Phospholipid Transfer Protein

PR – Pathogenesis-Related

PRRs – Pattern Recognition Receptors

Pst – *Pseudomonas syringae tomato*

PTI- PAMP – Triggered Immunity

R protein – Resistance protein

SA – Salicylic Acid

SABP2 – Salicylic Acid Binding Protein 2

SAMT – Salicylic Acid Methyl Transferase

SAR – Systemic Acquired Resistance

SBIP-470 – SABP2 Interacting Protein-470

SDS PAGE – Sodium Dodecyl Sulphate-Polyacrylamide Gel Electrophoresis

TAE – Tris-Acetate EDTA

T-DNA – Transfer DNA

TMV – Tobacco Mosaic Virus

βME – beta mercaptoethanol

μg – Micro gram

μl – Micro litre

APPENDIX B – Buffers and Reagents

0.1% Diethyl Pyrocarbonate (depc) Treated Water (0.1 L)

Diethyl pyrocarbonate = 0.1 ml

Add to 100 ml distilled water

Incubate at 37°C for ~12 hours

Autoclave at 121°C and 15 psi atmospheric pressure for 20 minutes

1X PBS (1 L)

10X PBS = 100 ml

Distilled water = 900 ml

1X PBS Plus 3% Tween Twenty (1 L)

10X PBS = 100 ml

Distilled water = 870 ml

Tween twenty = 30 ml

1X PLTP Buffer (1 L)

Tris-HCl pH 7.4 (M.W: 157.60 g/mol) = 1.576 g, final concentration = 10 mM/L

NaCl (M.W: 58.44 g/mol) = 8.766 g, final concentration = 150 mM/L

EDTA (M.W: 292.24 g/mol) = 0.29224 g, final concentration 1mM EDTA

1x Western Blotting Transfer Buffer (1 L)

Cold water = 800 ml

100% methanol = 100 ml

10x transfer buffer = 100 ml

2x SDS-PAGE Loading Dye (100 mL)

1M Tris-Cl, pH 6.8 = 10 mL, final concentration = 100 mM

SDS = 0.4 g, final concentration = 0.4%

Glycerol = 20 ml, final concentration, 20%

Bromophenol blue = 0.2 g, final concentration = 0.2%

Add 5 mL of β ME before use

3% BSA in PBS-T (100 ml)

10X PBS: 10 ml

Water: 80 ml

BSA = 3 g, final concentration 3%

Tween-20 = 100 μ l, final concentration 0.1%

Adjust volume to 100 ml with water

4x SDS-PAGE Stacking Gel Buffer (1 L)

Tris base (M.W: 121.1 g/mol) = 60.56, final concentration 0.5 M

Adjust pH to 6.8

Add 0.4 g SDS, final concentration 0.04%

10 mM Magnesium Chloride (1 L)

Magnesium Chloride = 0.952 g

Adjust the volume to 1 liter with distilled water

10x Phosphate Buffer Saline (10X PBS) (1 L)

Sodium Phosphate dibasic (M.W: 141.96 g/mol) = 10 g, final concentration: 70 mM

Sodium Chloride (M.W: 58.44 g/mol) = 76 g, final concentration: 1.3M

Sodium Phosphate monobasic (M.W: 119.96 g/mol) = 4.1 g, final concentration = 30 mM

10x SDS-PAGE Running Buffer (1 L)

Tris base (M.W: 121.1 g/mol) = 30 g

Glycine (M.W: 75.07 g/mol) = 144 g

SDS = 10 g

10x Western Blotting Transfer Buffer (1 L)

Tris base (M.W: 121.1 g/mol) = 30.3 g, final concentration 125 mM

Glycine (M.W: 75.07 g/mol) = 72.06 g, final concentration 960 mM

20% Ammonium Persulfate (1 mL)

Ammonium persulfate = .2 g

Water = 1 ml

50 mM Sodium Phosphate Buffer (1 L)

Monosodium phosphate monohydrate ($\text{NaH}_2\text{PO}_4 \cdot \text{H}_2\text{O}$) = 2.9181 g

Disodium phosphate (Na_2HPO_4) = 7.733 g

Maintain pH 7

Maintain 1 liter with distilled water

Edward's Solution 1 L

Tris-HCl, Ph 7.5, (M.W: 157.60 g/mol) = 31.52 g, final concentration = 200 mM/L

Sodium chloride (M.W: 58.44 g/mol) = 14.61 g, final concentration = 250 mM/L

EDTA (M.W: 292.23 g/mol) = 7.30575 g, final concentration = 25 mM/L

SDS (M.W: 288.38 g/mol) = 5 g, final concentration 0.5% (w/v)

Adjust volume to 1 liter with water

Extraction Buffer

Edward's solution: 100 ml

TE buffer (pH 8): 900 ml

KING'S B Medium (1 L)

Potassium phosphate dibasic = 1.50 g

Protease peptone = 20 g

Magnesium sulfate = 1.50 g

Glycerol = 10 ml

Adjust volume to 1 liter with distilled water

Adjust pH to 7.0

Agar: 17.50 g (only for solid medium)

Autoclave at 121°C and 15 psi atmospheric pressure for 20 minutes

MS Media with Gamborg's Vitamins 1 liter

MS media = 4.4 g, final concentration = 4.4 g/L

Myo-Inositol (M.W: 180.2) = 100 g, final concentration 100 mg/L

Nicotinic Acid (1 mg/L) = 1 mg

Pyridoxine. HCl (1 mg/ml) = 1 mg

Thiamine. HCl (10 mg/ml) = 10 mg

MS Media with Gellan Gum

Murashige and Skoog basal medium = 4.4 gm, final concentration = 4.4 g/L

Sucrose = 10 g, final concentration = 1% (W/V)

Gellan gum powder = 4 g, final concentration = 0.4% (W/V)

Ni-NTA Binding Buffer (1 L)

Sodium phosphate monobasic (M.W: 137.99 g/mol) = 6.89 g, final concentration 50 mM/L

Sodium chloride (M.W: 58.44 g/mol) = 17.53 g, final concentration 300 mM/L

Imidazole (M.W: 68.08) = 0.6808, final concentration 10 mM/L

Ni-NTA Elution Buffer (1 L)

Sodium phosphate monobasic (M.W: 137.99 g/mol) = 6.896 g, final concentration 50 mM/L

Sodium chloride (M.W: 58.44 g/mol) = 17.53 g, final concentration 300 mM/L

Imidazole (M.W: 68.08) = 17.02 g, final concentration 250 mM/L

Ponceau S Stain (100 mL)

Ponceau S = 0.1 g, final concentration = 0.1%

Acetic acid = 5 ml, final concentration = 5%

SDS Gel Loading Buffer (2 X)

50mM Tris-HCl (pH 6.8)

100mM DTT

2% (w/v) SDS

0.1% (w/v) bromphenol blue

10% (v/v) glycerol

TE Buffer 1 L

Tris-HCl (M.W: 157.60 g/mol) = 1.576 g, final concentration = 10 mM/L

Adjust pH to 8

Adjust volume to 1 liter with water

Western Blocking Buffer (200 mL)

1x PBS buffer = 200 mL

Dry Milk = 2 g, final concentration 1%

BSA = 6 g, final concentration 3%

VITA

DANDA PANI CHAPAGAI

- Education: East Tennessee State University, Johnson City, TN, USA, M.S.,
Biology, December 2014.
Purbanchal University, Biratnagar, Nepal, B.S., Biotechnology,
2011.
- Professional Experience: Graduate Assistant, East Tennessee State University, Department
of Biological Science, Johnson City, TN, USA, 2012-2014.
President, Biotech Association of Nepal for Research and
Development, Gairidhara, Kathmandu, Nepal, 2009-2012.
Research Intern, Everest Biotech Pvt. Ltd., Lalitpur, Nepal,
2008-2009.
- Presentations: Chapagai D, and Kumar D. (2014). *Role of a Putative Lipid
Transfer Protein/SBIP-470 in SA-mediated defense pathway.*
Appalachian Student Research Forum. Johnson City, TN.
Chapagai D, and Kumar D. (2013). *Role of a Putative Lipid
Transfer Protein/SBIP-470 in SA mediated defense pathway.*
Appalachian Student Research Forum. Johnson City, TN.
Chapagai D, Donald D, Zhao B, and Kumar D. (2013).
*Involvement of a Putative Lipid Transfer Protein/SBIP-470 in
SA Mediated Signaling.* Poster presentation at 52nd Annual
Meeting of the Phytochemical Society of North America.
Corvallis.

Chapagai D. (2010). *Inter linkage between PP2A, NANOG and Aromatase in Human Breast Cancer*. Thesis presentation at SANN International College, Gairidhara, Kathmandu-3. Nepal.

Honors and Awards:

FRANK AND MARY LOEWUS TRAVEL AWARD by
Phytochemical Society of North America.

Research Grant on “Virus free pre basic potato seed Production, Commercialization and Entrepreneurship development” by
Ministry of Youth and Sport, Government of Nepal.